Synthesis of Polyisoxzolidines As Potential Corrosion Inhibitors

BY

ABDULLAH LAJAMI

A Thesis Presented to the
DEANSHIP OF GRADUATE STUDIES

KING FAHD UNIVERSITY OF PETROLEUM & MINERALS

DHAHRAN, SAUDI ARABIA

In Partial Fulfillment of the
Requirements for the Degree of

MASTER OF SCIENCE

In

CHEMISTRY

MARCH 2010

KING FAHD UNIVERSITY OF PETROLEUM AND

DAHRAN 31261, SAUDI ARABIA

DEANSHIP OF GRADUATE STUDIES

This thesis, is written by **Abdullah Ali Lajami** under the direction of his advisor and approved by his thesis committee, has been presented to and accepted by the Dean of Graduate Studies, in partial fulfillment of the degree of

MASTER OF SCIENCE IN CHEMISTRY

Thesis committee

Dr. H. AL-MUALLEM. (Advisor)

Prof. S.A. ALI. (Member)

Dr. A.J. AL-HAMDAN. (Member)

Dr. Abdullah J. Al-Hamdan
Department Chairman

Dr. Salam Zummo
Dean of Graduate Studies

20/6/10

Date

DEDICATED TO MY FAMILY

ACKNOWLEDGEMENT

In the name of Allah, the Most Gracious, the Most Merciful. Praises and thanks be to Allah, the Cherisher and Sustainer of the worlds for providing me the blessings, strength, patience and guidance to complete this work, and blessings be to the last messenger and prophet, Mohammad, peace be upon him, his family and companions,.

Acknowledgements are due to the King Fahd University of Petroleum & Minerals for providing the facilities, and to SABIC for providing the financial support (under the grant SAB-070007) to carry out this research. I would like to express my gratitude and appreciation to this university for the valuable opportunity to continue my Master's degree with professional and bright people.

The deepest and sincerest gratitude are due to my thesis advisor, Dr. Hasan A. Al-Muallem, whose experience, patience and guidance added considerably to my graduate experience. I highly appreciate his knowledge, skills and countless sacrificing of time for helping in completing this thesis. Appreciation also goes to Professor Shaikh Asrof Ali for all his unequalled effort and help. I appreciate his vast knowledge, skills and assistance he has offered me while working in the lab and in writing the thesis. I certainly would like to thank Dr. Abdullah Al-Hamdan for his participation and support as a committee member as well as Chairman of the Department of Chemistry. My gratefulness also goes to all the faculty members and staff of the Department of Chemistry who provided me with education, technical support and who have improved the quality of my research experience at KFUPM.

I appreciate the efforts of Mr. Mohammad Arab in teaching and training me on using the NMR and FTIR instruments. I am really grateful to all my colleagues and friends for their encouragement and help during my research work. Special thank goes to my classmate and labmate Basem Al-Musa.

Finally, I would like to thank my family for their prayers and support that they provided me throughout my entire life and in particular during working in this thesis. I must acknowledge with utmost gratefulness and gratitude my parents and my wife, without whose encouragement, I would never be able to finish this thesis.

TABLE OF CONTENTS

LIST OF TABLES

LIST OF FIGURES

ABSTRACT

FULL NAME: ABDULLAH ALI AHMAD LAJAMI

TITLE OF STUDY: SYNTHESIS OF POLYISOXZOLIDINES AS POTENTIAL CORROSION INHIBITORS

MAJOR FIELED: CHEMISTRY

DATE OF DEGREE: March 2010

Several polyisoxazolidines, a new class of polymers, were synthesized using 1,3-dipolar cycloaddition reaction of some alkene-nitrones, and cocycloaddition of dialkene and dinitrones. Hydroxylamine, *N*-(10-undecenyl)hydroxylamine and aldehyde, *p*-allyloxybenzaldehyde and *p*-10-undecen-1-yloxybenzaldehyde were employed to synthesize the alkene-nitrone monomers. The dialkene, *p*-diallyloxybenzene, and dinitrones, *N,N*'-dimethyl-*p*-phenylenedinitrone and *N,N'*-dimethyl-1,5-pentylidenedinitrone were used to synthesize the polyisoxazolidines via cocycloadditions. IR, ^{1}H, and ^{13}C NMR spectroscopy were used to characterize the various synthesized monomers as well as the polymers. The kinetics of the polymerization processes was investigated by ^{1}H NMR spectroscopy. Kinetic data is helpful in controlling the molar mass of the polymers. End group analysis by ^{1}H NMR spectroscopy was used to determine the average molar mass of the polymers. In order to stabilize the molecular mass of the polymers, the end group of the living polymers was capped by reacting with monofunctional reactive alkene, like methyl acrylate. The synthesized polyisoxazolidines, containing multiple donor atoms (N, O), quaternary ammonium group, π-electrons, and electron-rich aromatic group, were used to study their efficiencies on the corrosion inhibition of mild steel in acidic solutions (1 M HCl and 0.5 M H_2SO_4) at 60 ^{o}C using gravimetric and electrochemical methods. Most of the compounds have shown very good corrosion inhibition efficiency (IE%) in HCl solution as measured by the gravimetric method. Comparable results were obtained by the electrochemical method using Tafel plots for the inhibition efficiency of some of the selected synthesized compounds. It is evident from the Tafel plots that in most of the compounds the inhibitor adsorption shifted the corrosion potential (E_{corr}), in the negative direction with reference to the blank in 1 M HCl, signifying that suppression of the cathodic reaction is the main effect of these corrosion inhibitors.

MASTER OF SCIENCE DEGREE

KING FAHD UNIVERSITY OF PETROLEUM AND

DAHRAN, SAUDI ARABIA

ملخص الرسالة

الاسم: عبدالله علي أحمد لاجامي

عنوان الرسالة: تحضير بوليميرات الايزوكسازوليدين لتطبيقها كمثبطات لعملية الصدأ

التخصص: الكيمياء

التاريخ: ربيع الآخرة 1431هـ (مارس 2010)

تم تحضير صنف جديد من البوليمرات هو بوليمرات أيزوكسازوليدين باستخدام تفاعل إضافة حلقية (3،1) ثنائي القطب لبعض الألكينات النيترونية، و تفاعلات إضافة حلقية بين ألكينات ثنائية و نيترونات ثنائية. و قد تم استخدام المركبات N-(10-اندسين)هيدروكسيل امين ، و *p*- أليلوكسي بنزالدهيد و *p*- (10-اندسين-1-يلوكسي بنزالدهيد) لتحضير الألكينات النيترونية. كما أن الألكين الثنائي *p*- داي اليلوكسي بنزين ، والنيترونات الثنائية N,N'-ثنائي مثيل *p*- فينيل ثنائي النيترون و N,N'-ثنائي مثيل 1,5- بنتثنائي نيترون قد استخدمت لتحضير الأنواع الأخرى من بوليميرات الايزوكسازوليدين . تم استخدام مطياف الاشعة تحت الحمراء ومطياف الرنين المغناطيسي لكل من الهيدروجين والكربون- 13 لتحديد الصيغة البنائية لكل من المنومرات والبوليمرات . كما تمت دراسة حركية البلمرة ، و التي على ضوئها يمكن التحكم في الأوزان الجزيئية للبوليمرات. كما تم أيضاً استخدام مطياف الرنين النووي المغناطيسي لتحليل المجموعات الوظيفية الطرفية و ذلك بهدف تحديد الأوزان الجزيئية للبوليمرات. و من أجل تثبيت الأوزان الجزيئية للبوليمرات فقد تم مفاعلة المجموعات الطرفية في هذه البوليمرات الحية مع ألكينات أحادية المجموعة الوظيفية مثل ميثيل أكرلات . و جرى دراسة بوليمرات الأيزوكسازوليدين و بعض مشتقاتها التي تحتوي على ذرات مانحة للألكترونات (N, O)، و أيونات أمونيوم رباعية , و ألكترونات باي (π), و مجموعات أروماتية غنية بالإلكترونات، من حيث كفاءاتهم في منع تآكل الفولاذ المطاوع في الأوساط الحمضية في كل من 1 مولار من حمض الكلور و نصف مولار من حمض الكبريت و ذلك باستخدام طرق التحليل الوزنية و الكهروكيميائية . معظم المركبات أعطت نتائج جيدة ج داً في حمض الكلور كما اوضحته نتائج التحليل الوزنية . و قد تم الحصول على نتائج مشابهة باستخدام الطرق الكهروكيميائية. إن المعلومات التي تم استخلاصها من منحنيات التافل تبين ان طاقة مزع الصدأ (E_{corr}) تتجه نحو المنطقة السالبة عند مقارنتها مع منحنى حمض الكلور الذي استخدم كمرجع، وهذا يدل على أن هذه المواد تعمل بشكل رئيسي كمثبطات لتفاعلات الاختزال التي تحدث في المهبط

درجة الماجستير في العلوم

جامعة الملك فهد للبترول والمعادن

الظهران ، المملكة العربية السعودية

CHAPTER 1

POLYISOXAZOLIDINES VIA NITRONE CYCLOADDITON REACTIONS

1.1 Introduction

A nitrone **(1)** is the *N*-oxide of an imine or any compound that has azomethine *N*-oxide system. Among a plethora of functional groups in organic chemistry, the nitrone functionality has secured an important place in the arsenal of synthetic chemists. A nitrone is an 1,3-dipole in 1,3-dipolar cycloadditions (**Scheme 1**).[1] It reacts with alkenes **(2)** to give five-membered isoxazolidines (**3**).

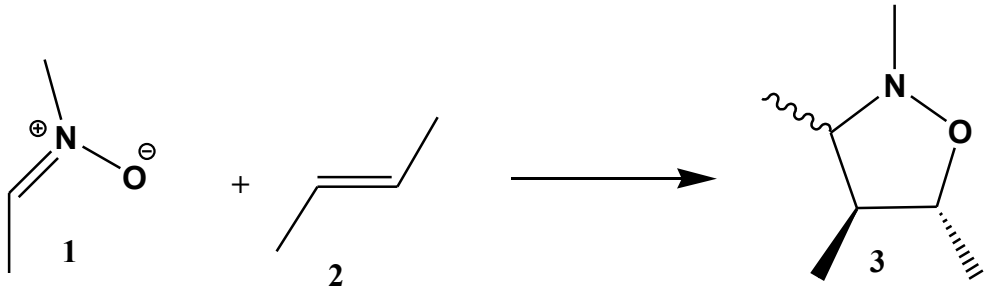

Scheme 1.

Nitrones have been known for more than a century, and there is a great interest in their reactivity towards olefins. Nitrones were discovered by E. Beckmann in 1890 by N-alkylation of oximes.[2] This observation was not given much attention until the systematic studies of Huisgen in 1960s who established the stereochemistry of dipolar cycloadditions. Applications of the cycloaddition have appeared in synthesizing various natural products.[3, 4]

Early researchers suggested the name "nitrone", which is a combination of the words "nitrogen" and "ketone", to emphasize the striking similarity between the newly discovered functional group and the already rich chemistry of the carbonyl group.[2] Now, it is clearly known that the similarity depends on the mesomeric effects which predominate in both classes of compounds, making the nitrone group behaves as carbonyl function (**Scheme 2**).

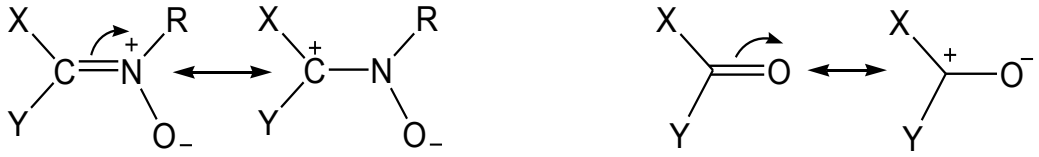

4 **5**

Scheme 2.

The (3 + 2) cycloadditions, also known as 1,3-dipolar cycloadditions (1,3-DC), are similar to Diels–Alder cycloadditions since both processes feature the involvement of [$\pi_{4s} + \pi_{2s}$] electrons.[1,5,6] Although 1,3-dipoles are formally charged species, these charges are stabilized by resonance between the two forms of the dipolar compound.[5] The highest electron density is located at the terminal oxygen atom[5], hence these species are referred to as 1,3-dipoles (**Scheme 3**).[7]

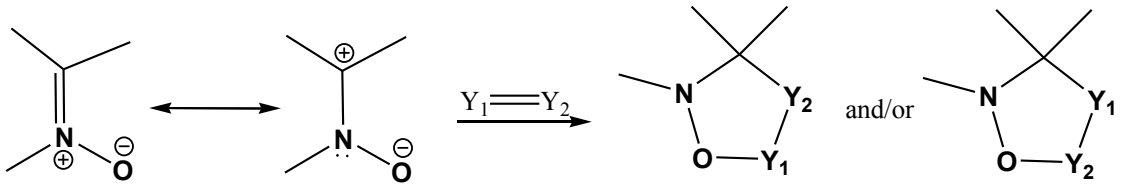

6 **7** **8**

Scheme 3.

The 1,3-dipolar addition of nitrones to olefins is the most useful method for synthesizing isoxazolidines[4], which can be converted to many useful compounds,

including 1,3-amino alcohols, *N*-substituted 1,3-amino alcohol (**Scheme 4**)[1], 1,3-keto alcohols, α,β-unsaturated carbonyl compounds, and the synthesis of natural and non-natural heterocyclic compounds.[4, 8]

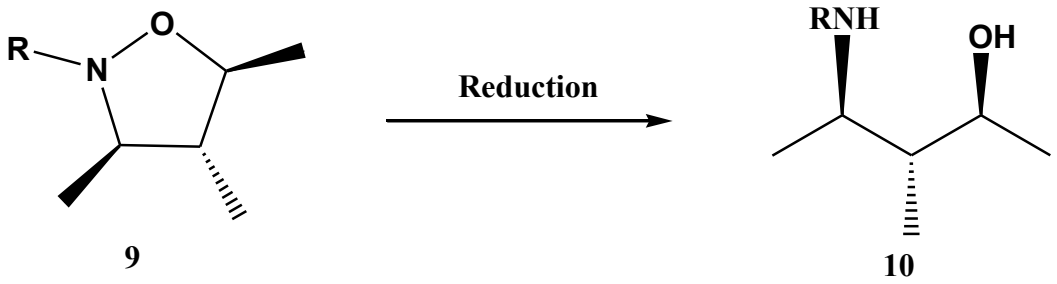

Scheme 4.

1.2 Mechanism of 1,3-dipolar cycloaddition reactions of nitrones

1,3-DC reaction of nitrones with alkenes is a concerted [$\pi_{4s} + \pi_{2s}$] reaction (**Scheme 5**). The lack of significant dependence of nitrone-olefin cycloaddition reactions on the nature of the solvent used over a wide range of dielectric constant indicates an early and highly ordered transition state.

Concerted Mechanism

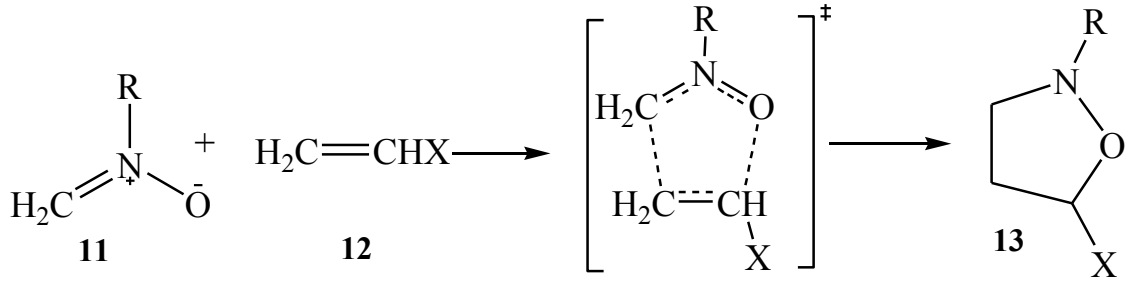

Scheme 5.

Perhaps the backbones of evidence that support the concerted mechanism are the stereospecific and regioselective bond formation of nitrone cycloaddition reaction **(Scheme 6)**.[4, 6]

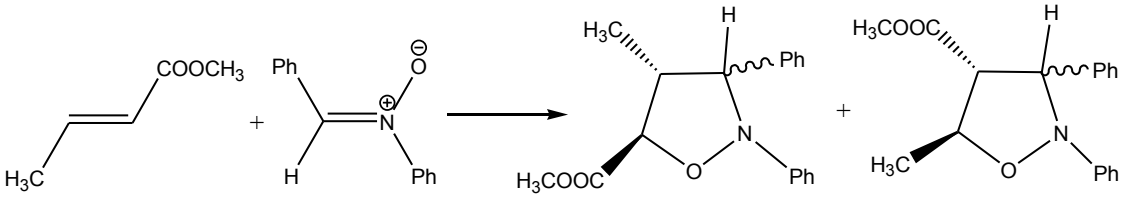

14 **15** **16** **17**

~ 0% ~100%

Scheme 6.

1.3 Regioselectivity and stereoselectivity of the nitrone cycloadditions reaction

Regioselectivity and stereoselectivity of the 1,3-DC reaction with various substituted alkenes have been heavily theorized and researched. Although recently other theories have been developed, the frontier molecular orbitals (FMO) theory contributes important insights into the majority of the 1,3-DC reactions. The frontier molecular orbitals in the dipolarophile and in dipole are presented in Fig. 1.

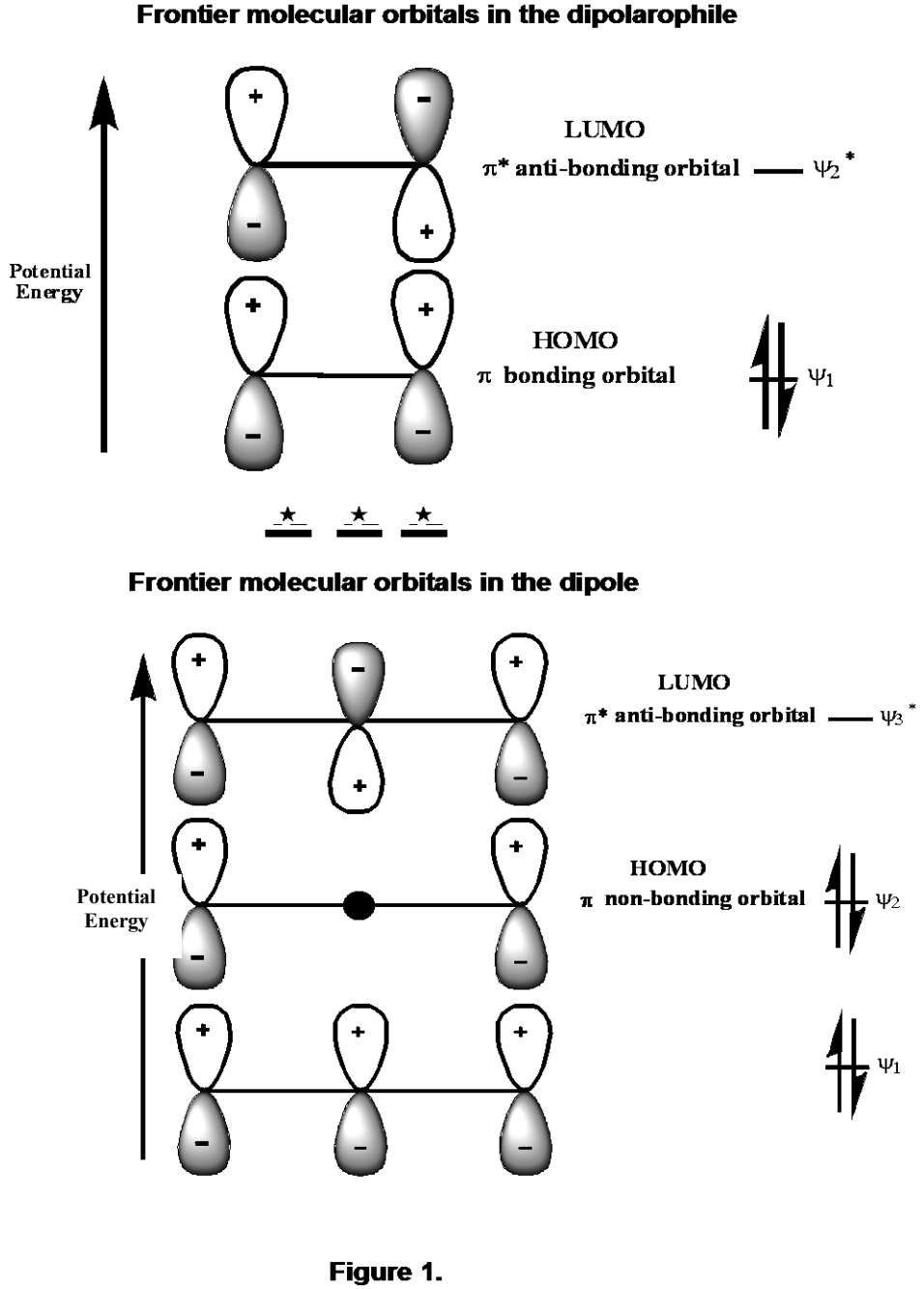

Figure 1.

Cycloadditions have been categorized by Sustmann[9] into three different types (**Fig. 2**).[1] The 1,3-DC reaction of nitrones is believed to correspond to **type II** of Sustmann classification. In this type, the similarity of the lowest unoccupied molecular orbitals (LUMO) and the highest occupied molecular orbitals (HOMO) energies in the dipole and the dipolarophile implies that both HOMO-LUMO interactions stabilize the transition state involved in the cycloaddition.[1, 4-6]

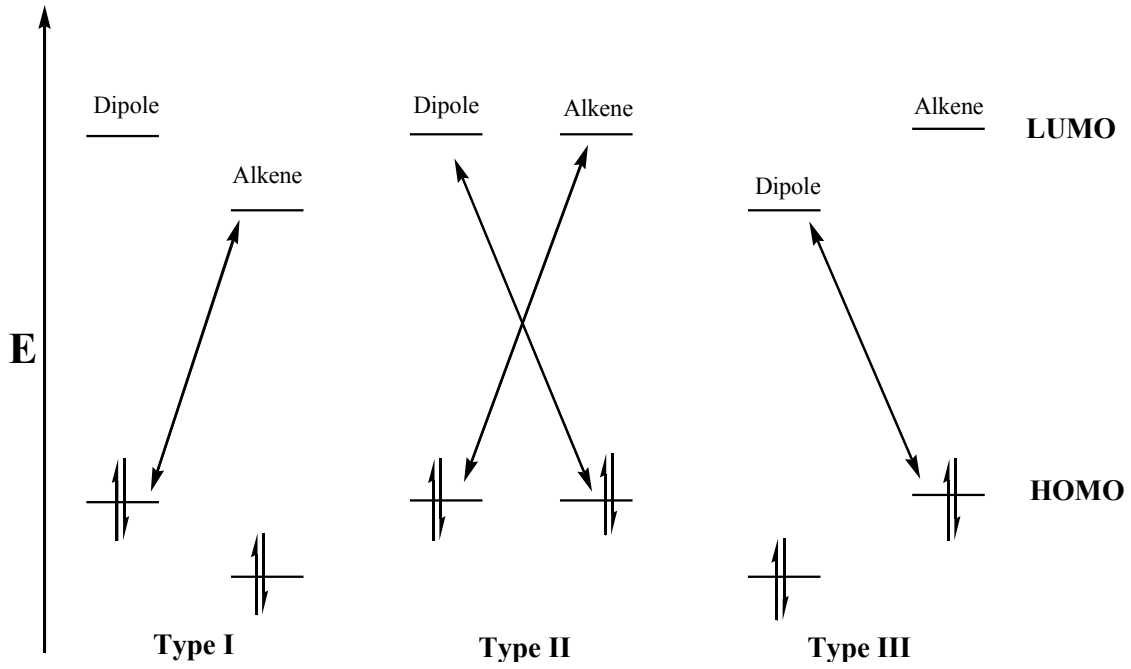

Figure 2.

FMO theory holds that the orbitals that overlap best are closest in energy. The energy gap between the dipole and dipolarophile depends on the type of substituent on both of them. In electron-rich dipolarophiles (**12**), where X = alkyl or OR, raises the energy level of $HOMO_{dipolarophile}$; the dominant interaction is that of $LUMO_{dipole}$ and $HOMO_{dipolarophile}$. In electron-poor dipolarophiles, such as in the case of X =NO_2, lowering the energy level of $LUMO_{dipolarophile}$, the dominant interaction is that of $HOMO_{dipole}$ and $LUMO_{dipolarophile}$.[4]

Although reactivity is rationalized in terms of relative energy differences of the reactant frontier orbitals, the coefficients associated with the atomic orbitals in each of the frontier molecular orbitals dictate the regiochemistry of the cycloadditions. Needless to say that the best overlap of orbitals is between those of similar size. The atomic orbital coefficient of the $LUMO_{nitrone}$ is seen to be larger at carbon than at oxygen; in $HOMO_{dipolarophile}$ with electron donating substituent, the coefficient will be larger on the unsubstituted carbon. This leads to 5-substituted isoxazolidine. For very electron-deficient dipolarophile, the dominant interaction involves $HOMO_{dipole}$-$LUMO_{dipolarophile}$. The transition-state orientation will lead to 4-substituted isoxazolidine (**Fig. 3**). [4, 6]

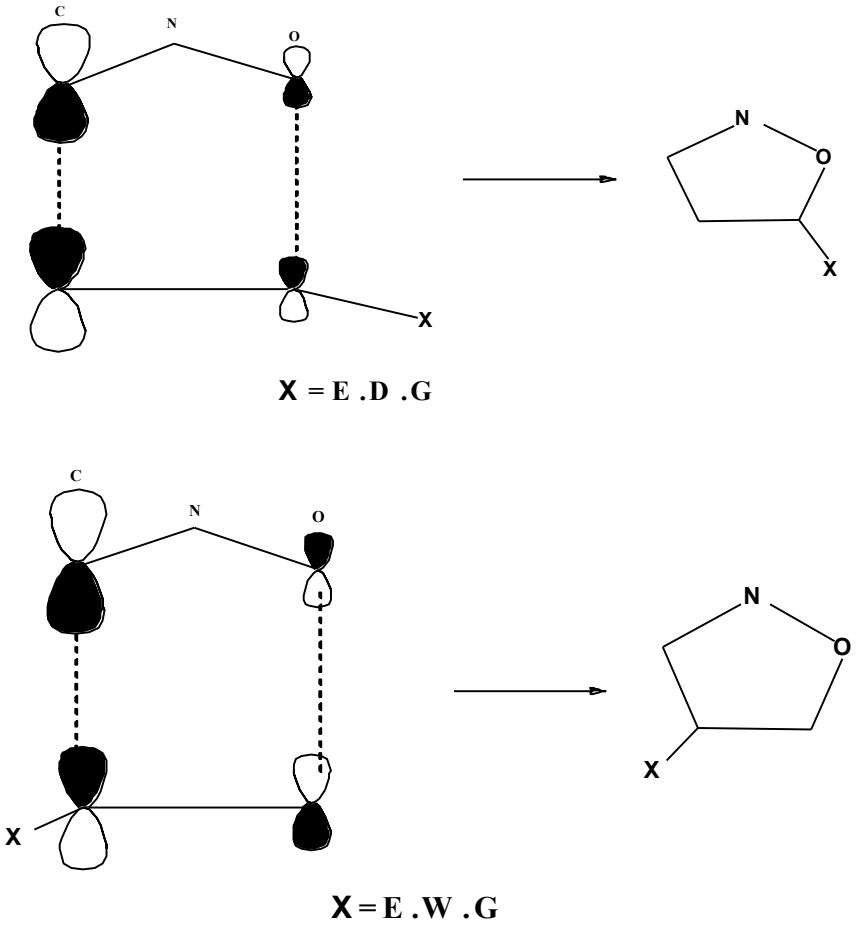

Figure 3.

It has been observed that with various mono-substituted alkenes, up to four products may result. These products can be classified according to their regiochemistry, as either the 4- or 5- regioisomer, and their stereochemistry, as either *endo* or *exo* attack of the dipolarophile.

1.4 Nitrone-alkene cycloaddition polymerization

Despite the widespread use of nitrone reactions, there are very few instances that deal with the formation of polyisoxazolidines.[5] Manecke and Klawitter have synthesized poly(isoxazolidine)s *via* (3 + 2) cycloaddition polymerization of monomers containing nitrone moieties by using two techniques.[10,11] The first technique involved cocycloaddition reaction of alkadiene (A-A Type) (e.g. **20**) and dinitrone (N-N Type) (e.g. **18**). The bisnitrones **18** and **19** were reacted, in turn, with bismaleimides **20** in dimethylformamide at 110 ^{o}C (**Scheme 7**) to give poly(isoxazolidine)s.[10, 11]

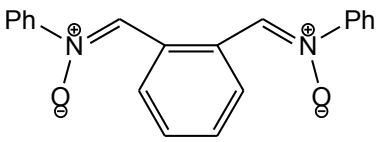

18

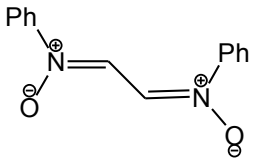

19

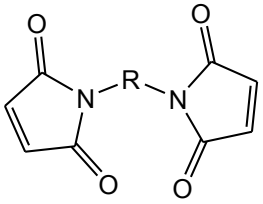

20

20a R= m-phenyl
20b R= p-phenyl

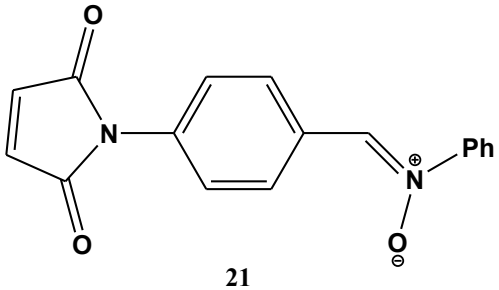

21

Scheme 7.

The polyisoxazolidines produced through this method possessed low molecular weights (M_n values ranging from 2400 to 3600). In addition, Manecke and Klawitter

employed (A-N type) monomers utilizing *p*-maleimidophenyl-N-phenylnitrone (**21)**. The M_n values of the homopolymerization of the A-N monomer that was synthesized in 86% were up to 6200. These polyisoxazolidines were soluble in common organic solvents such as dimethyl sulfoxide and dimethylformamide, but not in ethanol or acetone.[10, 11]

The desired high molecular weight poly(isoxazolidine)s were not produced because the conditions chosen for the cycloaddition reaction involved exposing of the nitrone group to heat for long periods and acidic (or basic) reaction conditions. These conditions result in degradation of the nitrone functionality **22** prior to the occurrence of the desired 1,3-dipolar cycloaddition to give the corresponding amides **23** and O-methyl oximes **24**, respectively (**Scheme 8**).[5]

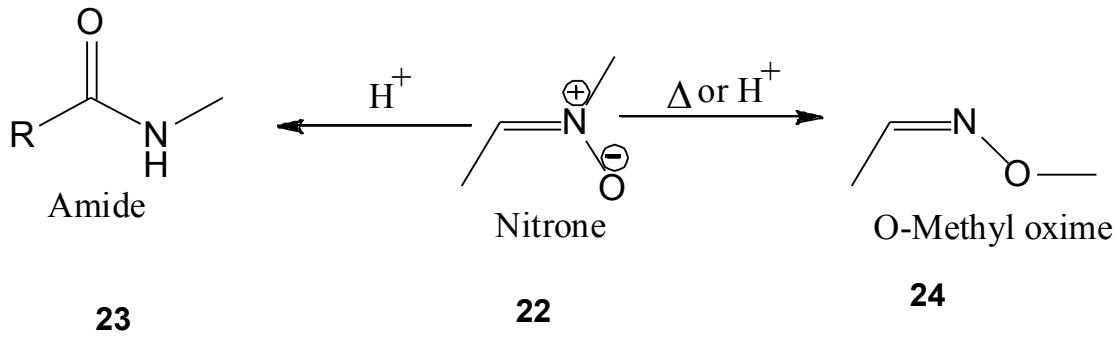

23 **22** **24**

Scheme 8.

Although the cycloaddition reactions are high yielding in nature and the involvement of difunctional monomers are suitable for polymerization, there are very few examples of polymers that have been produced via nitrone cycloaddition reaction. The reactivity can lead to deleterious side reactions between the nitrone and the olefin such as dimerizations, rearrangements, and intramolecular reactions between the nitrone moiety and the alkene group in AN-type monomer.[1, 5]

Wayne Hayes *et. al.* produced a diverse range of poly(isoxazolidine) architectures up to 30 kDa by using high pressure reaction condition. (A-A type) and (N-N type) polymerization strategy was employed in order to tailor these polyisoxazolidines.[12]

Nitrone-alkene cycloadducts, extensively used in the synthesis of various natural products of biological interest,[13] have also been introduced to the corrosion literature for the first time only recently. There are very few reports related to corrosion inhibition efficiencies of the isoxazolidines in the literature. [14-16]

Recently, polyisoxazolidines and polynitrones were attempted to be used for optical data storage applications, coatings applications, good high temperature performance, anti-bacterial, anti-fungal and biological activities.[7, 17-18] According to our literature search, there is no poly(isoxazolidine) used for testing the corrosion inhibition efficiencies.

1.5 Chemistry of Corrosion

Corrosion is a deterioration process that occurs to metals upon their interaction with the environment.[19-21] It is a very costly problem, and it is estimated that about 40% of the steel production goes to replace steel lost due to corrosion. Moreover, corrosion is injurious and can lead to serious accidents, explosions and environmental damage.

Corrosion reactions of metals in acidic solution are electrochemical in nature and involve the following reactions:

$$M \longrightarrow M^{n+} + ne^- \qquad \text{anodic}$$

$$H^+ + e^- \longrightarrow 1/2\ H_2 \qquad \text{cathodic}$$

At anodic sites on the surface, the metal atoms undergo oxidation and go into solution as ions. At cathodic sites, the electrons released from the anodic reaction react with some reducible component of the electrolyte. The corroding piece of metal is described as "mixed electrode" since simultaneous anodic and cathodic reactions are proceeding on its surface. The mixed electrode is a complete electrochemical cell on one metal surface.

Corrosion reactions are spontaneous due to thermodynamic stability of the corrosion product. In practical terms, it is not possible to eliminate completely all corrosion damage to metals. However, retarding either the anodic or cathodic reactions or both electrochemical reactions can reduce the rate of the corrosion. This can be achieved in several ways, namely cathodic protection, anodic protection, galvanization, organic coatings, inorganic coatings, ceramic/glass lining and addition of inhibitors.

A corrosion inhibitor is a chemical additive that reacts with a metallic surface to give it a certain level of protection and thus reduces the rate of metal wastage. Inhibitors are normally distributed from a solution or dispersion. Some are included in a protective coating formulation. Inhibitors slow corrosion processes by either increasing the anodic or cathodic polarization behavior, reducing the movement or diffusion of ions to the metallic surface, or by increasing the electrical resistance of the metallic surface. The efficiency of an inhibitor can be evaluated by comparing anodic and cathodic polarization curves and by comparing the corrosion rates estimated from corrosion current.

Inhibitors are used in a wide range of applications, such as the oil and gas exploration and production industry, the petroleum refining industry, the chemical industry, water treatment facilities, industrial water cooling systems, metal extraction plants, and domestic central heating systems. The largest consumption of corrosion inhibitors is in the oil industry, particularly in the petroleum refining industry. The total consumption of corrosion inhibitors in the United States has doubled from approximately $600 million in 1982 to nearly $1.1 billion in 1998. A study[22] published in September 2001 revealed that the total direct cost of corrosion was determined to be $279 billion per year, which is 3.2 percent of the U.S. gross domestic product (GDP). Indirect costs to the user (society costs) are conservatively estimated to be equal to the direct costs. This means that the overall cost to society could be as much as six percent of the GDP.

Chemical inhibitors are preferred in situation where the corrosive medium is being recycled, *e.g.,* water in cooling towers, acid solutions for acid pickling, acid cleaning, cooling system of automobiles and other equipment. A particular advantage of the use of

corrosion inhibitors is that they can be implemented or changed in situ without disrupting a process. Generally, the most commonly used inhibitors in HCl medium include alkyl and aryl amines, saturated and unsaturated nitrogen ring compounds, ketoximes, imidazoline derivatives, quaternary ammonium compounds, acetylenic alcohols and sulfur containing compounds. Almost all good inhibitors are proprietary (secret) mixture of several chemicals (with synergistic effect) the identity of which only the chemical companies know. Organic adsorption inhibitors usually coat metal with an oily surface layer to protect the metal. They displace water molecules from the metal surface and thus prevent solvation of metal ions by water and also prevent H^+ ions from cathode sites where reduction to H_2 could happen.

CHAPTER 2

CORROSION INHIBITION: LITERATURE REVIEW

The nature of inhibitor interaction during corrosion inhibition of metals and alloys has been deduced in terms of three types of adsorption characteristics of the inhibitors at the metal/solution interface:[23-26] (i) electrostatic adsorption, (ii) adsorption due to the influence of the π bond orbitals, and (iii) chemisorption. The adsorption is controlled by the chemical structure of the inhibitor and by the residual charge on the surface of the metal. Electrostatic adsorption on metal surface is a physical process, which involves relatively weak forces with low activation energy. The ions are not in direct physical contact with the metal. Usually, a layer of water molecule separates them and thus can be desorbed very easily. Chemisorption, however, involves strong interaction between the metal surface and an inhibitor molecule. A coordinate covalent bond involving transfer of electron from inhibitor to the metal surface is formed.[27] Availability of nonbonding electrons in heteroatoms, π-electrons in inhibitor containing multiple bonds or aromatic rings facilitates electron transfer from the inhibitor to the metal. The strength of the chemisorption bond depends upon the electron density on donor atom of the functional group and also the polarizability of the group. The following sequence describes the strength of the adsorption bond based on polarizability and electronegativity of the elements.

$$Se > S > N > O$$

Based on systematic study of corrosion inhibition of iron by organic amines, it was concluded that electron transfer from nitrogen to the metal surface is a chemisorption process. Hard and soft acid base principle (HSAB) was applied to explain the corrosion inhibition phenomenon. According to HSAB principle, soft acids react readily with soft

bases, whereas hard acids like to combine with hard bases. Thus, sulfur being more polarizable (*i.e.,* softer) than nitrogen tends to interact with the neutral metal atoms (soft acid) more strongly than nitrogen-containing inhibitors.[28-30]

The most significant criteria involved in the selection of inhibitors are hydrophobicity,[31] molecular structure,[32] electron density at the donor atom of the inhibitor,[33] solubility and dispersibility of the inhibitor,[34] and length of hydrocarbon chain and the number of aromatic rings.[35]

Molecular structure plays a vital role on corrosion inhibition efficiency. The intimate relation between the chemical structure of the substances and their inhibiting action has been investigated[36-40]. In aromatic and heteroaromatic systems, the electron density on the donor atom of an inhibitor can be increased or decreased by introducing electron donating or electron withdrawing substituent, respectively, in suitable position of the ring structure. The corrosion inhibitor efficiency of various substituted organic inhibitors were correlated using Hammett's parameter which is a measure of the electron donating or withdrawing ability of the substituents.[41-43] In acid solutions, corrosion inhibition of iron by pyridinium and quinolinium compounds is thought to take place through π-electron system of the inhibitors.[44]

Amines having linear carbon chain and their derivatives are well known corrosion inhibitors.[45-52] The percent inhibition increases with carbon number in the chain to about 10 carbons, and with higher members little increase or decrease in the ability to inhibit corrosion occurs. Also, increase in the hydrocarbon chain length in homologous series of nitriles and mercaptans have been shown to result in an increase in the corrosion inhibition efficiency.[53]

Corrosion inhibition of iron in 6 M HCl by various diamines $H_2N(CH_2)_nNH_2$ has been reported. For a 'n' value of 3-8, better inhibition was recorded in comparison to the diamines with a 'n' value of greater than 8. The inhibitors with lower 'n' value may form adsorption binding through chelation of two amine groups.[54]

In the corrosion inhibition of carbon steel in HCl solution by 1-octyn-3-ol, it has been postulated that polymer type of film coating was formed on the metal surface.[55] Acetylenic derivatives form polymeric film and inhibitor with long alkyl chain covers the metal surface,[56] the barrier film thus formed may involve covalent bond (chemisorption bond), π-electron interactions or attractive lateral interactions. The film prevents mass transport and result in inhibition of corrosion.[56] An excellent work involving the electrochemical and quantum chemical studies on the formation of protective films by alkynols on iron has been reported.[57] The results supported the assumption that film formation on iron surfaces from alkynols took place in a two-step process: first chemisorption, then polymerization. The binding of alkynols to iron was studied in model electronic structure calculations, which indicated that a dative bond was formed between Fe and the triple bond.

Amphoteric surfactants (containing both an anionic and a cationic moiety in the same molecule) of the general structure shown in **Scheme 9** have also been used as corrosion inhibitors for mild steel in 0.5 M HCl solution.[58]

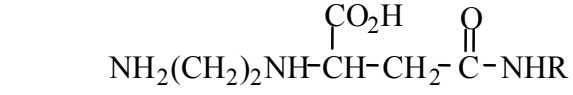

25

($R = C_{10}H_{21}$, $C_{11}H_{23}$, $C_{12}H_{25}$, $C_{13}H_{27}$, $C_{15}H_{31}$, $C_{17}H_{35}$)

Scheme 9.

At a given concentration of the surfactants, the percent inhibition increases with the increase of carbon chain length up to C_{13}. It is reasoned that these compounds (**Scheme 9**) are expected to exert a high retarding effect (due to additive effect of several functional groups) of the corrosion process of the mild steel in HCl.

Many researchers attempted to correlate the inhibition efficiency of organic inhibitors to the electron density of the functional groups.[58-61] It has been suggested[58] that inhibition of corrosion of iron by aliphatic amines is due to chemisorption of the amines on the metal surface. Increase in percent inhibition upto C_{13} is attributed to the increased in the number of electron donating methylene groups.

Some researchers have reported[60,61] that nitrogen containing compounds gave very little inhibition in presence of sulfuric acid and that the presence of halide ions is necessary to obtain good inhibition. High inhibition efficiencies (82%) have been achieved with polymers of macrocyclic inhibitors such as porphyrins and phthalocyanines.[62]

Inhibition of steel corrosion by polyaniline coatings in the presence of sulfuric and phosphoric acids has been found[65] to provide good corrosion protection. The inhibition effects of sodium dodecylbenzenesulfonate and hexamethylenetetramine on the corrosion of mild steel in sulfuric acid solution has been investigated.[66] Concentration regions showing synergistic and antagonistic inhibition behavior was identified.

The mechanism through which the corrosion inhibitors function has been ascribed to adsorption processes on the anodic or cathodic sites or both and for *e.g.,* acetylenic alcohols to subsequent polymerization on the steel surfaces. The essential requirements for a good protective film are

1) polar groups with high affinity to the metal surface.
2) long chain hydrocarbon tails, attached to the polar groups and hydrophobic in character.
3) polymeric compound formed in secondary reaction between the adsorbed inhibitor molecules.

It is difficult to combine the above requirements in a single component. Hence, commercial corrosion inhibitors are usually composed of a number of surface-active compounds. It has been reported that the effective formulations used in the corrosion

inhibition of oil field steel are mixtures of *N*-containing compounds, acetylenic compounds, surfactants, and aldehydes.[67]

Some inhibitors (like cinnamaldehyde and acetylenic alcohols) can be recovered as polymers from the metal surface indicating that the inhibitors may be interrupting a propagating process, which is initiated by H atoms (**Scheme 10**). It is common knowledge that the attack of HCl on iron pipe generates H atoms, which then leads to hydrogen embrittlement.

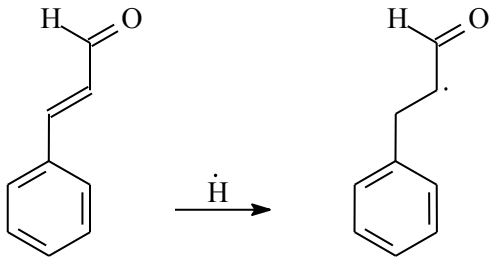

26 **27**

Scheme 10.

Polymeric materials for corrosion control with emphasis on fundamentals of metallic corrosion and factors influencing the corrosion protection performance of polymeric coatings was reviewed by Dickie and Floyd.[68] Numerous polymers have been used to provide coatings and adhesiveness to metals, including alkyd, acrylic, epoxy, polyester and polyurethane resins. These polymers are required to bond well to the metals and to provide good coverage, in order to provide corrosion resistance and adhesiveness to the metals.

A water-soluble acrylic polymeric corrosion inhibitors containing benzotriazole moiety was reported.[69] The polymer, poly(acrylic-co-4- (5-enzotriazole)amidophenyl-acrylate), has the structural formula shown in **Scheme 11**. The polymer was reported to

provide good coverage, good corrosion inhibition and excellent adhesiveness when applied to the surface of oxidizable metals.

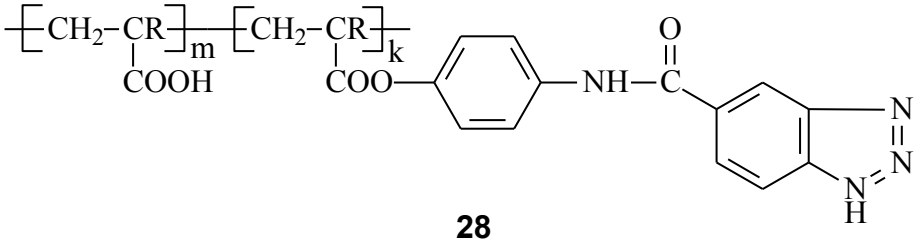

28

Scheme 11

Azole compounds or polybenzimidazoles (PBI) have been used to inhibit corrosion of, and provide adhesiveness to, copper metals, in particular copper lead frames. Azole compounds including benzotriazole (BAT) are advantageously used because they are water-soluble.

Cationic polymers (specifically polyquaternary amines) prepared from reacting mono- or polyamines with polyfunctional organic compounds, *e.g.,* epihalohydrins, organodihalides, and unsaturated dihalides, which are capable of both quaternizing and extending the molecular weight of the amine were patented three decades ago.[70] These polyquaternary amino polymers, having at least about 10% of the polymer units with quaternary amino units, were found useful as corrosion inhibitors for highly acid systems such as pickling inhibitors for ferrous metals and corrosion inhibitors in acidizing media employed in deep well petroleum and gas recovery.

Synthesis of a nitro-substituted polymeric compound that was found useful as a combined corrosion inhibitor and metal surface modification, particularly aluminum flake pigment surface modification has been reported.[71] The polymeric compound includes a pigment interactive nitro-containing substituent, a hydrophobic substituent, and a terminal hydrophilic substituent.

New classes of polymeric corrosion inhibiting compositions incorporating pendant heterocyclic groups (**Scheme 12**) which are surprisingly effective copper corrosion inhibitors were disclosed.[72] The polymers form a protective barrier on metallic components to aqueous systems and remain substantive on metallic surfaces over a wide pH range. Moreover, the polymers are resistant to oxidizing biocides, and are substantially impervious to repeated or prolonged exposure to corrosive agents.

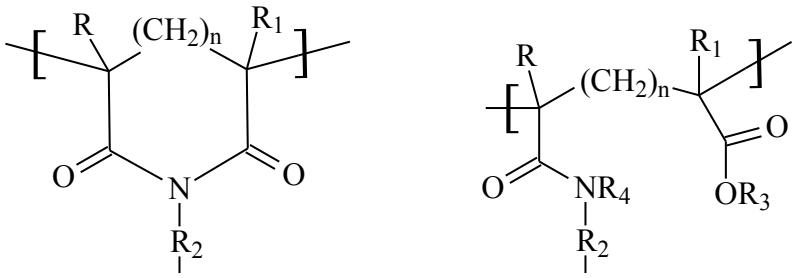

29 **30**

Scheme 12.

A composition for preventing or retarding the formation of gas hydrates during the transport of a fluid comprising water and a hydrocarbon through a conduit was reported.[73] The composition is a copolymer of vinyl caprolactam and vinyl pyridine (3-25%), and terpolymers thereof, with vinyl pyrrolidone. The polymers also may be quaternized, suitably with about a C_{1-18} alkyl halide; *e.g.,* an alkyl iodide. These polymeric corrosion inhibitors find special utility in the prevention of corrosion of pipe or equipment which is on contact with a corrosive oil-containing medium. The polymers exhibit advantageous dual corrosion and gas hydrate inhibitory characteristics.

The combinations of an unsaturated (a vinyl or acrylic monomers) and a peroxy compound, particularly methacrylonitrile-$K_2S_2O_8$ system, in aqueous acids was reported

to act as film-forming inhibitors of the acid corrosion of mild steel corrosion.[74] A modified poly(methacrylonitrile) film (**Scheme 13**) is formed on the metal surface which slows down both the anodic and cathodic partial reactions with the inhibiting efficiencies being near 99%. Inhibition was observed to occur over a wide range of pH and concentrations of the unsaturated compound. A drawback, however, is that methacrylonitrile is toxic.

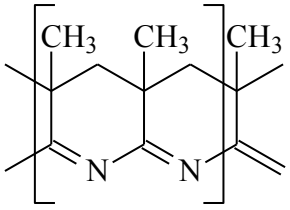

31

Scheme 13.

A few nitrones [$ArCH=N^{+}(O^{-})Ar$] have been synthesized and investigated[75] for evaluating their efficiency as inhibitors for the corrosion of mild steel in 1 M HCl. Substituted nitrones have been well known since the turn of the century.[2,6] Many methods of preparation have been described in the literature.[2,6] The condensation of aldehydes with phenylhydroxylamines[76,77] gives the corresponding nitrones in relatively high yields. The nitrone function is a typical 1,3-dipole which reacts with CC-double and CC-triple bond systems to form five-membered rings.[2,6]

A variety of isoxazolidines (**Scheme 14**) have been synthesized by nitrone cycloaddition reaction and tested[14] for the inhibition action on the corrosion of mild steel for the first time in 1 M HCl using gravimetric and polarization techniques. These isoxazolidines have polar head and nonpolar tail. The inhibition efficiency depends on the length of the hydrophobic alkyl chain R because a compound with larger nonpolar tail

will cover the surface with fewer molecules compared with one with a smaller tail. These new inhibitors exhibited excellent inhibition efficiency.

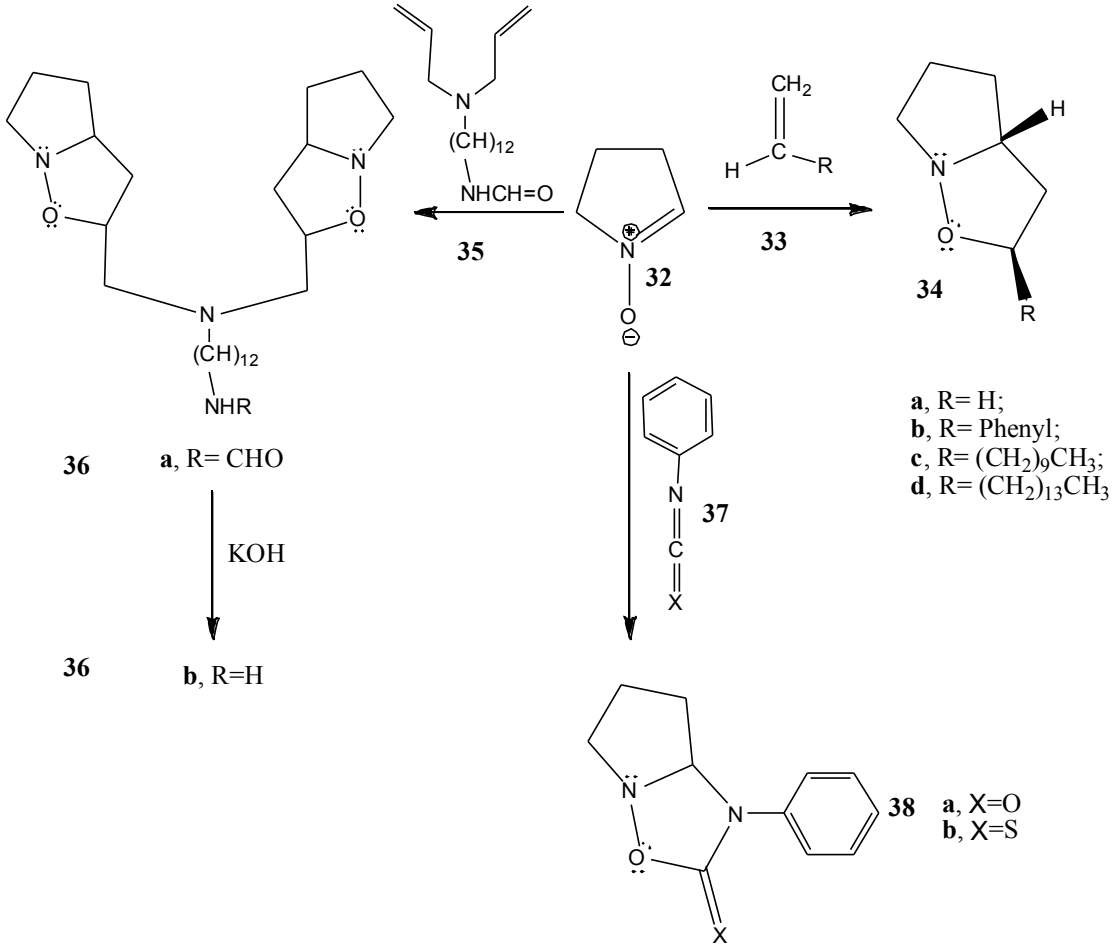

Scheme 14.

S.A. Ali *et al*. synthesized several new isoxazolidines[15] using cycloaddition reactions of different alkenes with various nitrones (**Scheme 15**). These new cycloadducts with different degree of steric crowding and hydrophobic chain length were tested for corrosion inhibitions of mild steel in 1 M and 5 M HCl by gravimetric and electrochemical methods. It was found that the isoxazolidines with long hydrophobic tails

and having the most crowded environment around the nitrogen center are excellent inhibitors.

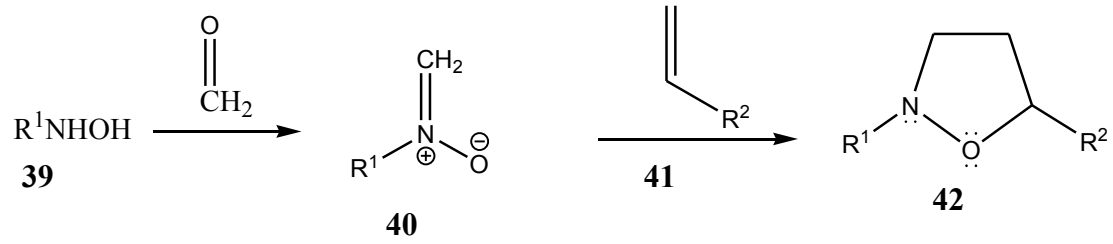

a, $R^1 = CH_3$
b, $R^1 = CH(CH_3)_2$
c, $R^1 = C(CH_3)_3$

a, $R^1 = CH_3$; $R^2 = (CH_2)_5CH_3$
b, $R^1 = CH_3$; $R^2 = (CH_2)_{11}CH_3$
c, $R^1 = CH(CH_3)_2$; $R^2 = (CH_2)_{11}CH_3$
d, $R^1 = C(CH_3)_3$; $R^2 = (CH_2)_{11}CH_3$

Scheme 15.

A. Yildirim and M. Cetin synthesized various derivatives of isoxazolidine. These different kinds of isoxazolidine are obtained by normal 1,3-dipolar cycloaddition reactions of three different long chain alkenes containing **O** or **S** as hetero atoms and **C**,**N**-diphenyl nitrone in toluene for long time (**Scheme 16**).[16] Corrosion inhibition efficiencies (IE%) for synthesized compounds were tested in 2 M HCl for 20 hours at room temperature and gave very good result.

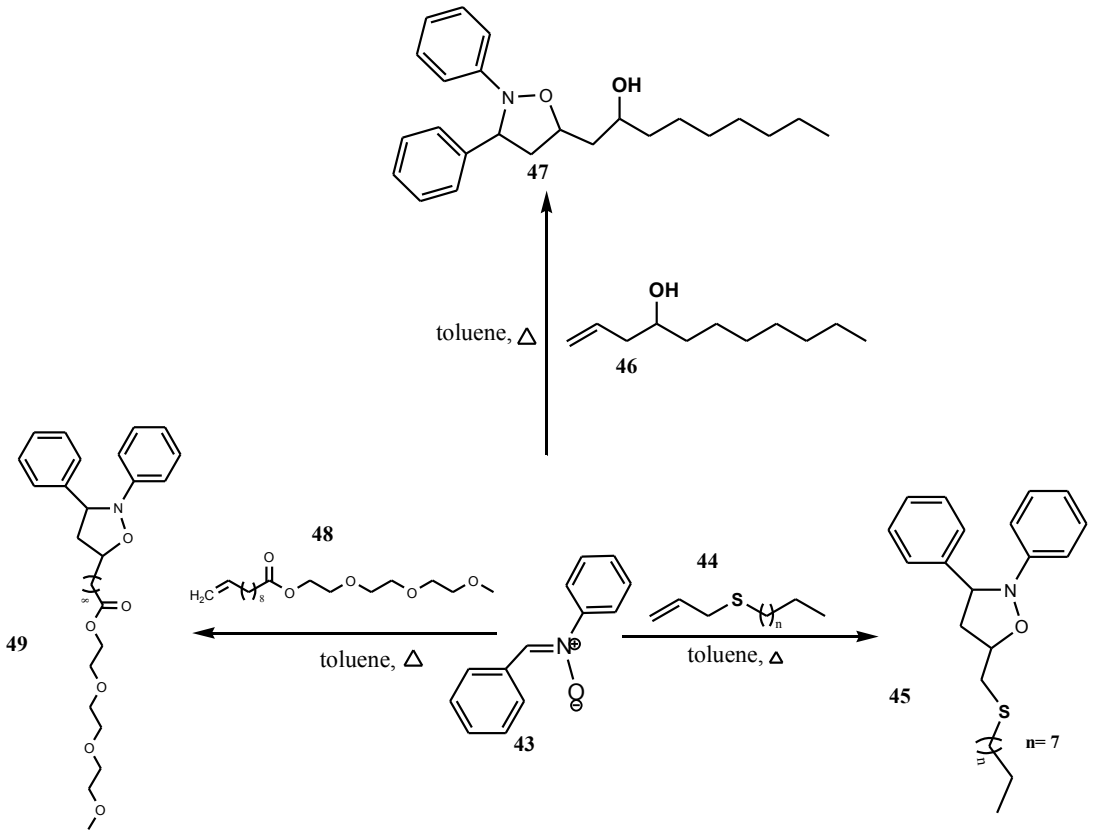

Scheme 16.

Polymerization by 1,3-dipolar cycloaddition reactions of α ,α'-(*p*-phenylene) bis(*N*-phenylnitrone) **50** with diolefins *m*-phenylenebismaleimide **51** which gave a polymer **52** that did not melt at 300^{o} was reported by Iwakura *et. al.* (**Scheme 17**).[78]

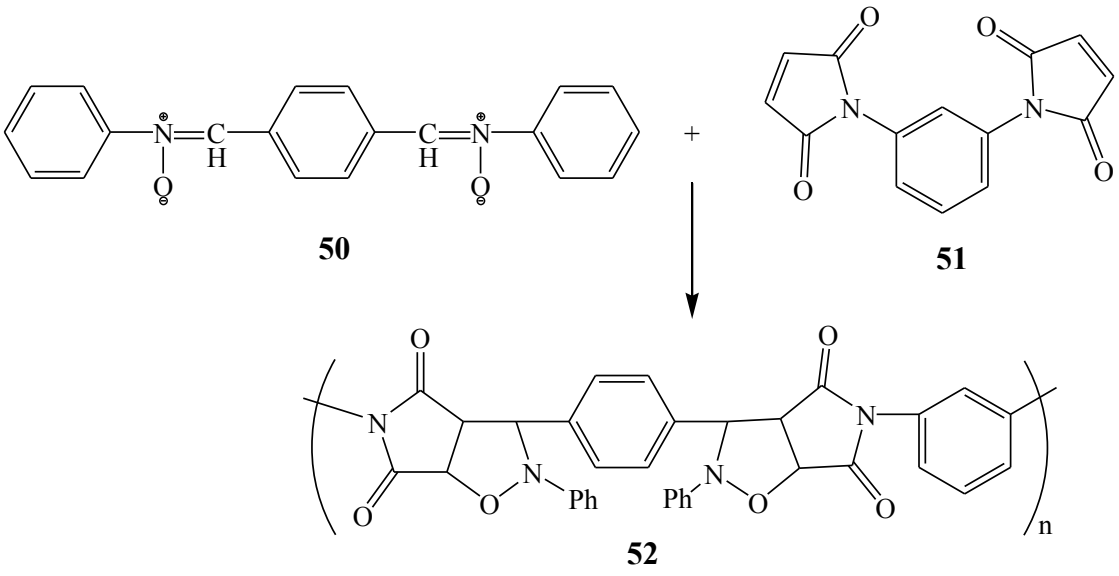

Scheme 17.

Recently, the synthesis of various high molecular weight polymers bearing isoxazolidine ring has been reported by Ritter *et. al.*[7] Namely, polymer **55** was prepared via 1,3-dipolar polycycloaddition of *N,N*'-dimethyl-*p*-phenylenedinitrone **(53)** with *N,N*'-(1,4-phenylene)dimaleimide **(54)** (**Scheme 18**).

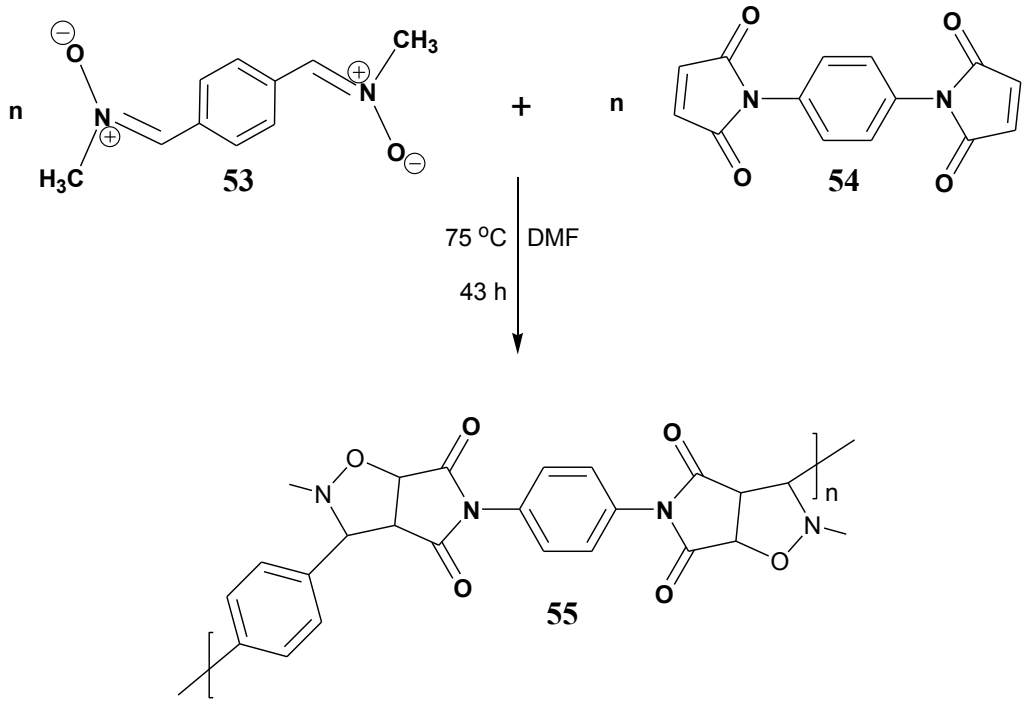

Scheme 18.

To reduce steric hindrance in the main chain, some bis(nitrone)s with flexible aliphatic spacer between two *N*-methylnitrone functions were utilized for next polycycloaddition (**Scheme 19**). Completely mechanically stable transparent coatings were obtained even directly from the reaction mixture of this synthesis.

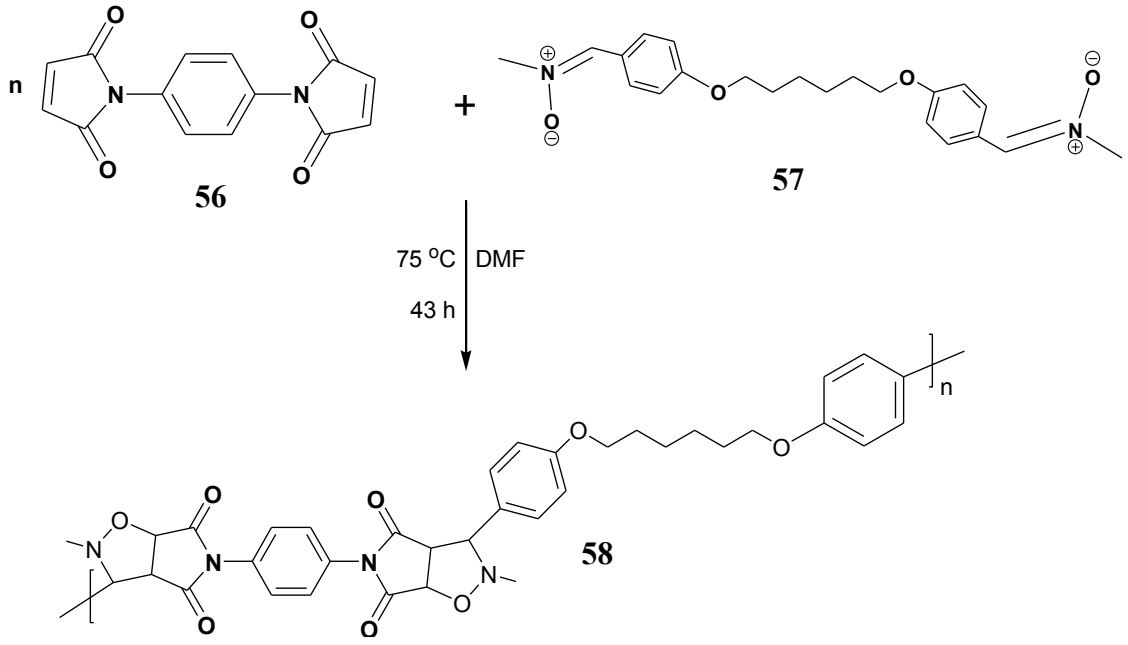

Scheme 19.

(A_2 + N_2) cycloaddition polymerization has been employed to synthesize various linear poly(isoxazolidine)s by Wayne Hayes *et. al*. **(Scheme 20)**.[12] Bisnitrone **53** was copolymerized with monomers featuring electron deficient maleimide (**59** and **60**) and acrylic moieties (**63- 65**). The polymerization was made under high pressure (4.5 kbar, 40 ^{o}C, DMF) over a period of 6 days to give mainly *endo*-cycloadducts as determined by ^{1}H NMR. The poly(isoxazolidine)s obtained *via* this strategy possessed molecular weights ($\mathbf{M}_w$) up to 30.4 kDa as decided by GPC.

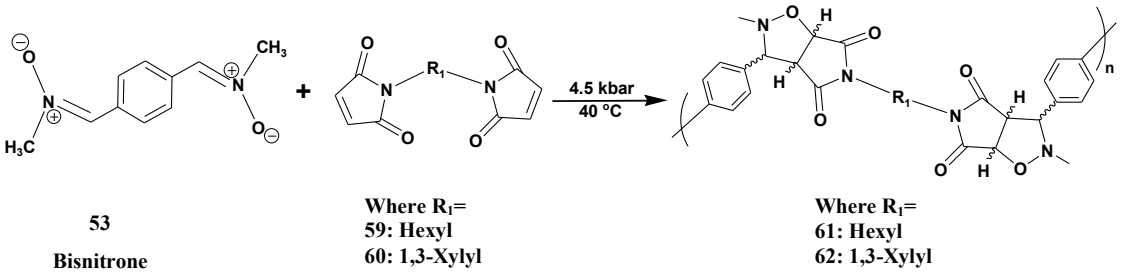

53
Bisnitrone

Where R_1=
59: Hexyl
60: 1,3-Xylyl

Where R_1=
61: Hexyl
62: 1,3-Xylyl

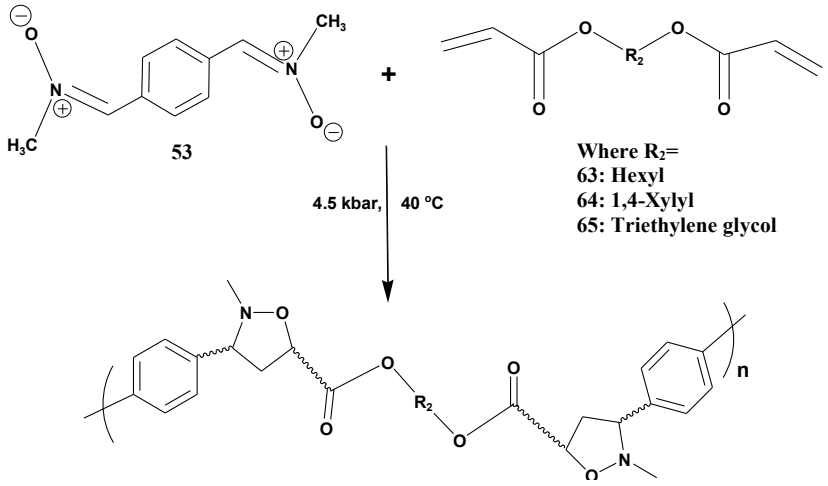

53

Where R_2=
63: Hexyl
64: 1,4-Xylyl
65: Triethylene glycol

Where R_2=
66: Hexyl
67: 1,4-Xylyl
68: Triethylene glycol

Scheme 20.

Homopolymerization of 4-(methacryloyloxy)benzaldehyde-phenylnitrone **(69)** using AIBN as free radical initiator failed as reported by Helmut Ritter and Michael Heinenberg (**Scheme 21**).[79] Also, copolymerization of **69** with methyl methacrylate (MMA) did not give expected polymethacrylate. FD-mass-spectra signals reveals that there are oligomers as the nitrone groups tend to undergo 1,3-dipolar cycloadditions with unsaturated groups.

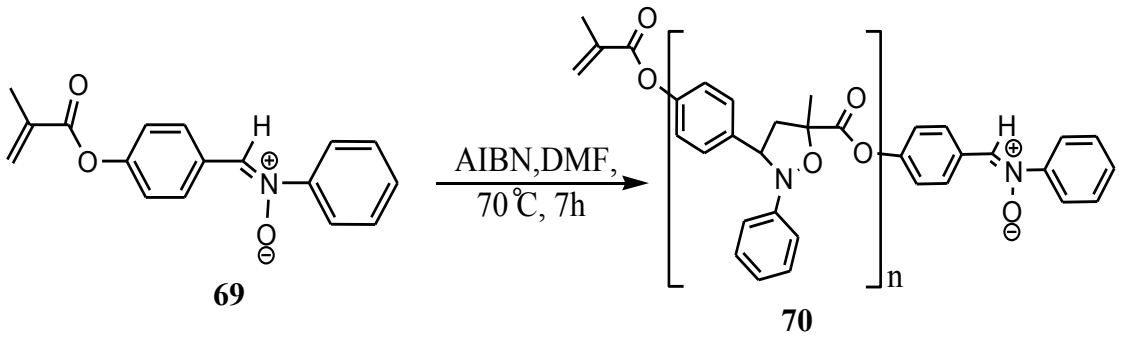

69 **70**

Scheme 21.

For a successful preparation of polymers containing nitrone groups in the side chain, it was intended to synthesize polymers with free aldehyde functions which can be converted to nitrones in the final step by reacting the polyaldehydes with phenylhydroxylamine. The monomers that contain aldehydes can be copolymerized with MMA radically at 70 ^{o}C using AIBN (**Scheme 22**). The new polymers are photosensitive materials since they include nitrone moieties.

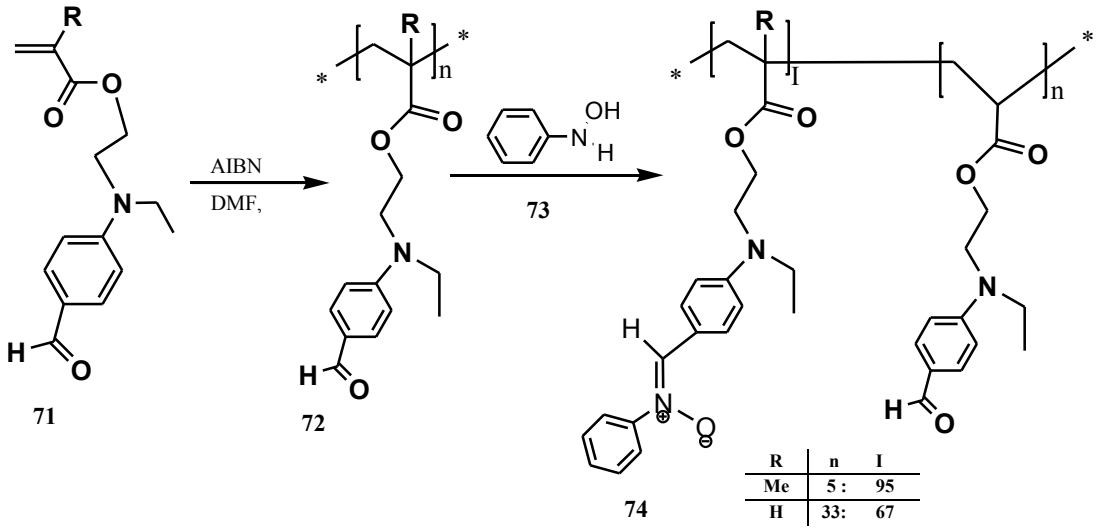

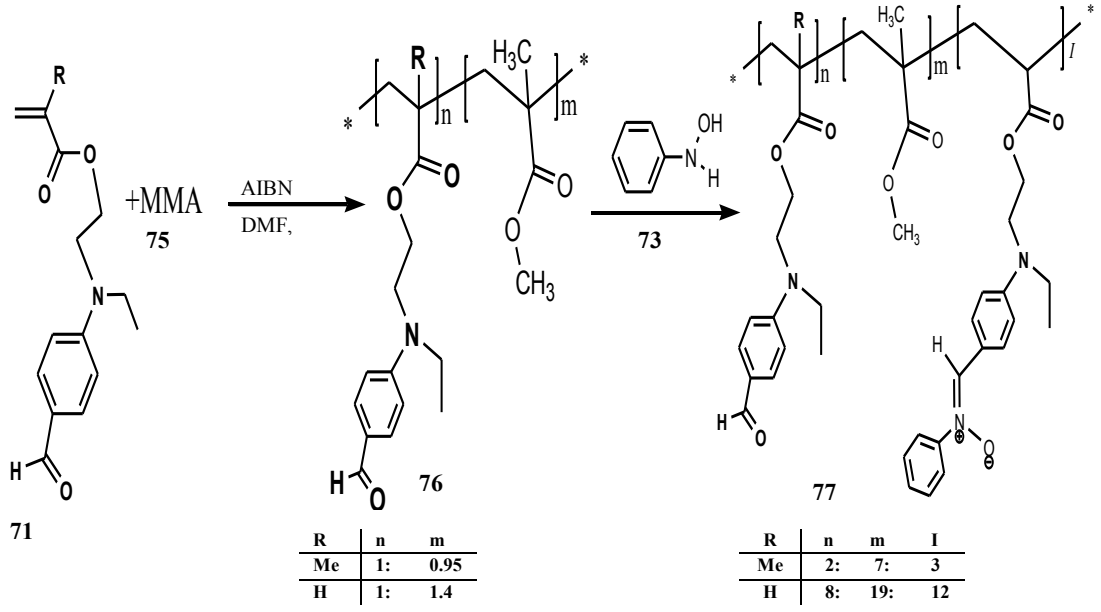

Scheme 22.

Various vinylbenzaldehydes were polymerized using AIBN as initiator at 70 °C for 24 h to yield the corresponding homopolymers as reported by Helmut Ritter *et. al.*[18]

Polymeric nitrones were produced by converting the free aldehydes groups to nitrones when the aldehydes functions react with excess of N-isopropylhydroxylamine (**Scheme 23**). Nitrones which are photosensitive moieties were irradiated and examined for the change in the refractive indices for all polymers.

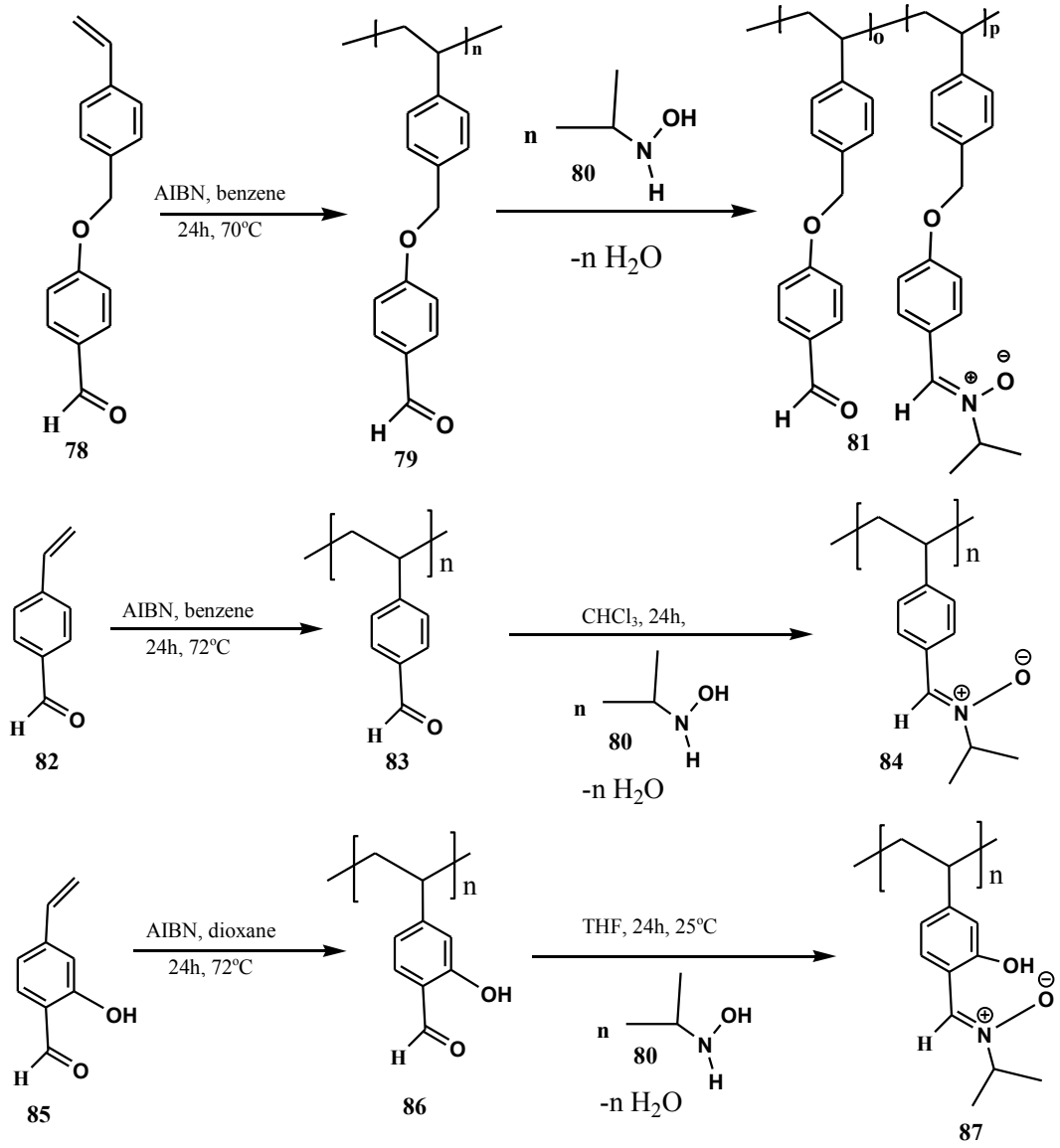

Scheme 23.

Kenta Tanaka *et. al.*[80] successfully produced poly(methyl methacrylate) (PMMA) containing a diarylnitrone derivative as side group by radical copolymerization (**Scheme 24**). Demonstrating steric hindrance, the two methyl groups introduced into the ortho positions on the *N*-arylbenzene ring almost completely suppressed the 1,3-dipolar cycloaddition of MMA to the nitrone moiety. This copolymer was synthesized in order to study refractive index which may be controlled by irradiation because the polymer has the photoreactive nitrone group.

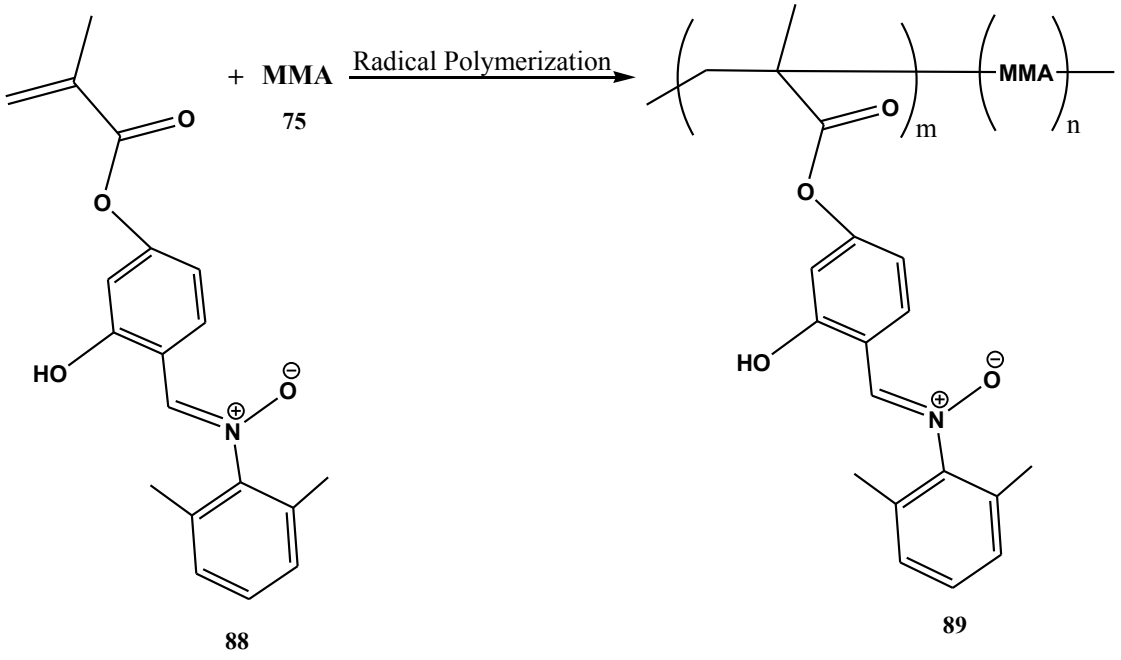

Scheme 24.

Chapter 3

THE OBJECTIVES AND THE WORK PLAN OF THE STUDY

3.1 General Objectives

From basic research point of view, the objective of this work is to study various aspects of alkene-nitrone polycycloaddition reactions involving A-N-type and N-N and A-A-type monomers (A denotes alkene; N denotes nitrone). Polymerization kinetics would indeed be of help in judiciously controlling the length of the polymer chain. The effects of spacer alkyl chain and molecular weight on solubility in aqueous media, and on the coverage of metal surface would be of great interest in corrosion inhibition study.

From applied research point of view, the objective is to study the efficiencies of the new polyisoxazolidines in corrosion inhibition of mild steel in corrosive environments. To the best of our knowledge, the use of polyisoxazolidines in corrosion inhibition study has so far not been reported. The synthetic utility of nitrone cycloaddition reactions in most cases deals with construction of low molecular weight five-membered heterocyclic ring systems. To the best of our knowledge, only minor pieces of information are available about the application of nitrone cycloaddition reactions to prepare linear polyisoxazolidines. The corrosion inhibition study involving polyisoxazolidines has not been reported so far.

Following are the specific objectives of the study:

1. Synthesis of specialty alkene-N-hydroxylamines, alkene-nitrones, dialkene and dinitrones **(Scheme 25 and Scheme 26**).

2. Exploring kinetics of polymerization of alkene-nitrones to polyisoxazolidines (**Scheme 27**).

3. End-capping for some of the living polymers (**Scheme 33)**.
4. Characterization of the synthesized compounds/polymers using various spectroscopic techniques.

5. Measurements of corrosion inhibition efficiency of the synthesized polyisoxazolidines (in various concentrations) in acidic solutions (1M HCl and 1N H_2SO_4).

3.2 Characterization Techniques

IR, ^{1}H, ^{13}C NMR spectroscopy will be used to characterize the various synthesized monomers as well as the polymers. The average molecular weight of the polymers will be determined by end-group analysis using NMR spectroscopy.

3.3 Corrosion Testing of the Polyisoxazolidines

The newly developed corrosion inhibitors are organic in nature and are tailored to provide protection to mild steel in corrosive acidic environment. Corrosion tests are comprised of gravimetric measurements and potentiodynamic polarization curves.

3.3.1 Gravimetric Measurements

Corrosion inhibition tests in acid solution are performed using coupons measuring about 2.5 x 1.5 x 0.1 cm^3 prepared from mild steel of known elemental composition. A solution of 1 M HCl is prepared from concentrated HCl using deionized water. The mild steel coupons are polished with emery papers, then degreased with acetone and washed with deionized water. The coupons are dried and kept in a dessicator. Inhibitor efficiency are determined at 60 ºC for 6 h by hanging the coupon into the acid solution (150 cm^3) (in open air) containing various amount (0 (blank), 50, 100, 200, 400 ppm) of the synthesized inhibitors. After the elapsed time, the cleaning procedure is consisted of wiping the coupons with a paper tissue, polishing lightly with emery paper, washing with distilled water, acetone followed by oven drying at 110ºC. Percent inhibition (%IE) will be determined using the following equation:

$$\%IE = \frac{\text{Weight loss (blank) - weight loss (inhibitor)}}{\text{Weight loss (blank)}}$$

Weight loss (blank) and weight loss (inhibitor) represent weight loss in absence and presence of inhibitor, respectively.

3.3.2 Electrochemical Measurements: Tafel Extrapolation Method

For potentiodynamic polarization studies, mild steel coupons embedded in araldite (affixing material) with an exposed area of 2.0 cm^2 are used, and experiments are carried out in 100 cm^3 of solution containing 0 and 200 ppm inhibitors at 60ºC until a steady-state open circuit potential is obtained. The electrochemical cell is assembled in a 250 ml round-bottomed flask consisting of mild steel working electrode; the graphite electrode of approximately 5 mm diameter works as a counter electrode, and a saturated calomel electrode (SCE) is used as a reference electrode. All three electrodes are connected to a potentiostat (Model 283, EG&G PARC) through an electrometer. Potential range of ±250mV with respect to open circuit potential and a scan rate of 1.6 mV/s are applied.

The Tafel plots of each tested inhibitor in 1 M HCl solution and of 1 M HCl (blank) are plotted. Each pair of Tafel plots is analyzed to obtain corrosion current density and corrosion potential. The corrosion rate is determined in mills per year (mpy) using:

$$CR = 0.129\frac{a * i}{n * D}$$

where,

CR = corrosion rate in mpy

a = atomic weight of the metal

n = number of electrons in the reduction of the metal ions.

D = density of the metal in g/cm^3.

i = corrosion current density $\mu A/cm^2$.

Finally, the corrosion inhibition efficiencies of each solution are determined by:

$$\text{Corrosion Inhibition Effeciency} = \frac{CR_{blank} - CR_{inhibitor}}{CR_{blank}}$$

CHAPTER 4

RESULTS AND DISCUSSION

4.1 Synthesis of Monomers

11-Bromo-1-undecene **(90)** upon treatment with excess hydroxylamine hydrochloride in the presence of NaOH afforded *N*-(10-undecenyl) hydroxylamine **(91)** in moderate yield (**Scheme 25**). The hydroxylamine when reacted with formaldehyde (**92a**) or ethanal (**92b**) afforded the corresponding new nitrones **93a** and **93b**, respectively. ^{1}H and ^{13}C NMR spectra confirmed the structure of the nitrones. The signals at δ 6.31 (1H, d, *J* 7.7 Hz) and 6.49 (1H, d, *J* 7.7 Hz) ppm were assigned to the methylene protons of carbon terminal of the nitrone functionality in **93a**, while the alkene protons appeared at δ 4.91 (2H) and 5.77 (1H) ppm. For the alkene-nitrone **93b**, proton attached to the nitrone moiety was displayed at δ 6.75 (1H, q, *J* 5.8 Hz) ppm. As expected, the carbon of the nitrone functionality and alkene moieties appeared at 138.90 and (113.94, 134.11) ppm, respectively. The strong IR absorptions at 1606 and 1183 indicated the presence of nitrone moiety.[81]

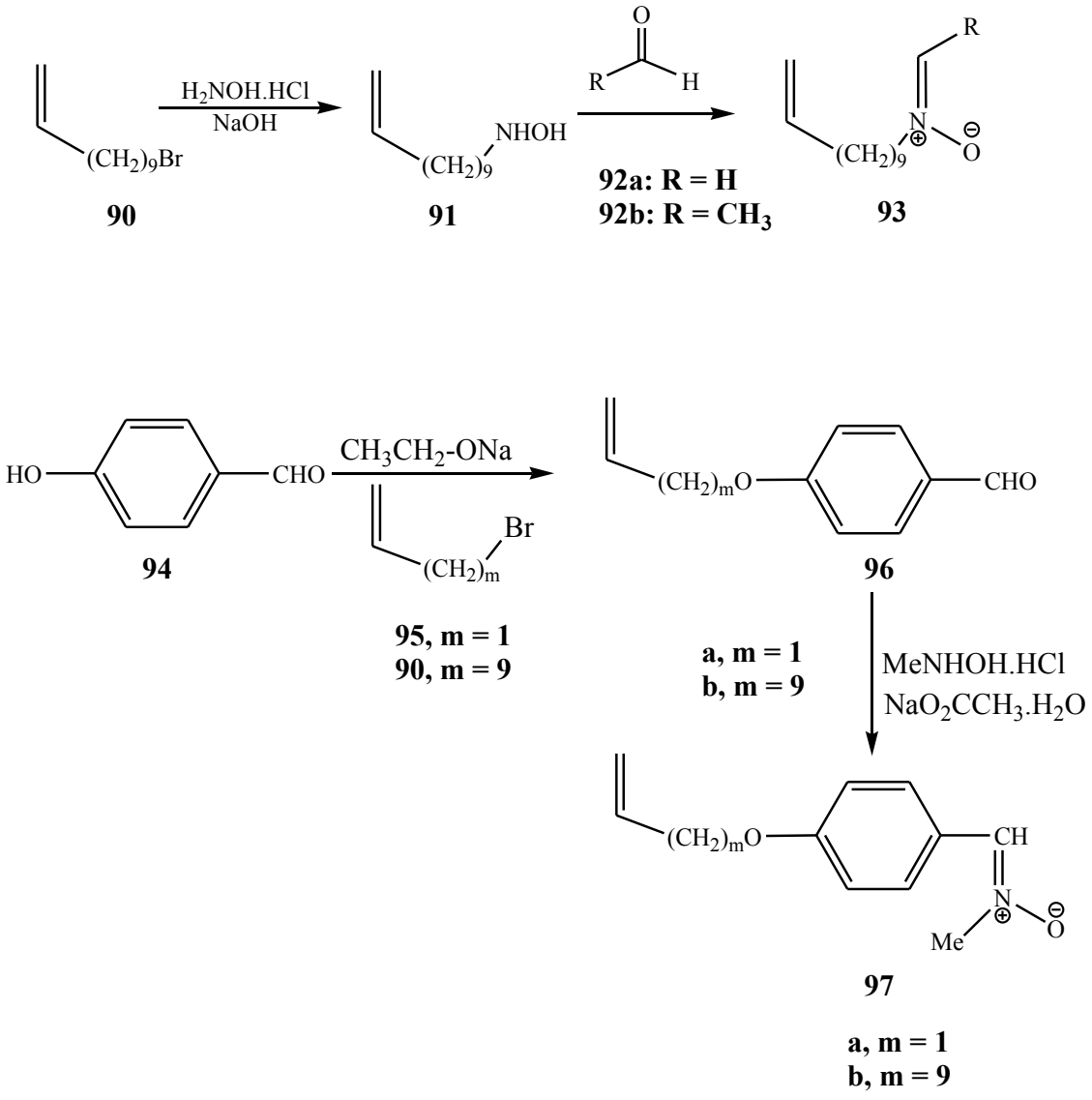

90 **91** **92a: R = H** **92b: R = CH_3** **93**

94 **95, m = 1** **90, m = 9** **96** **a, m = 1** **b, m = 9** **97** **a, m = 1** **b, m = 9**

Scheme 25

Another type of alkene-nitrones **97** was prepared for the first time using procedure as outlined in Scheme 25. Thus, inexpensive starting material *p*-hydroxybenzaldehyde (**94**), on treatment with ethoxide followed by allyl bromide (**95**) or 11-bromo-1-undecene (**90**), gave the alkenyloxybenzaldehydes **96a** and **96b**, respectively, in excellent yields.

The alkene-aldehydes **96a** and **96b**, on condensation with N-methylhydroxylamine, afforded the alkene-nitrone **97a** and **97b**, respectively (**Scheme 25**).

p-Dihydroxybenzene (**98)** was diallylated to give the diallyloxybenzene **(99)**. The dialdehyde compounds **100** and **102** were converted to the dinitrones **101** and **103** respectively, by reacting with N-methylhydroxylamine (**Scheme 26**).

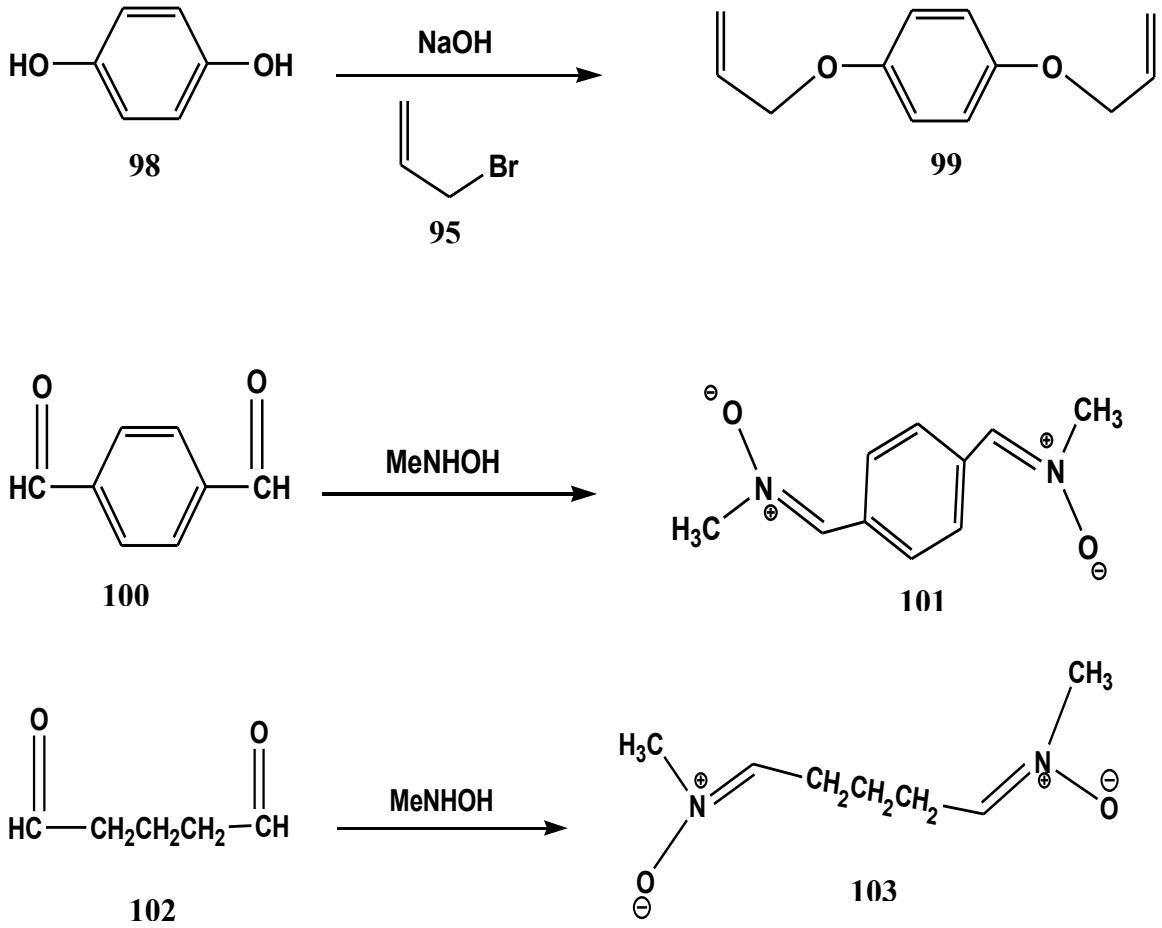
HO
OH
NaOH
Br
98
95
99
O
HC
CH
MeNHOH
100
101
CH3
N
H3C
CH2CH2CH2
102
103

Scheme 26.

4.2 Polymerization of the alkene-nitrones

4.2.1 Polymerization of the alkene-nitrone 93a

4.2.1.1 Synthesis of polyisoxazolidines and kinetics of polymerization reactions

The nitrone **93a** was allowed to undergo polymerization to **104a** at 65°C in $CDCl_3$ **(Scheme 27)**, and ^1H NMR spectra were recorded at several intervals **(Fig. 4)** to get the rate constant for the second order kinetics

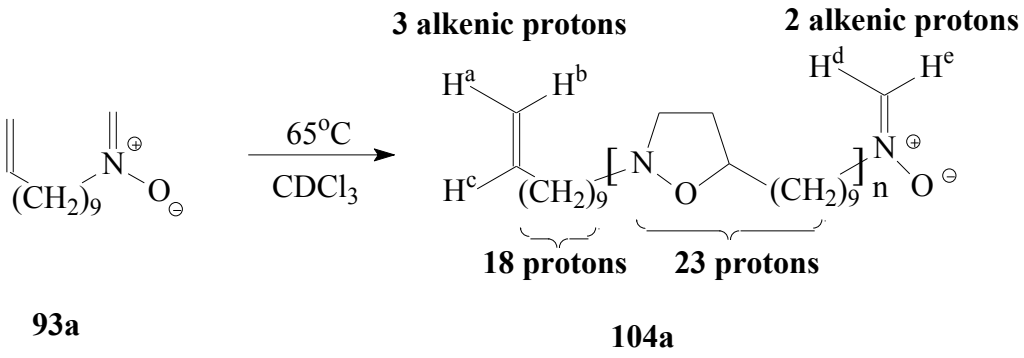

Scheme 27.

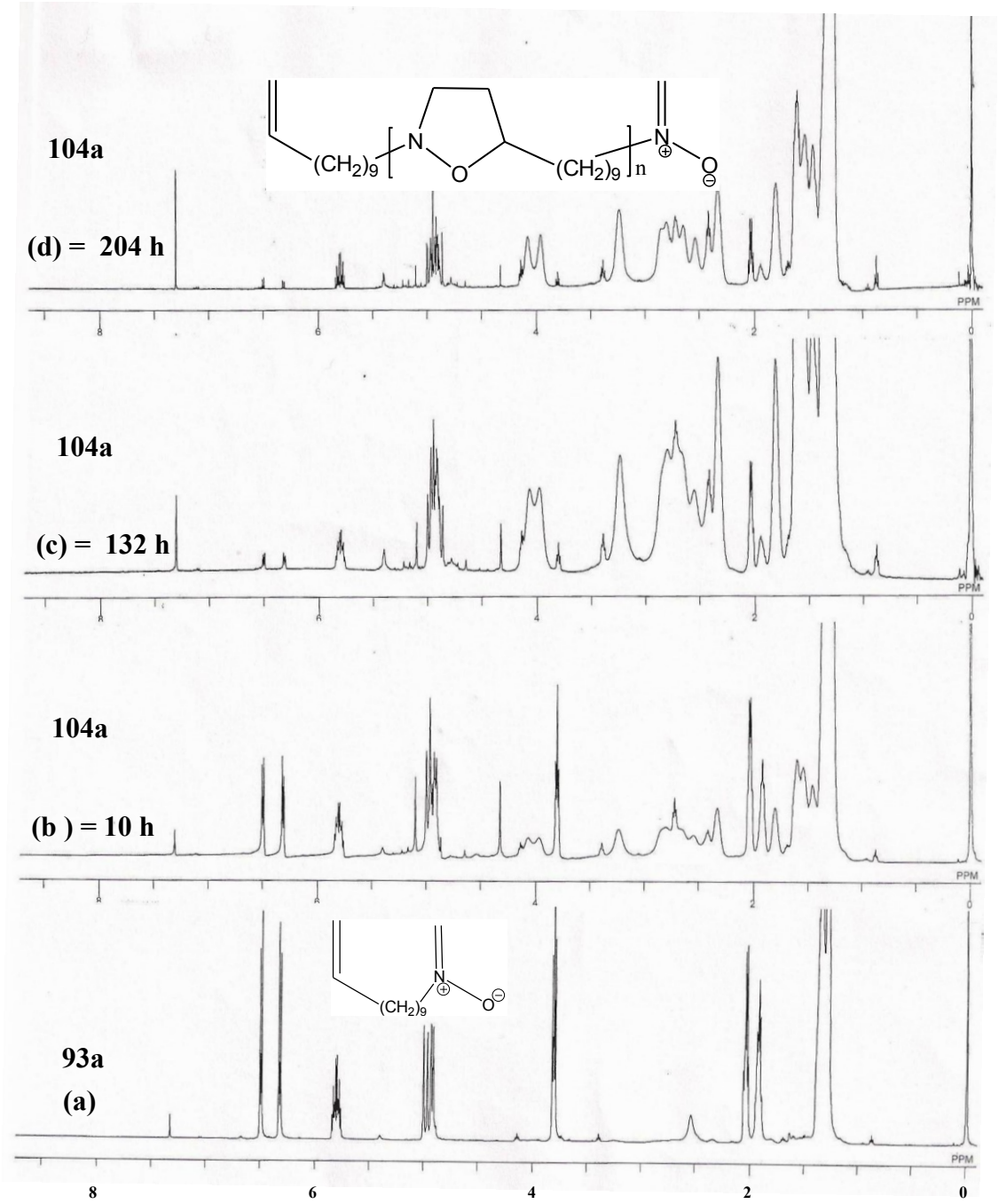

Figure 4: ^{1}H NMR Spectra of (a) alkene-nitrone **93a** and **104a** oligomer at (b) 10 hours, (c) 132 hours and (d) 204 hours, respectively.

4.2.1.2 Determination of degree of polymerization:

The end groups of the polyisoxazolidine **104a** have a total of 5 alkenic and 18 aliphatic protons. The NMR signals for the end group aliphatic protons (18) and the 23 protons of the repeating unit in the polymer, all appear below δ 4.2 ppm. However, area (A) under the alkenic proton H_c at δ 5.77 ppm permitted us to calculate the area of the 18 end group aliphatic protons as (A×18). So, the 23 protons of the repeating unit in the polymer will account for an area of [T – (A×18)], where T is the total area of signals appear below δ 4.2 ppm. Therefore, area of a single proton belonging to the repeating unit equals [T – (A×18)]/23. Thus, the value of 'n' and the degree of polymerization (DP) could then be equated to:

$$n = \frac{\text{Area of a single proton of the repeating unit}}{\text{Area of an alkene end group proton } H_c} = \frac{[T-(A\times 18)]/23}{A}$$

and the degree of polymerization (DP) would then equal 'n +1'.

$$DP = n + 1$$

The results of the polymerization of a 0.467 M solution of nitrone-alkene **93a** in $CDCl_3$ at 65°C are given in Table 1. The second order rate of the polymerization reaction yields the following equations:

$$\frac{-d[\text{alkene}]}{dt} = k[\text{alkene}]^2$$

Integration of the above equation yields:

$$\frac{1}{[M]} - \frac{1}{[M]_o} = kt$$

Since, $[M] = [M]_o - [M]_o p = [M]_o(1-p)$

$$\frac{1}{[M]_o(1-p)} - \frac{1}{[M]_o} = kt$$

$$\frac{1}{1-p} - 1 = M_o kt$$

$$DP - 1 = [M]_o kt$$

$$DP = [M]_o kt + 1$$

Where $[M]_o$ and [M] are the concentration at the initial and at various times, 'p' is the fraction of alkene functionality reacted and 1/(1-p) denotes the DP. The DP versus t plot is given in Figure 5 which indicates a straight line plot at the lower t values, but the plot takes a downward trend at higher times. This happens presumably as a result of degradation of the nitrone functionality prior to the occurrence of the desired 1,3-dipolar cycloaddition.[5] As evident from the Table 1, the ratio of the alkene/nitrone functionality increases with time while they remain close to 1 at lower range of times. So, the DP versus t plot at lower range of times is given in Figure 6 which gave a straight line plot and resulted in the rate constant (k) value of 6.34×10^{-5} L mol^{-1} s^{-1}. The polymer, rather the oligomer, **104a** has a DP of 12 at the end of 204 hours of polymerization.

Table 1: The results of the polymerization of nitrone-alkene **93a** in $CDCl_3$ at 65°C.

Time (h)	n	DP (i.e. n+1)	Ratio of H_c/H_d
1	0.25	1.25	1.00
2	0.32	1.32	1.11
3	0.49	1.49	1.25
4	0.59	1.59	1.27
5	0.67	1.67	1.30
6	0.77	1.77	1.35
10	1.33	2.33	1.50
14	1.65	2.65	1.76
19	2.46	3.46	1.98
33	3.21	4.21	2.30
40	4.04	5.04	3.09
62	5.21	6.21	3.10
132	8.88	9.88	5.21
204	11.0	12.0	11.9

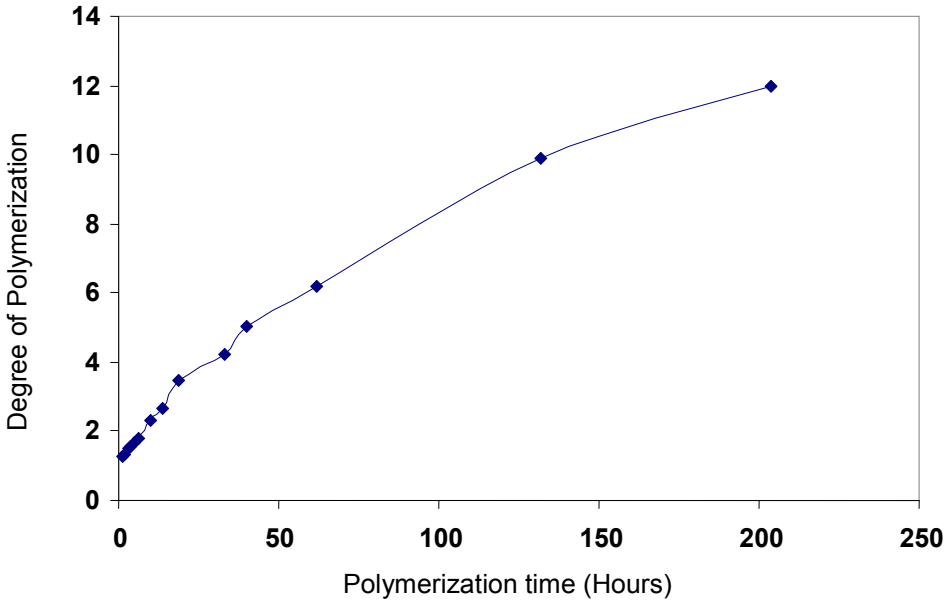

Figure 5: Degree of polymerization versus time of the polymerization of alkene-nitrone (**93a)** in $CDCl_3$ at 65 ^{o}C.

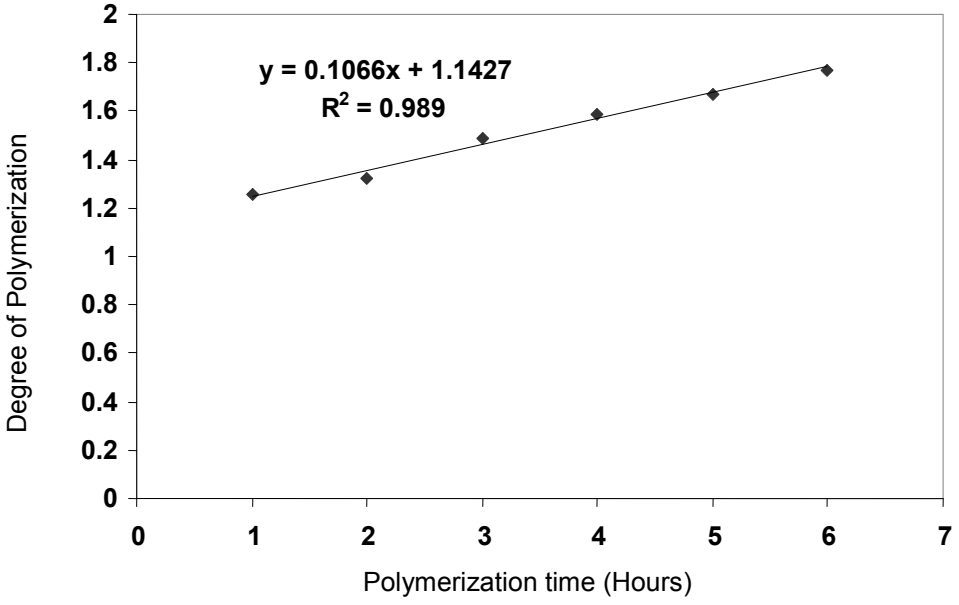

Figure 5: Degree of polymerization versus time of the polymerization of alkene-nitrone (**93a)** in $CDCl_3$ at 65 ^oC at lower range of times.

The polymerization reaction was also carried out in toluene at 80°C, and ^{1}H NMR spectra were recorded at several intervals. There were no ^{1}H NMR signals for the nitrone functionality, whereas the excess alkene protons remained as can be seen in Figure 7. The spectra remained unchanged after 24 h or 48 h of heating. The DP of ~5 remained unchanged. This happens, as discussed earlier, as a result of degradation of the nitrone functionality prior to the occurrence of the desired 1,3-dipolar cycloaddition.[5] This sample was used for the corrosion inhibition tests.

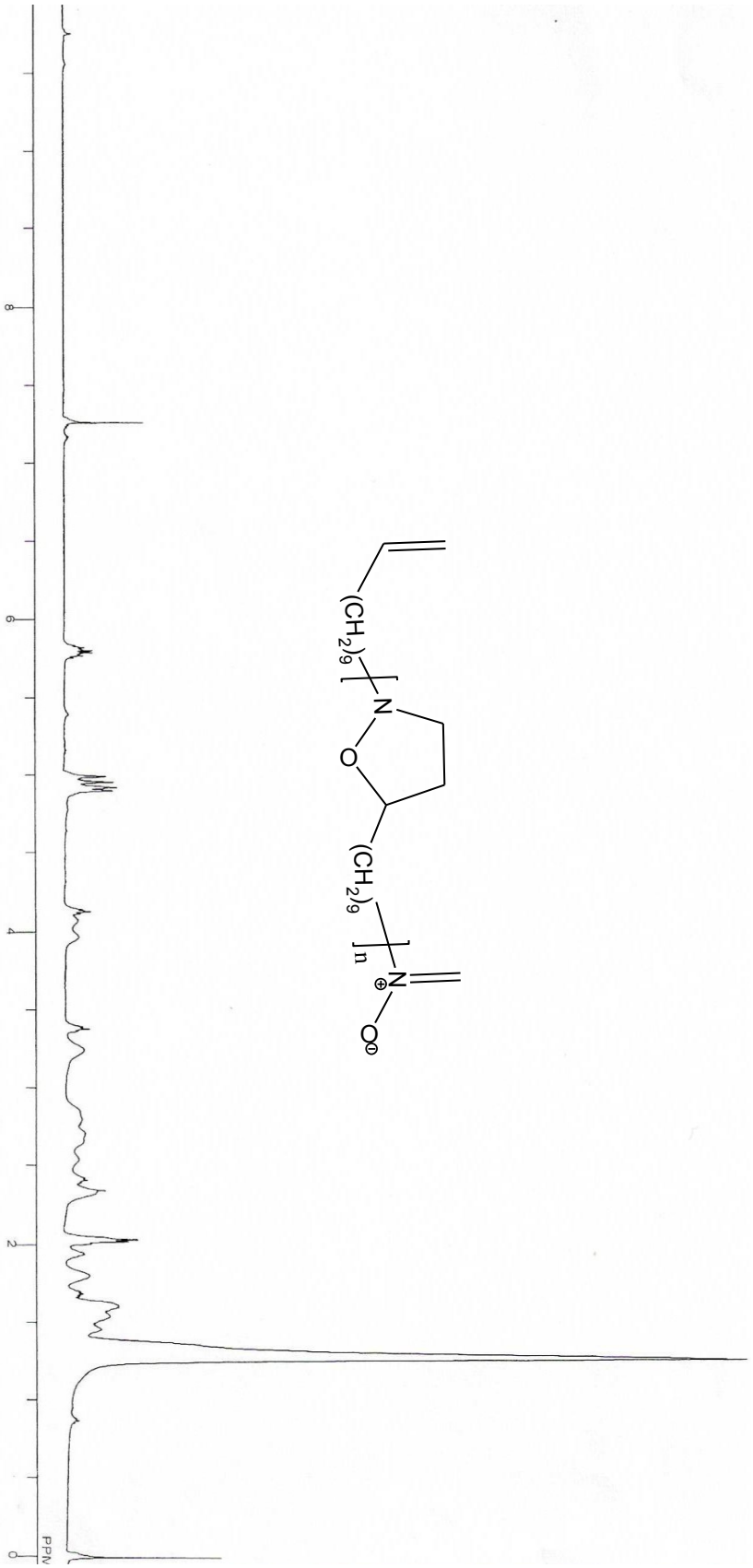

Figure 7: ^{1}H NMR Spectrum of polymerization of **93a** in toluene for 48 hours at 80 °C.

4.2.2 Polymerization of the alkene-nitrone 93b

The alkene-nitrone **93b** was allowed to undergo polymerization at 65°C in $CDCl_3$ **(Scheme 28)**, and ^1H NMR spectra were recorded at several intervals to get the rate constant for the second order kinetics.

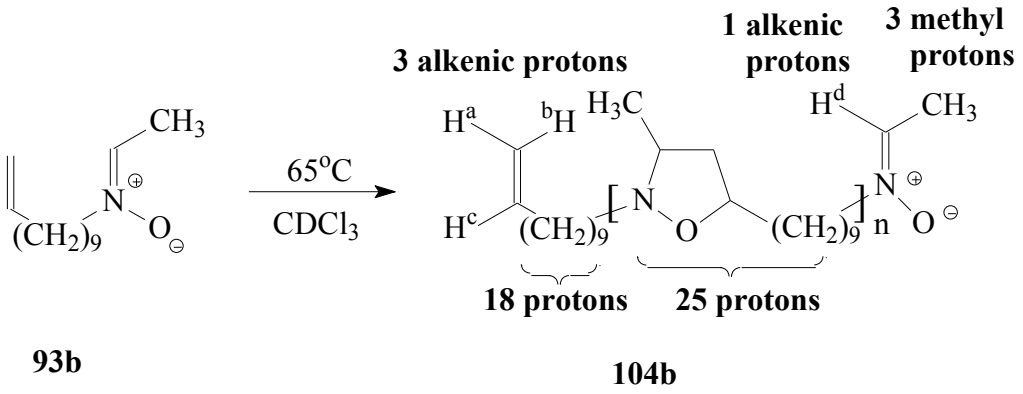

Scheme 28.

The polymerization of alkene-nitrone **93b** was found to be very slow at 80 or 90°C in toluene-d_8. Extensive decomposition of the nitrone functionality happened before the cycloaddition reaction could happen. A solution of the nitrone **93b** (0.437 mmol) in toluene-d_8 (1 cm^3) was thermolyzed in a NMR tube at 100°C. The ^1H NMR spectra of the nitrone **93b** at zero time and that of the reaction mixture after 80 h of thermolysis at 100°C are given in Figure 8. The NMR spectra remained similar after 30, 50 or 80 h of thermolysis. The polymerization equations used for the polymerization of nitrone **93a** (vide supra) are modified for **93b** for which the end groups have a total of 4 alkeneic and 21 (i.e. $(CH_2)_9$ and N-Me) aliphatic protons and the repeating unit has 25 protons. Now the modified equations are:

$$n = \frac{\text{Area of a single proton of the repeating unit}}{\text{Area of an alkene end group proton } H_c} = \frac{[T-(A\times 21)]/25}{A}$$

and the degree of polymerization (DP) would then equal ‘n +1’. The spectral analysis revealed the value of DP as 1.9 only.

$$DP = n + 1$$

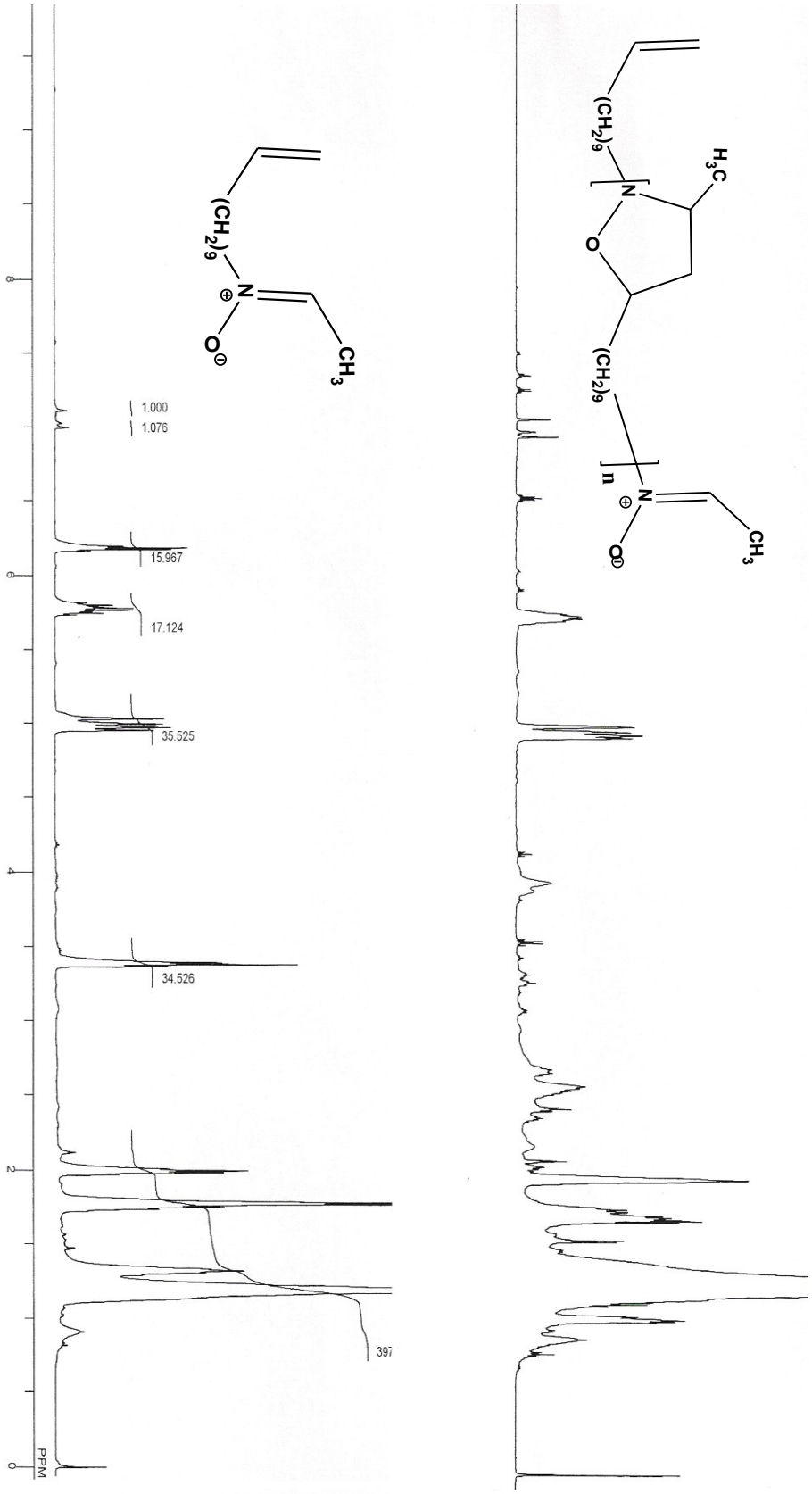

Figure 8: ^{1}H NMR Spectrum of (a) nitrone **93b** and (b) oligomers **104b** after 80 hours

4.2.3. Polymerization of the alkene-nitrone 97a

4.2.3.1. Synthesis of polyisoxazolidines 105a

A 1.26 M solution of nitrone **97a** in toluene was allowed to undergo polymerization at 120°C (**Scheme 29**), and ^{1}H NMR spectra were recorded at several intervals (**Fig. 9**) to get the rate constant for the second order kinetics.

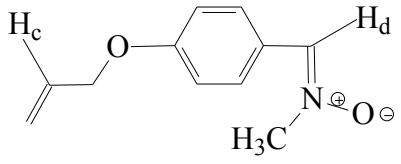

97a

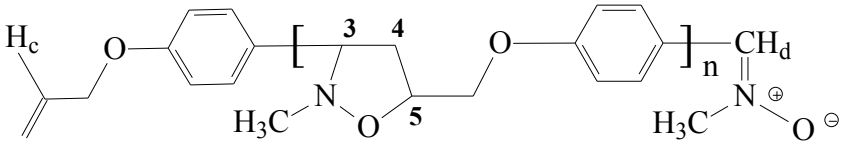

105a

a total of 4H of the polymer repeating unit at C-3, C-5, and C(5)CH_2O and 5H (NMe and CH_2O of end groups) appear in the δ range 3.3 ppm - 4.6 ppm

Scheme 29.

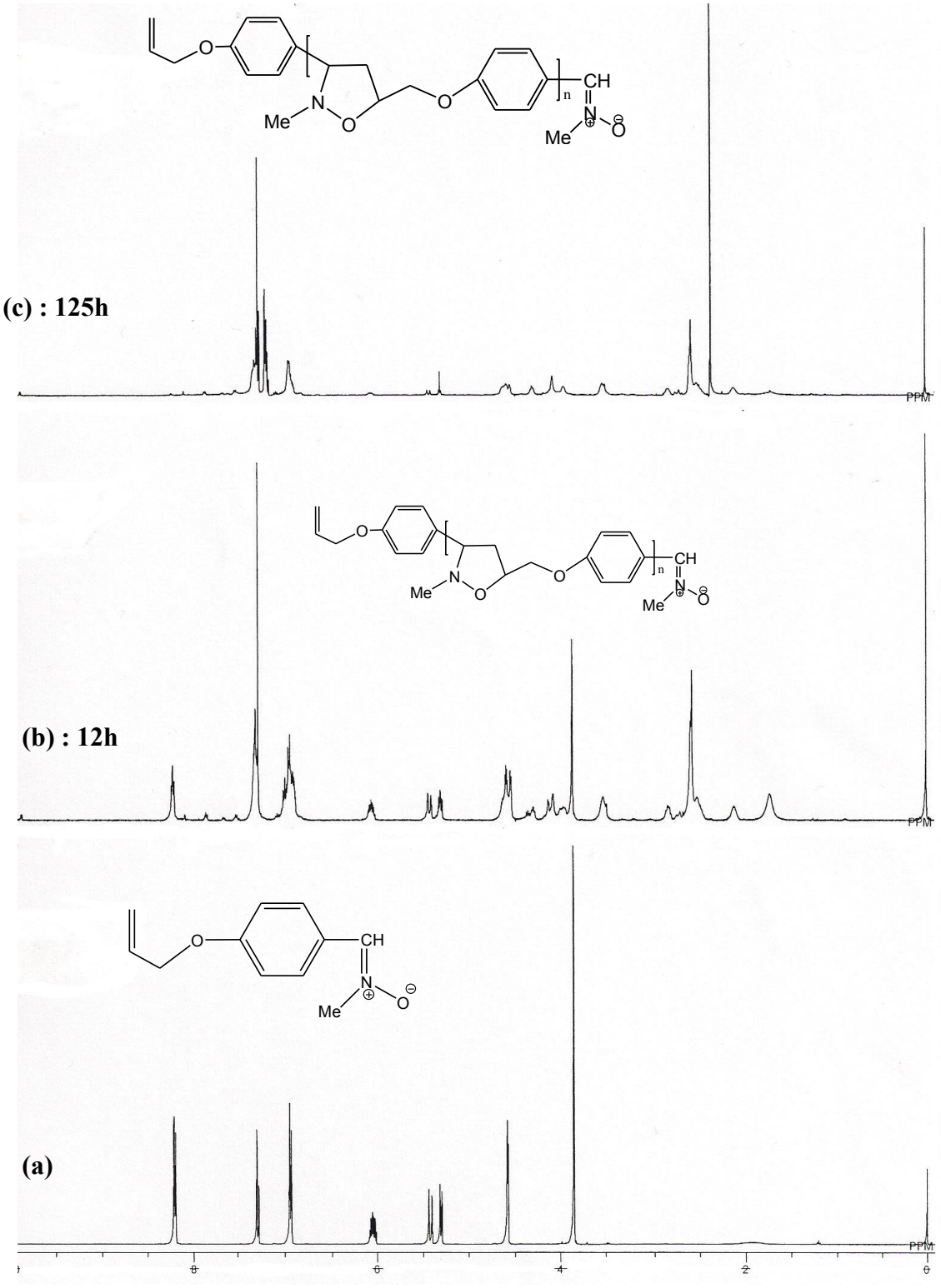

Figure 9: ^{1}H NMR Spectra of (a) alkene-nitrone **97a** , and oligomers **105a** at (b)12 hours and (c)125 hours, respectively

4.2.3.2 Determination of degree of polymerization:

Five protons (NMe and CH_2O) of the end groups and 4 protons of the repeating unit appear in the δ range 3.3-4.6 ppm. Area (A) under the alkenic proton H_c at δ 6.04 ppm permitted us to calculate the area of the 5 end group aliphatic protons in the δ range 3.3-4.6 ppm as (A×5). So, the 4 protons of the repeating unit of the polymer in the same δ range will account for an area of [T – (A×5)], where T is the total area of signals appear in the δ range 3.3-4.6 ppm. Therefore, area of a single proton belonging to the repeating unit equals [T – (A×5)]/4. Thus, the value of 'n' could then be equated to:

$$n = \frac{\text{Area of a single proton of the repeating unit}}{\text{Area of an alkene end group proton } H_c} = \frac{[T-(A\times5)]/4}{A}$$

and the degree of polymerization (DP) would then equal 'n +1'.

The results of the polymerization of a 1.26 M solution of nitrone-alkene **97a** in toluene at 120°C are given in Table 2. As discussed earlier, the second order rate of the polymerization yields the following equations:

$$DP - 1 = [M]_o kt$$
$$DP = [M]_o kt + 1$$

Where, $[M]_o$ is the initial monomer concentration. The DP versus t plot is given in Figure 10 which indicates a straight line plot. As evident from the Table 2, the ratio of the alkene/nitrone functionality remained close to 1. So, the DP versus t plot at lower range of times (**Figure 10**) gave a straight line plot and resulted in the rate constant (k) value of 1.52×10^{-5} L mol^{-1} s^{-1}. The polymer, rather the oligomer, **105a** has a DP of 6.4 at the end of 125 hours of polymerization.

Table 2: The results of the polymerization of **97a** in toluene at 120°C**.**

Time (h)	n	DP (i.e. n+1)	Ratio of H_c/H_d
2	0.35875	1.36	1
4	0.60875	1.61	1
8	0.85875	1.86	1
12	1.10875	2.11	1
41	3.355	4.36	1.1
72	5.1315	6.13	1.1
125	5.3815	6.38	1.2

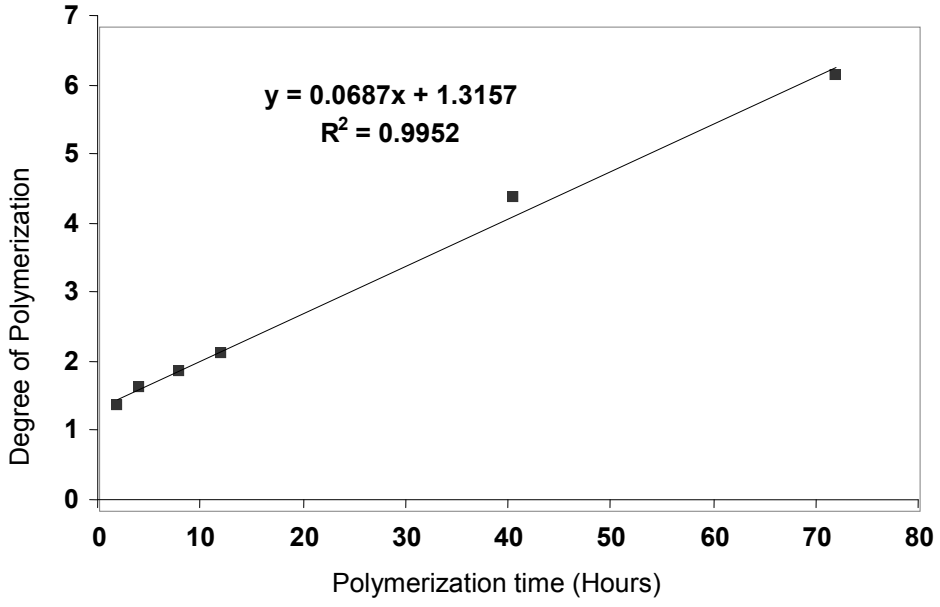

Figure 10: Degree of polymerization versus time of the polymerization of alkene-nitrone (**97a**) in toluene at 120 ^{o}C

4.2.4 Polymerization of the alkene-nitrone 97b

Monomer **97b** (1.01 g, 3.33 mmol) in moisture-free toluene (5.97 g, 6.9 cm^3) (total volume 7.22 cm^3, i.e. 3.33/7.22 = 0.461 M) was homopolymerized (**Scheme 30**) for 162 h at 120 ^oC. ^1H NMR spectra were recorded at several intervals (**Fig. 11**) to get the rate constant for the second order kinetics as described in the polymerization of **97a.** The DP was calculated as described for the case of **97a.** The end groups in polymer **105b** (similar to **105a**) have a total of 5 protons (NMe and CH_2O) and the repeating unit has a total of 4 protons appear in the δ range 3.3-4.6 ppm.

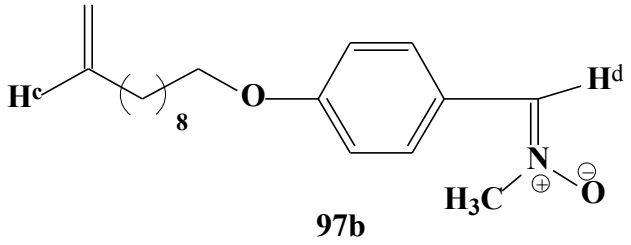

97b

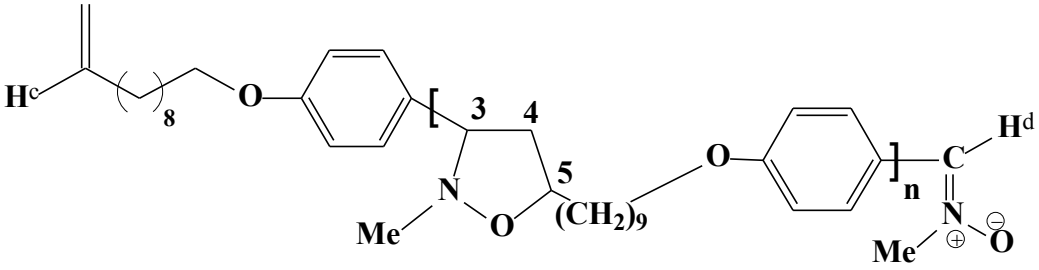

105b

A total of 4H of the polymer repeating unit at C-3, C-5, and C(5)-CH_2-O-ph and 5H (NMe and CH_2O of end groups) appear in the δ range 3.3 ppm -4.6 ppm

Scheme 30

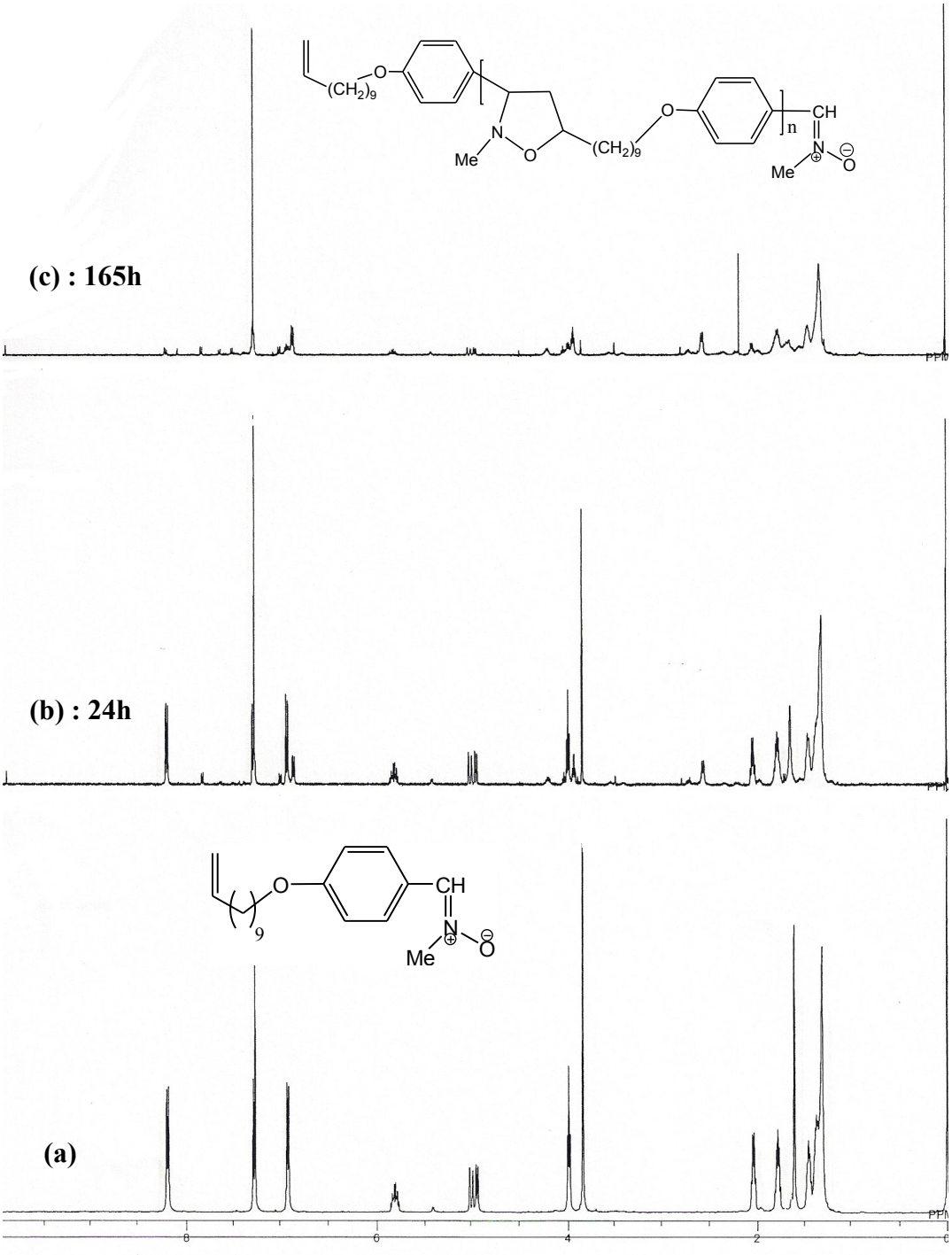

Figure 11: ^{1}H NMR Spectra of (a) alkene-nitrone **97b** , and oligomer **105b** at (b) 24 hours and (c) 165 hours, respectively

As evident from the Table 3, the ratio of the alkene/nitrone functionality remained close to 1. The DP versus t plot is given in Figure 12 which gave a straight line plot and resulted in the rate constant (k) value of 9.22×10^{-6} L mol^{-1} s^{-1}. The polymer, rather the oligomer, **105b** has a DP of 3.7 at the end of 162 hours of polymerization.

Table 3: The results of the polymerization of **97b** in toluene at 120°C .

Time (h)	n	DP (i.e. n+1)	Ratio of H_c/H_d
24	0.64	1.64	1
48	0.98	1.98	1
72	1.28	2.28	1
162	2.74	3.74	1

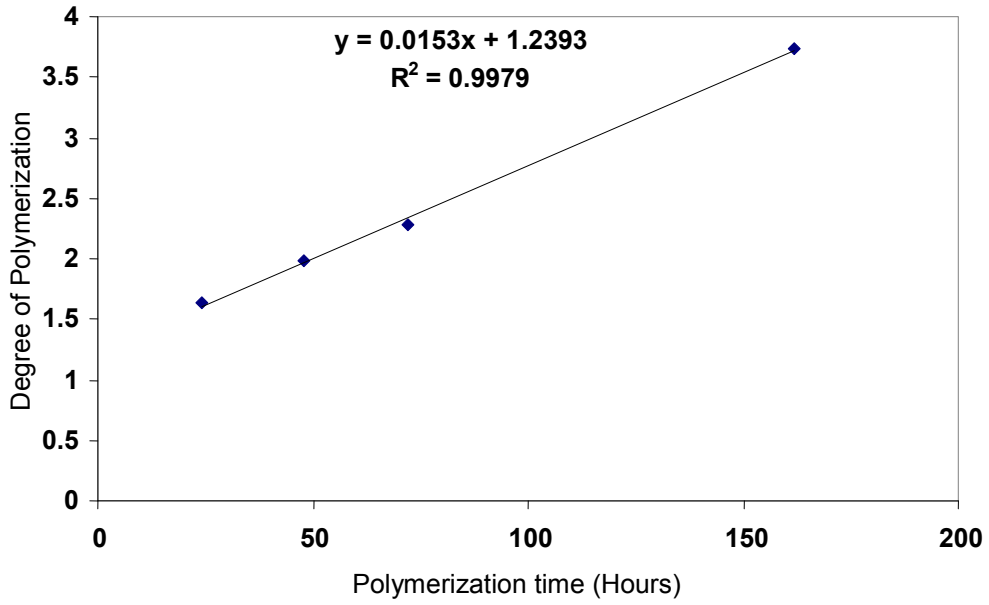

Figure 12: Degree of polymerization versus time of the polymerization of alkene-nitrone (**97b**) in toluene at 120 ^{o}C.

4.3. Copolymerization of dialkene 99 and dinitrone 101

4.3.1 Synthesis of polyisoxazolidine 106

The copolymerization of dialkene **99** and dinitrone **101** was carried out in DMF at 120 ^{o}C. Toluene as a solvent was avoided due to solubility problem**.** ^{1}H NMR spectra were recorded at several intervals (**Fig. 13**) to get the rate constant for the second order kinetics as described below.

4.3.2 Determination of degree of polymerization:

As shown in the Scheme 31, the end groups and the repeating unit in polymer **106** have 14 and 18 aliphatic protons, respectively in the δ range 1.5-4.6 ppm. The area for the proton signals of solvent DMF (Me_2NCHO) are excluded from the calculation. Area (A) under the alkenic proton H_c at δ 6.04 ppm permitted us to calculate the area of the 14 end group aliphatic protons in the δ range 1.5-4.6 ppm as (A×14). So, the 18 protons of the repeating unit of the polymer in the same δ range will account for an area of [T – (A×14)], where T is the total area of signals appear in the δ range. Therefore, area of a single proton belonging to the repeating unit equals [T – (A×14)]/18. Thus, the value of 'n' could then be equated to:

$$n = \frac{\text{Area of a single proton of the repeating unit}}{\text{Area of an alkene end group proton } H_c} = \frac{[T-(A\times 14)]/18}{A}$$

and the degree of polymerization (DP) would then equal '2n +1'.

$$DP = 2n + 1$$

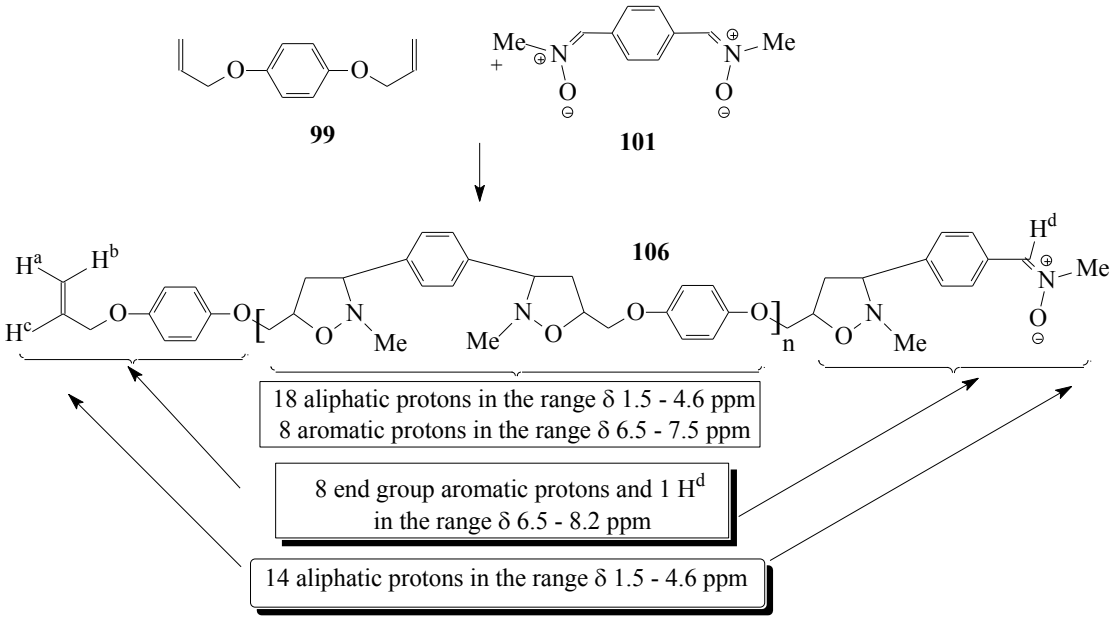
99
101
106
18 aliphatic protons in the range δ 1.5 - 4.6 ppm
8 aromatic protons in the range δ 6.5 - 7.5 ppm
8 end group aromatic protons and 1 Hd
in the range δ 6.5 - 8.2 ppm
14 aliphatic protons in the range δ 1.5 - 4.6 ppm

Scheme 31.

The results of the polymerization of a 1.62 M (concentration of the alkene and nitrone groups) solution of dinitrone **101** and dialkene **99** in DMF at 120°C are given in Table 4. The concentration of the reactants was 0.808 M in each, however, the concentration of the functional groups will be twice as much. As discussed earlier, the second order rate of the polymerization yields the following equations:

$$DP - 1 = [M]_o kt$$

$$DP = [M]_o kt + 1$$

Where, $[M]_o$ is the initial concentration. As evident from the Table 4, the ratio of the alkene/nitrone functionality remained close to 1. The DP versus t plot is given in Figure 14 which gave a straight line plot and resulted in the rate constant (k) value of 2.97×10^{-5} L mol^{-1} s^{-1}. The polymer, rather the oligomer, **106** has a DP of 21 at the end of 136 hours of polymerization.

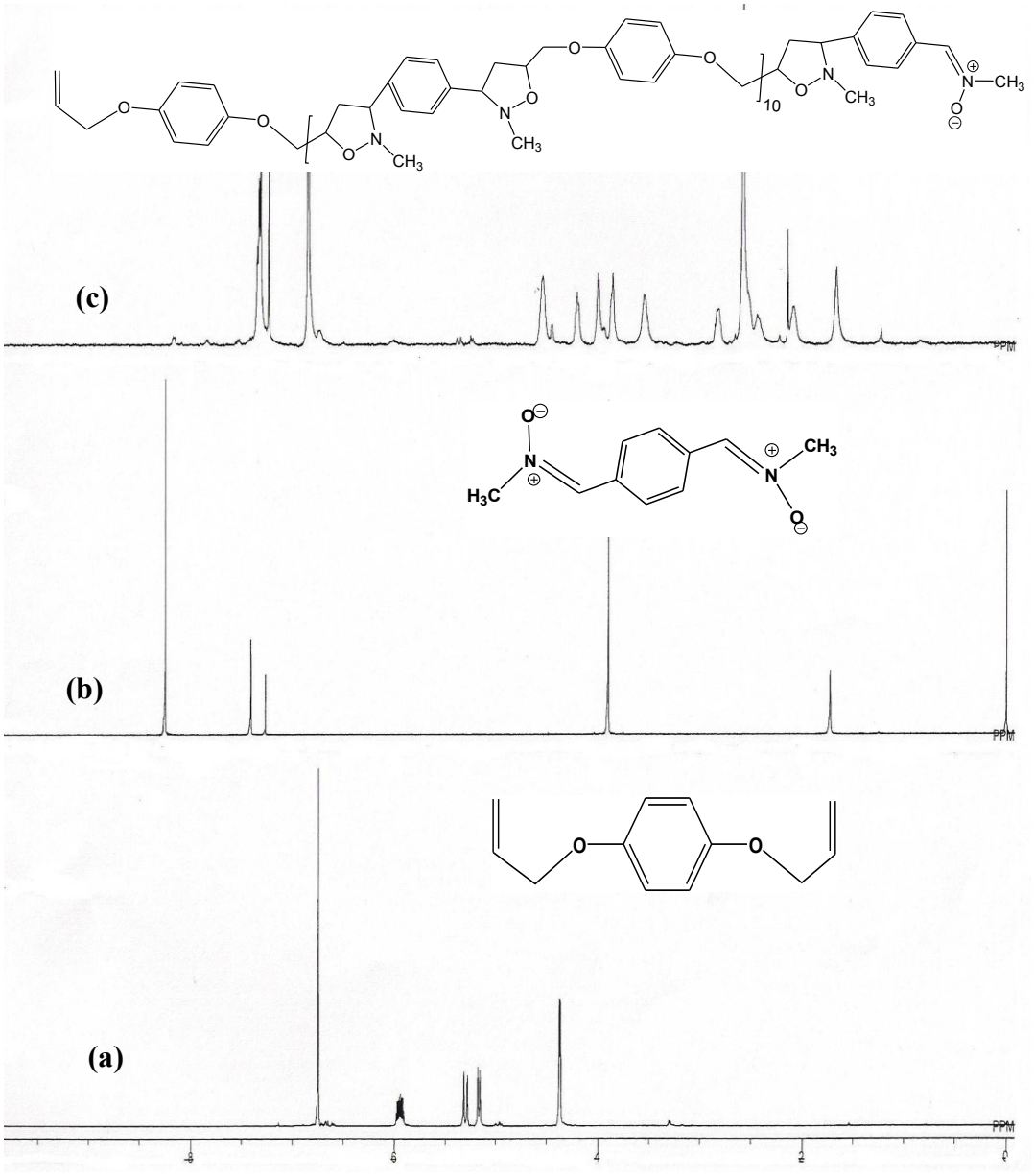

Figure 13. ^{1}H NMR Spectra of (a) dialkene **99** , (b) dinitrone **101** and (c) oligomer (**106**) at 24 hours

Table 4: The results of the polymerization of dialkene **99** and dinitrone **101** in DMF in toluene at 120 °C.

Time (h)	n	DP (i.e. 2n+1)	Ratio of H_c/H_d
32	0.95	2.90	1
68	3.57	8.13	1
100	6.15	13.3	1
136	10.0	21.0	1

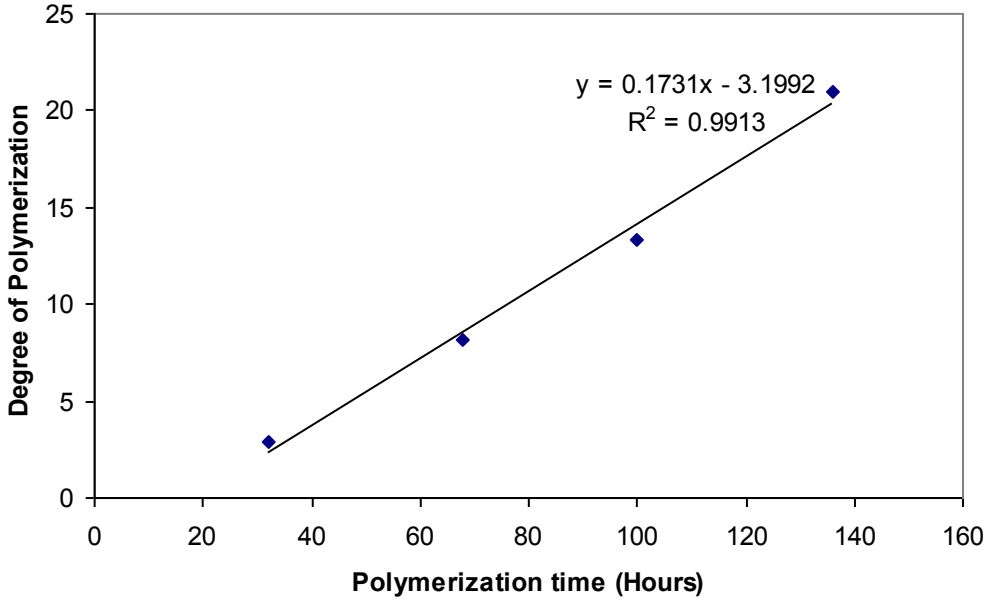

Figure 14: Degree of polymerization versus time of the polymerization of dialkene (**99**) and dinitrone (**101**) in DMF at 120 ^{o}C

4.4. Copolymerization of dialkene 99 and dinitrone 103

Finally, we attempted the polymerization of the *p*-diallyloxybenzene **(99)** and *N,N′*-dimethyl-1,5-pentylidenedinitrone **(103)** (**Scheme 32**) in a 1:1 ratio in toluene at 110 ^{o}C for about 92 h. The ^{1}H NMR spectrum revealed the absence of protons attributed to the nitrone functionality (CH=NO(CH_3) as shown in Figure 15, while the dialkene end group protons are present in considerable amount. In order to react with the terminal alkene end groups, more of the dintrone **103** (5.0 mmol) was added and the mixture was polymerized for a further 24 h to yield polymer **107** (**Scheme 32**). Since the proton spectrum failed to reveal the presence of end group proton, we were unable to determine the degree of polymerization. A pure sample of the dinitrone **103** was thermolyzed in toluene at 110 ^{o}C for 92 h. The ^{1}H NMR spectrum revealed the complete decomposition of the nitrone into intractable matter (**Fig. 16)**.

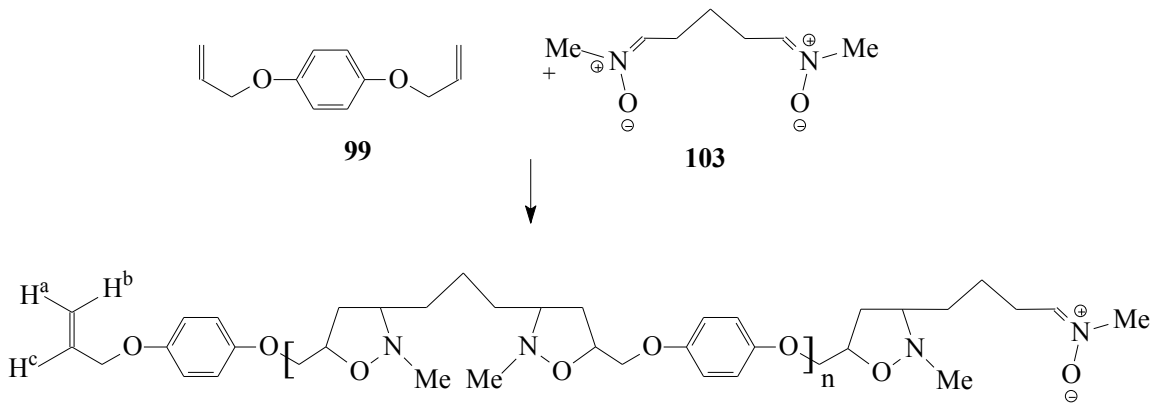

107

Scheme 32.

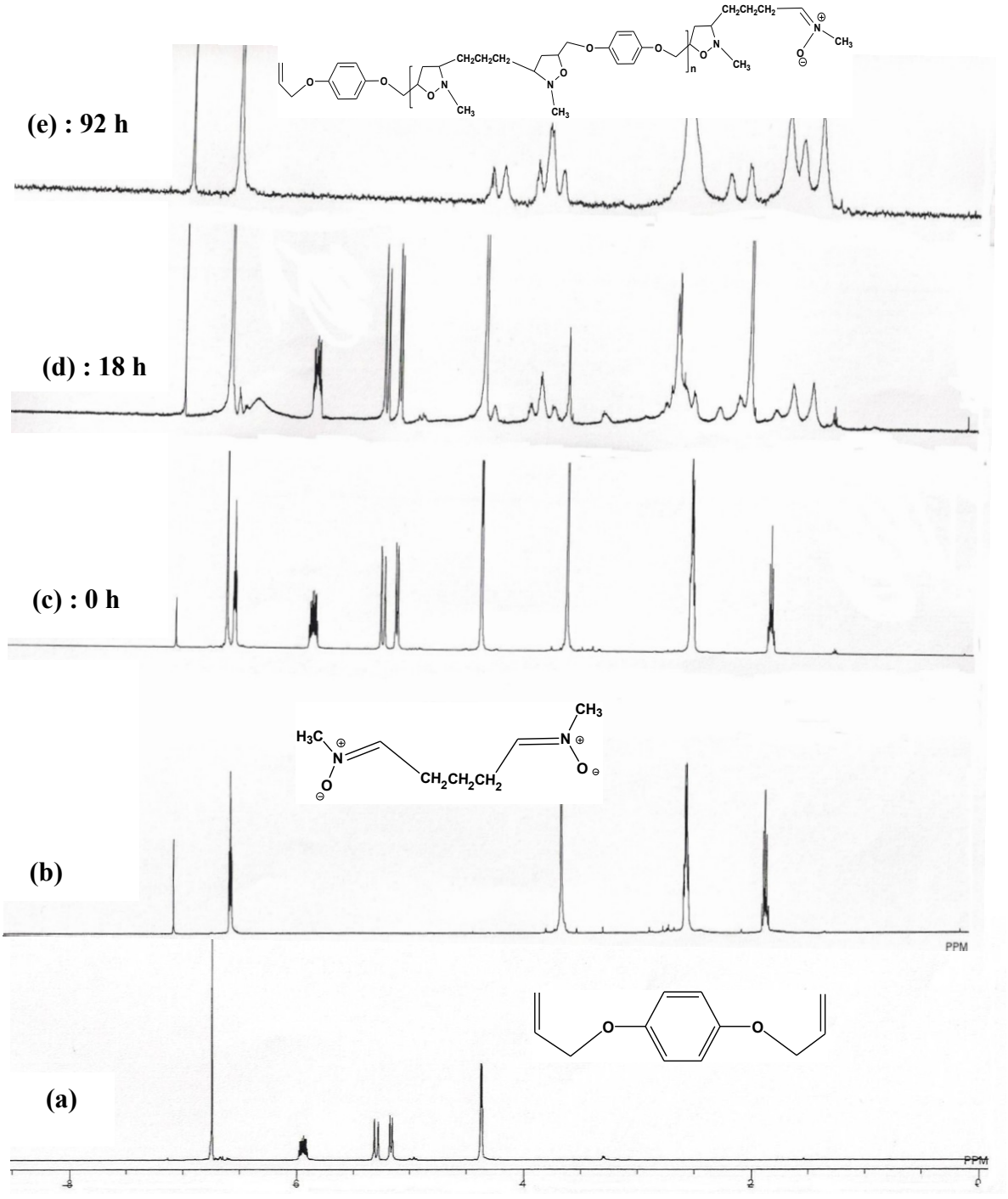

Figure 15: ^{1}H NMR Spectra of (a) dialkene **99** , (b) dinitrone **103**, (c) dialken-dinitrone mixture at 0 hours at room temperature, (d) oligomer **107**at 105^{o}C for 18 hours with excess dinitrone, and (e) **107** oligomer at 110^{o}C for 92 hours.

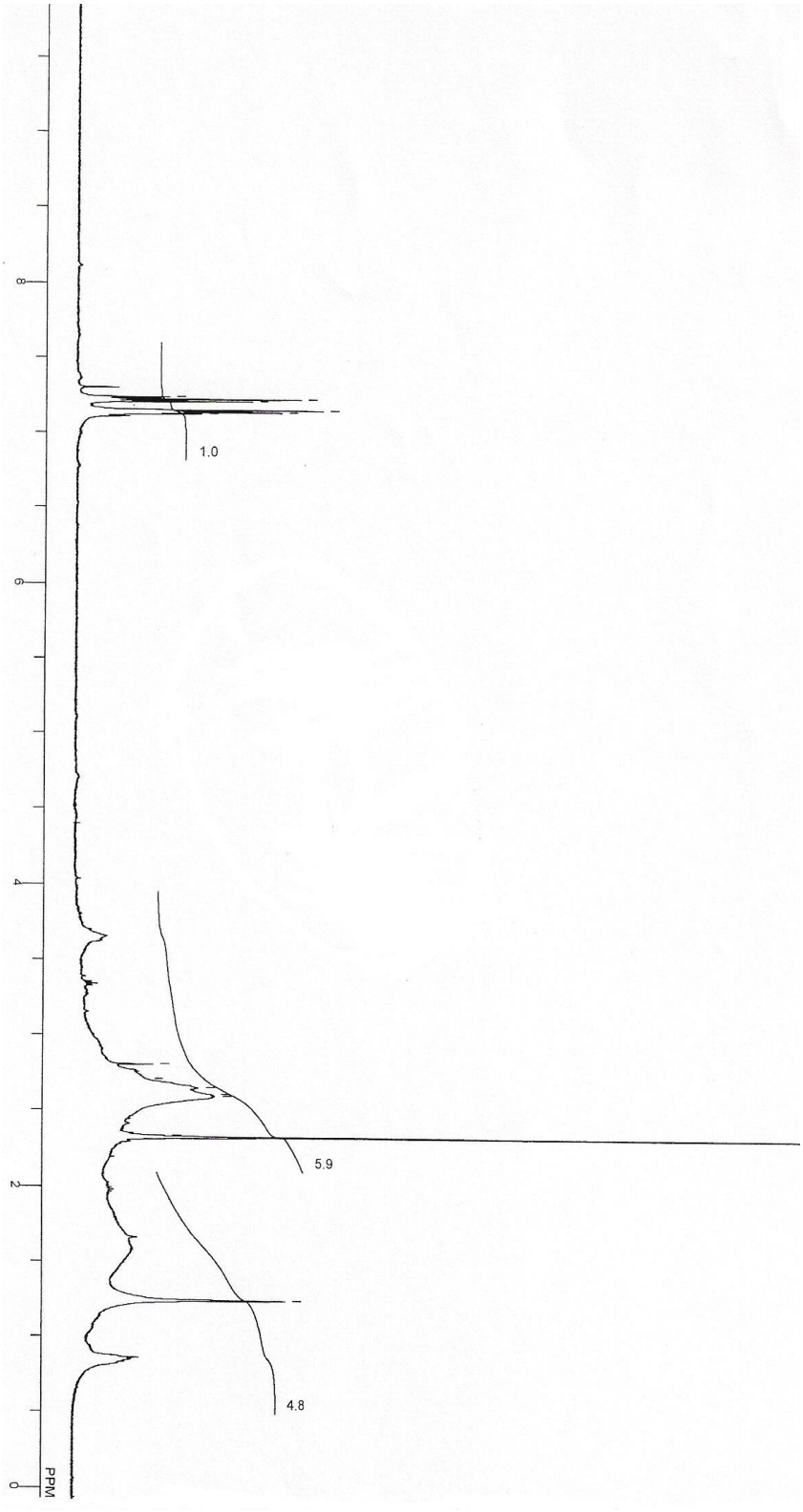

Figure 16: ^{1}H NMR Spectrum of dinitrone **103** thermolyzed in toluene at 110 ^{o}C.

4.5 End-capping of the living polymer(s)

The alkene-nitrone will give living polymers, one terminal of which could be capped by reacting with reactive alkenes like, methyl acrylate as shown in Schemes 33. The end-capping will stabilize the polymer chain with respect to the molar mass (**Fig. 17)**.

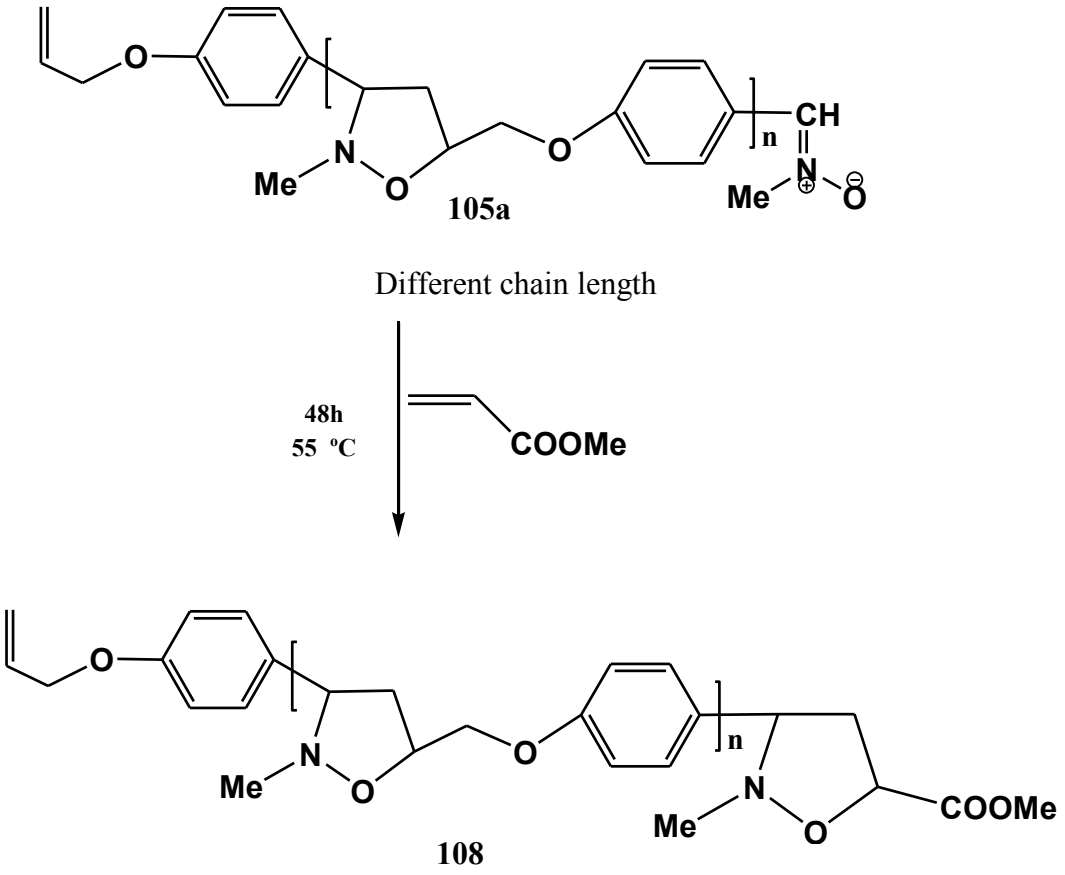

Scheme 33.

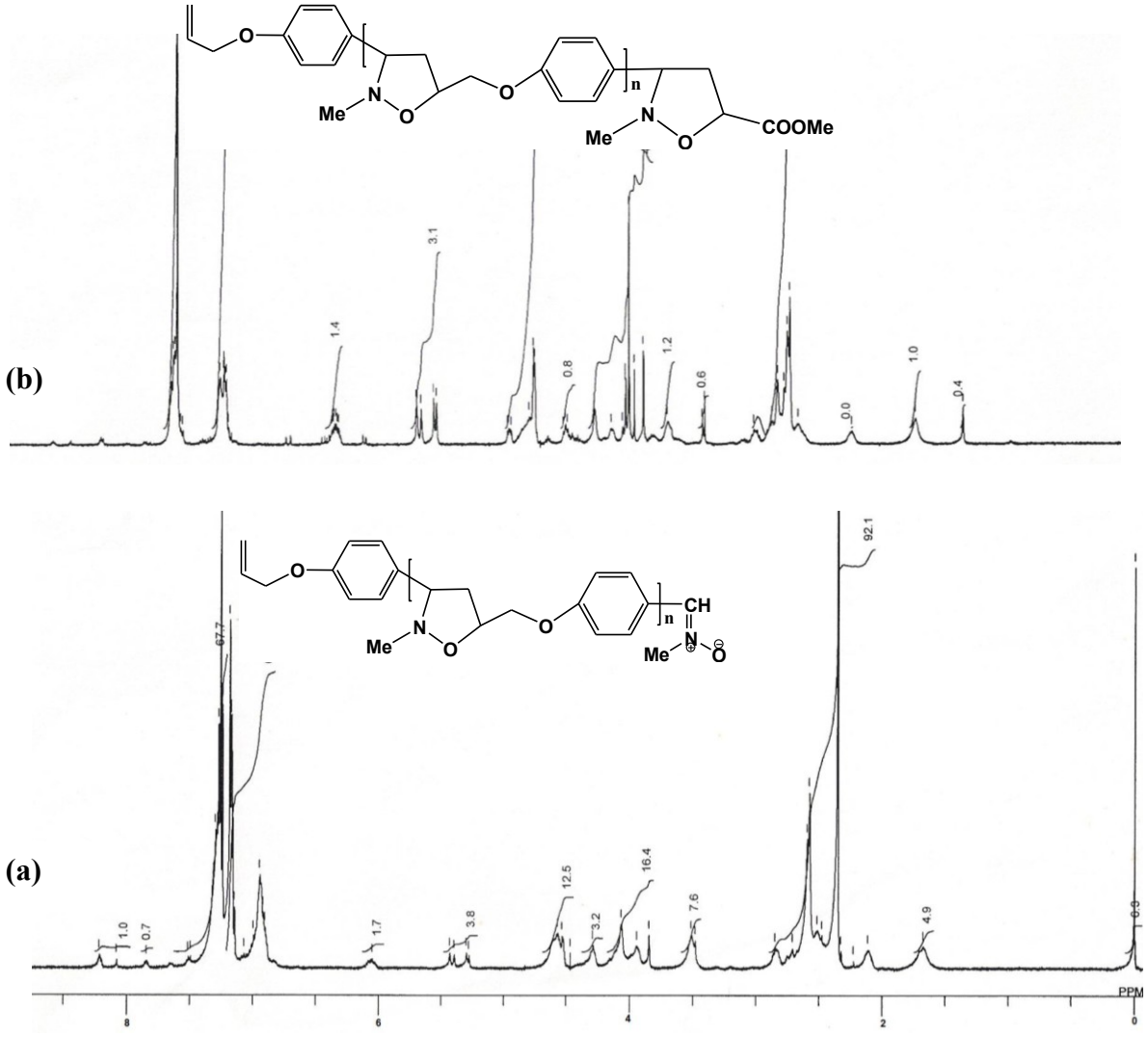

Figure 17: ^{1}H NMR Spectra of (a) oligomers **105a** at 46 hours and (b) oligomers **105a** end-capped with methyl acrylate

4.6. Gravimetric Measurements

The results of weight loss measurements for various concentrations of the inhibitor molecules at 60°C after 6 h of immersion in 1 M HCl and 0.5 M H_2SO_4 are reported in Table 5. The %IE was determined using the following equation:

$$\%\text{IE} = \frac{\text{Weight loss (blank)} - \text{Weight loss (inhibitor)}}{\text{Weight loss (blank)}} \times 100$$

Weight loss (blank) and weight loss (inhibitor) represent weight loss in absence and presence of inhibitor, respectively. Triplicate determinations were made with each of the inhibitors and with solutions containing no inhibitor. In some cases where the deviations are larger, the weight loss measurements were carried out for the fourth or even fifth time in order to get the desired standard deviation. Relative weight losses of the coupons were used to calculate the percent inhibition efficiency (%IE) as described.[14] In most of the cases, the coupons were of almost identical size and mass. However, in some cases where the masses differed, relative weight loss of the coupons were used to calculate the percent inhibition efficiency (%IE) using the following equation

$$\%\text{IE} = \frac{\Delta\overline{W}_o - \Delta W}{\Delta\overline{W}_o} \times 100$$

where $\Delta\overline{W}_o$ is the mean relative weight loss of the coupons in the blank solutions, and ΔW is the relative weight loss of the coupon in the inhibitor solution. In the following equations, W_{ib} and W_{fb} are the initial and final masses, respectively, of the coupons in blank solutions and W_{is} and W_{fs} are the initial and final masses of the sample coupon in the inhibitor solution.

$$\Delta\overline{W}_o = [\sum (W_{ib} - W_{fb}) / W_{ib}] / 3$$

$$\Delta W = (W_{is} - W_{fs}) / W_{is}$$

The average percent inhibition efficiency reported in the Tables 5, 6, and 8 is found to have a standard deviation of 0.3-3.5%. Results of Tafel plots and polarization resistance method of mild steel sample in solutions containing 200 ppm of the inhibitors in 1 M HCl at 60 ºC corroborated the results from gravimetric method.

Table 5: Inhibition efficiency (%IE) using gravimetric measurements for different concentrations of inhibitors for the inhibition of corrosion of mild steel in 1 M HCl and 0.5 M H_2SO_4 exposed for 6 h at 60ºC.

Compoun	%IE in HCl at ppm						%IE in H_2SO_4 at ppm		
d	10	25	50	100	200	400	50	100	200
97a	6.0	19	30	53	69	83	11	15	24
97b			24	31	39		2	5	7
104a	44	63	65	77	89	94	ND[a]	ND[a]	ND[a]
104b	34	53	59	80	96	99	ND[a]	ND[a]	ND[a]
105a[b]			88	91	91		77	83	86
105a[c]			91	92	91		78	80	87
105a[d]			90	91	92		79	82	83
105b			55	57	67		3.4	39	57
106			89	91	92		44	49	48
107			86	86	89		45	21	16

[a]ND: not determined;

[b]sample of DP = 2;

[c]sample of DP = 4;

[d]sample of DP = 6.4.

4.7 Electrochemical Measurements

4.7 .1 Polarization Curves

Each pair of Tafel plots was analyzed to obtain corrosion current density and corrosion potential.[14] The results of Tafel plots for mild steel in 1 M HCl (blank) and 1 M HCl solution containing 200 ppm of the inhibitors at 60°C are summarized in Tables 6 and 7. Results of Tafel plots for mild steel sample in solutions containing 200 ppm of the inhibitors in 0.5 M H_2SO_4 at 60 ºC are summarized in Tables 8 and 9. The Tafel plots for mild steel in 1 M HCl (blank) and 1 M HCl solution containing 200 ppm each of the monomers **97a** and **97b** and each of the inhibitors **104a**, **104b**, **105a**, **105b**, **106** and **107** at 60 ^{o}C are shown in Figs. 18-30. The Tafel plots for mild steel in 0.5 M H_2SO_4 (blank) and 0.5 M H_2SO_4 solution containing 200 ppm each of the monomers **97a** and **97b** and each of the inhibitors **104a**, **104b**, **105a**, **105b**, **106** and **107** at 60 ^{o}C are shown in Figs. 31-40.

4.7.2 Linear Polarization Resistance

The inhibition efficiency (IE) in 1 M HCl and 0.5 M H_2SO_4 at 60 ºC from linear polarization technique was calculated as follows:

$$\%IE = \left(\frac{R'_p - R_p}{R'_p}\right) \times 100$$

Where, R_p and R'_p are the polarization resistance in the absence and presence of various concentrations of the inhibitors, respectively. Values of R'_p and R_p and the corresponding inhibition efficiency for each inhibitor are given in Tables 6-9.

Table 6: Results of Tafel plots and polarization resistance method of mild steel sample in solutions containing 200 ppm of the inhibitors in 1 M HCl at 60 ºC.

Solution	Tafel plots					Polarization resistance	
	E_{corr} *vs SCE* (mV)	β_a (mV/dec)	β_c (mV/dec)	i_{corr} ($\mu A/cm^2$)	%IE	R_p *(Ω)*	%IE
Blank[a]	-453	40.1	85.6	2559	–	2.2	–
97a	-510	64.4	134.9	636.5	75	11.2	80
104a	-483	96.3	169.9	310.9	88	36.7	94
104b	-469	82.3	173.8	134.8	95	70.6	97
107	-488	41.8	56.6	24.4	99	31.7	93

[a]A solution of 200 ppm of each compound was used. The blank was a 1.0 M HCl solution.

Table 7: Results of Tafel plots and polarization resistance method of mild steel sample in solutions containing 200 ppm of the inhibitors in 1 M HCl + 2 ml DMF at 60 ºC.

Solution	Tafel plots					Polarization resistance	
	E_{corr} *vs SCE* (mV)	β_a (mV/dec)	β_c (mV/dec)	i_{corr} ($\mu A/cm^2$)	%IE	R_p *(Ω)*	%IE
Blank[a]	-501	72.0	144	1668	–	5.0	–
97b	-512	64.7	146	1724.5	-3.4	5.26	4.2
105a[b]	-479	115	144	294.7	82	30.2	83
105a[c]	-446	85.5	93.1	227.4	86	34.3	85
105a[d]	-444	74.9	88.3	193.7	88	64.1	92
105b	-492	88.8	127	125	93	70.6	93
106	-469	59.1	109	64.1	96	115.	96

[a]A solution of 200 ppm of each compound was used. The blank was 1 M HCl + 2 ml DMF solution; [b]sample of DP = 2; [c]sample of DP = 4; [d]sample of DP = 6.4.

Table 8: Results of Tafel plots and polarization resistance method of mild steel sample in solutions containing 200 ppm of the inhibitors in 1 N H_2SO_4 at 60 ºC.

Solution	Tafel plots					Polarization resistance	
	E_{corr} *vs SCE* (mV)	β_a (mV/de)	β_c (mV/dec)	i_{corr} ($\mu A/cm^2$)	%IE	R_p *(Ω)*	%IE
Blank[a]	-499	71.1	149.1	2354	–	3.9	–
97a	-509	87.2	177.2	2835	-20	4.8	10
104a	-435	21.5	159.5	209.8	91.1	32.9	88
104b	-447	36.5	276.7	749	68.2	13.0	71
107	-486	60.2	144.1	1574	33	7.3	47

[a]A solution of 200 ppm of each compound was used. The blank was a 1.0 N H_2SO_4 solution.

Table 9: Results of Tafel plots and polarization resistance method of mild steel sample in solutions containing 200 ppm of the inhibitors in 1 N H_2SO_4 + 2 ml DMF at 60 ºC.

Solution	Tafel plots					polarization resistance	
	E_{corr} *vs SCE* (mV)	β_a (mV/dec)	β_c (mV/dec)	i_{corr} ($\mu A/cm^2$)	%IE	R_p *(Ω)*	%IE
Blank[a]	-511	101	175	3844	–	3.2	–
97b	-503	-41.5	172	1389.5	63.9	10.0	68
105a[b]	-486	40.7	170	930	75.8	14.4	78
105b	-493	41.0	114	645.5	83.2	8.9	64
106	-464	31.8	137	577.5	85	12.8	75

[a]A solution of 200 ppm of each compound was used. The blank was a 1 N H_2SO_4 + 2 ml DMF solution. [b]sample of DP = 6.4

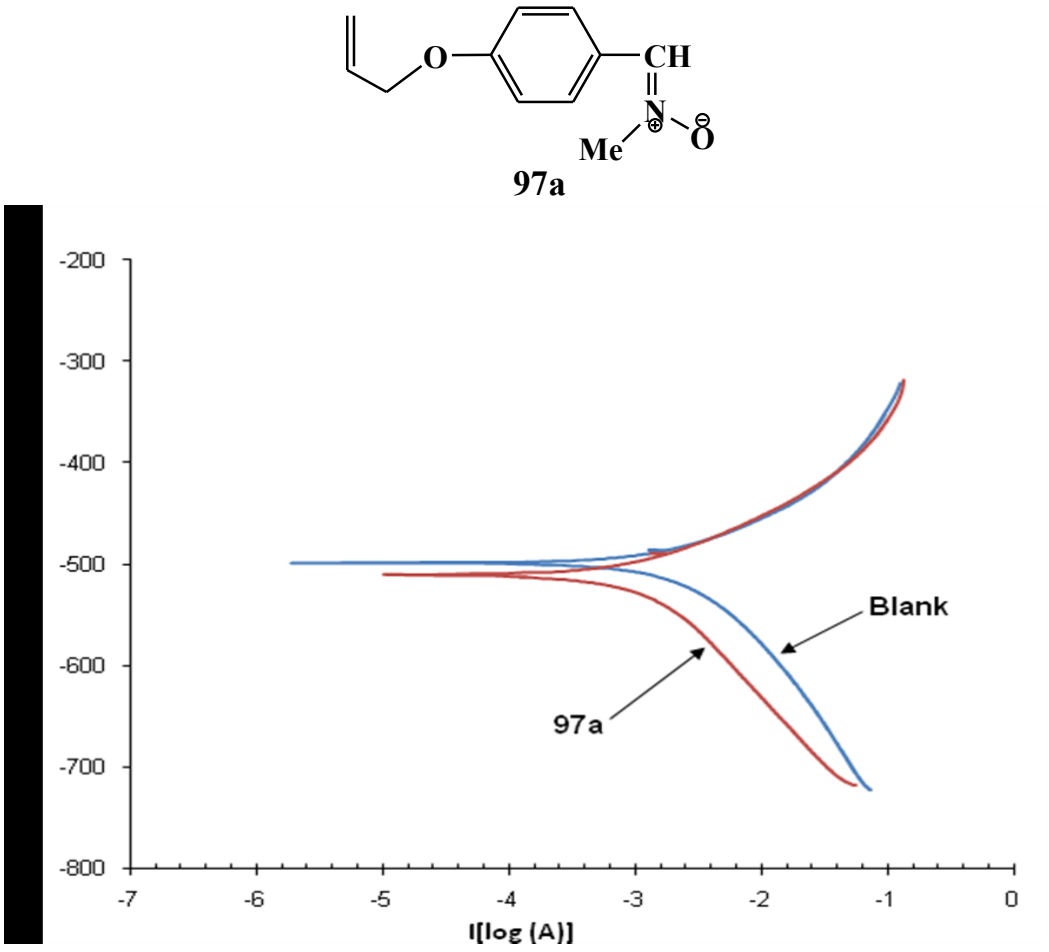

Figure 18. Potentiodynamic polarization curves for mild steel in 1 M HCl (blank) and 1 M HCl containing 200 ppm of the monomer **97a** at 60 ^{o}C.

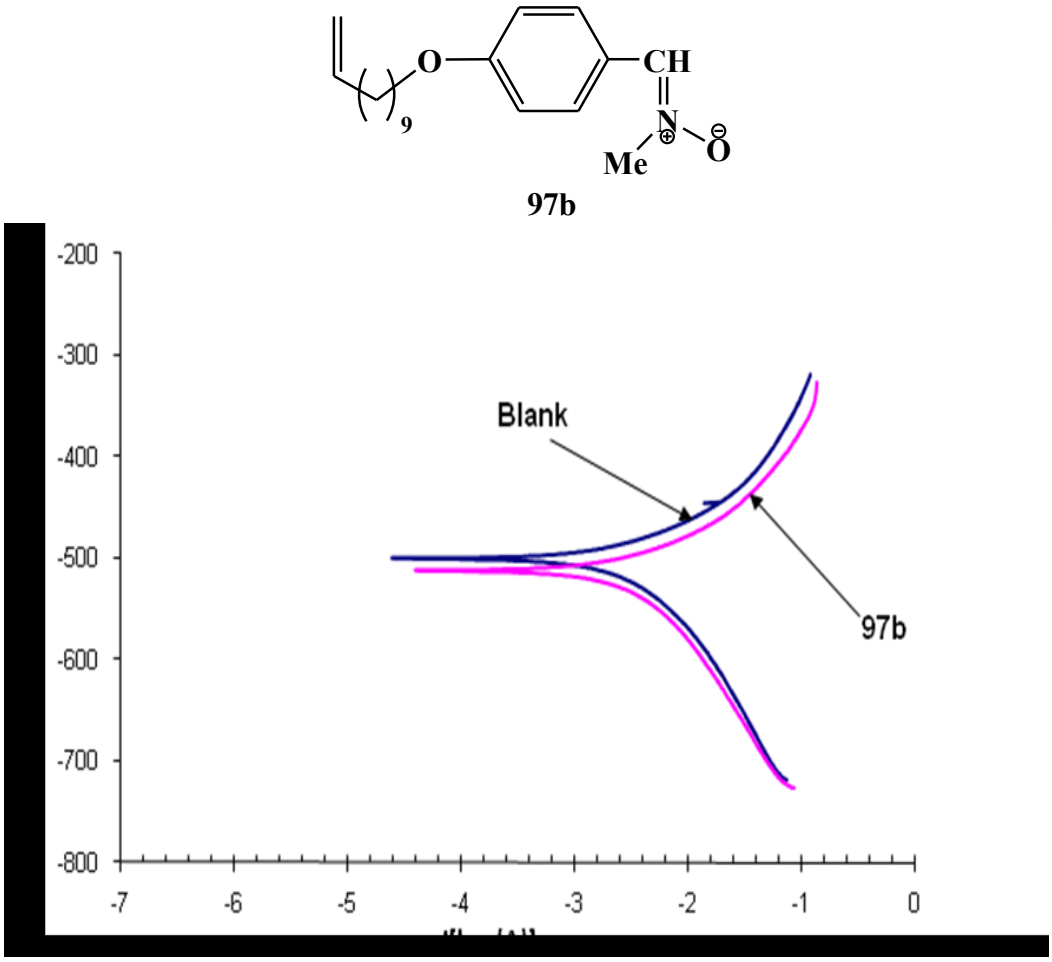

Figure 19. Potentiodynamic polarization curves for mild steel in 1 M HCl + 2 ml DMF (blank) and 1 M HCl + 2 ml containing 200 ppm of the monomer **97b** at 60 ^{o}C.

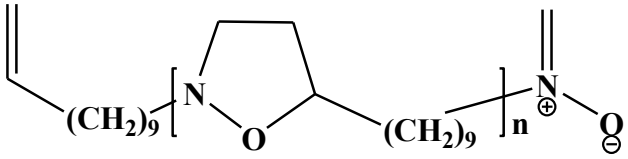

104a

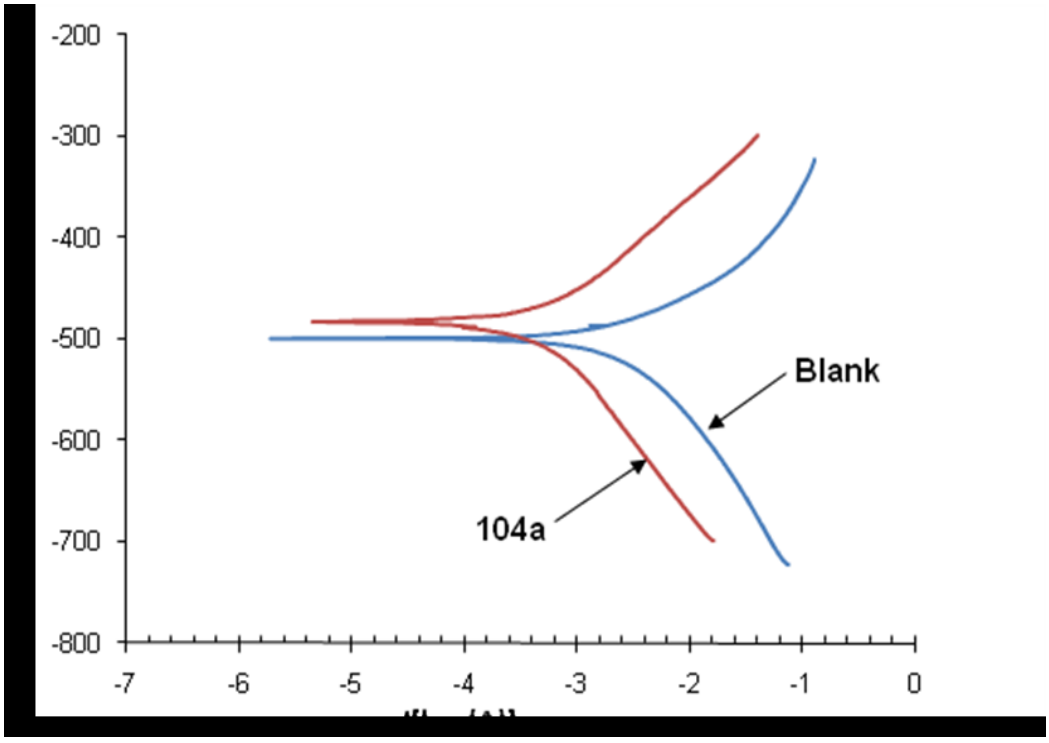

Figure 20. Potentiodynamic polarization curves for mild steel in 1 M HCl (blank) and 1 M HCl containing 200 ppm of the polyisoxazolidine **104a** at 60 ^{o}C.

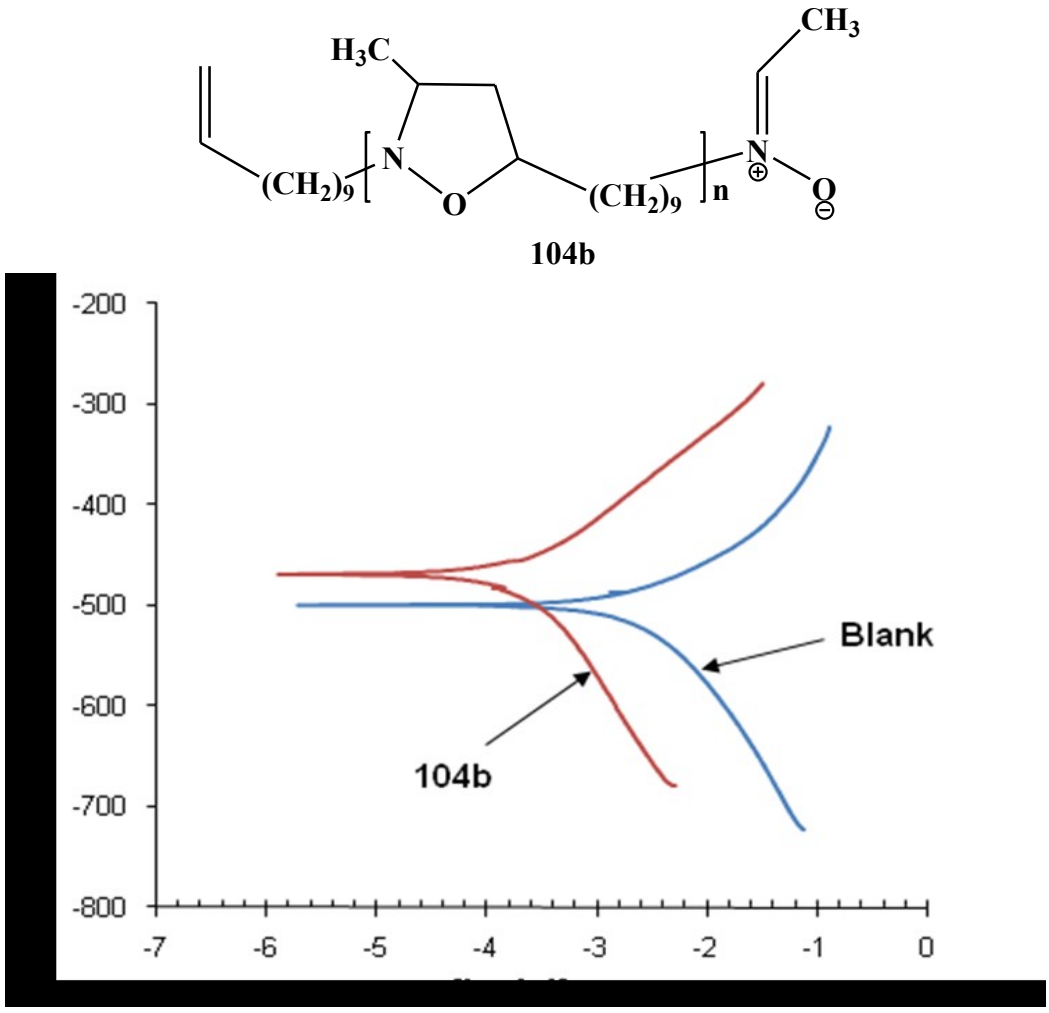

Figure 21. Potentiodynamic polarization curves for mild steel in 1 M HCl (blank) and 1 M HCl containing 200 ppm of the polyisoxazolidine **104b** at 60 ^{o}C.

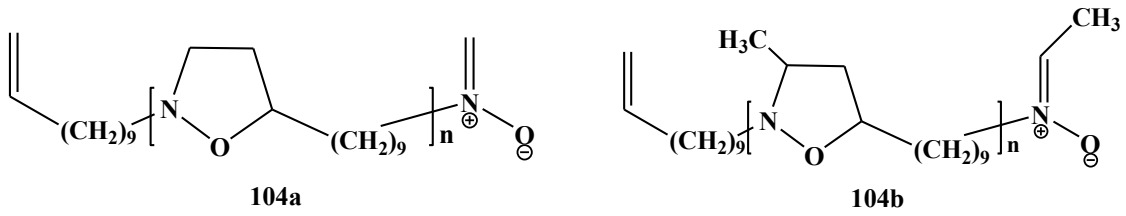

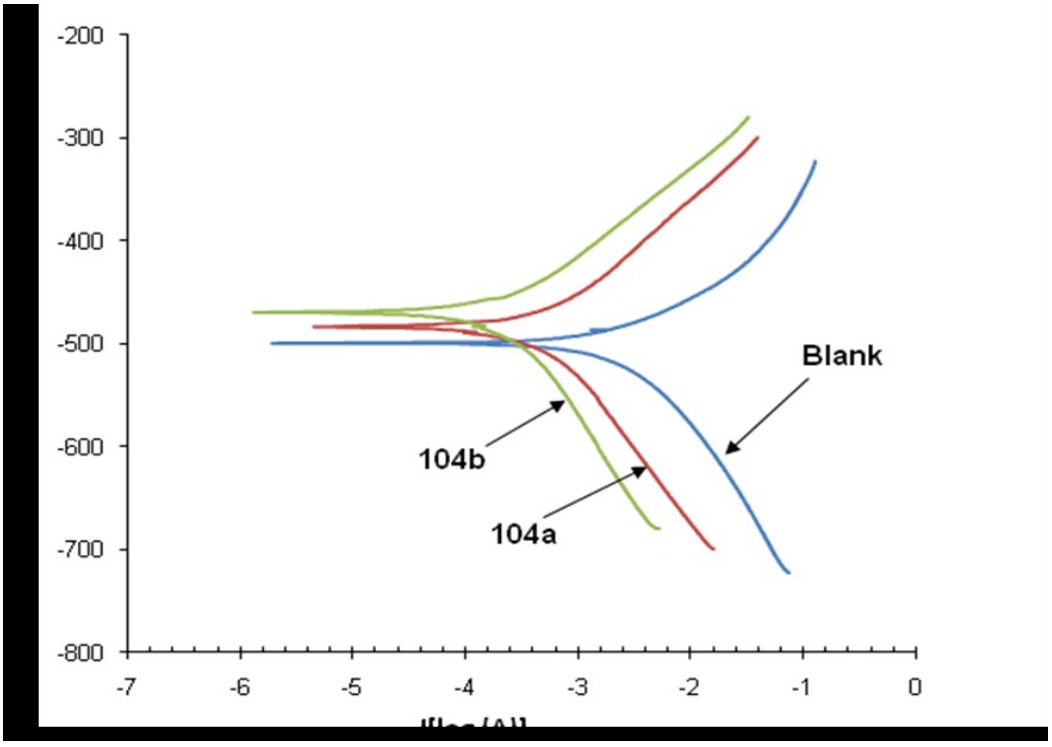

Figure 22. Potentiodynamic polarization curves for mild steel in 1 M HCl (blank) and 1 M HCl containing 200 ppm of the polyisoxazolidine**s 104a** and **104b** at 60 ^{o}C.

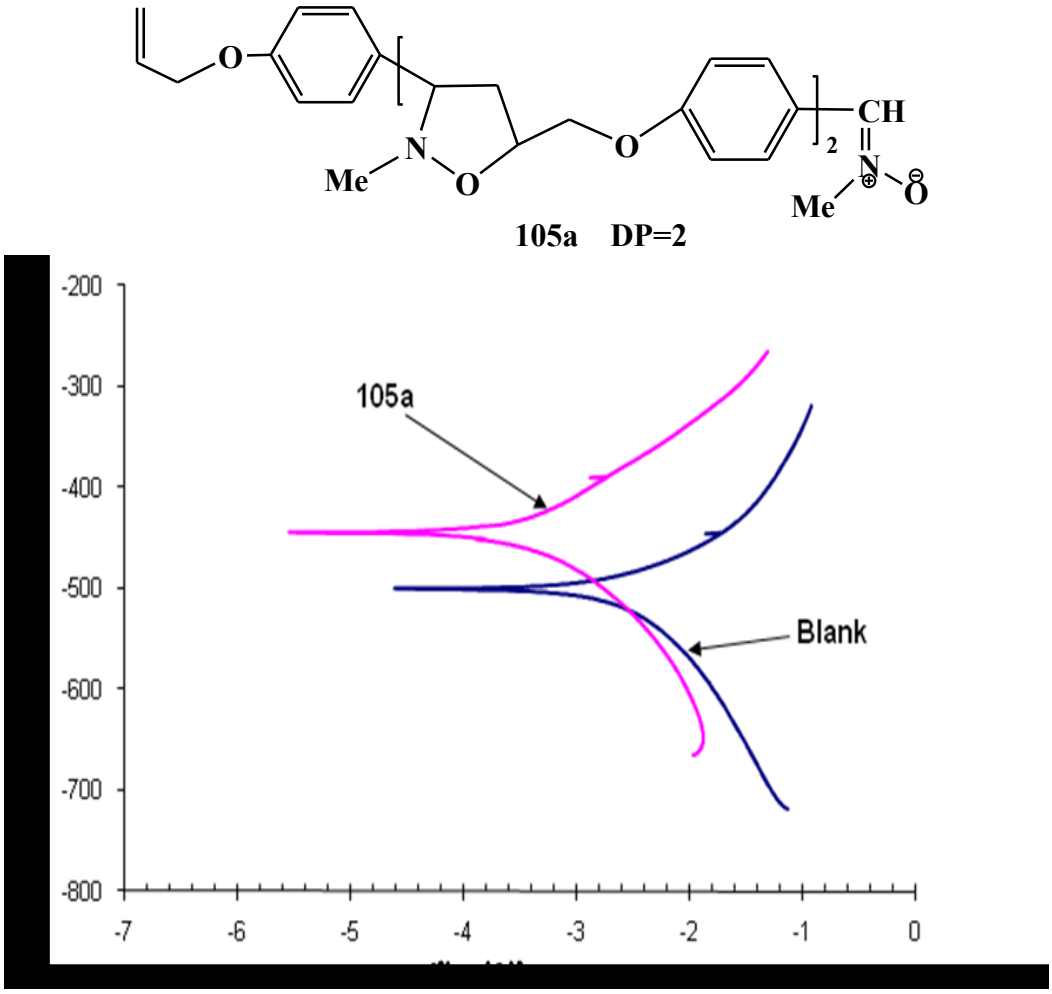

Figure 23. Potentiodynamic polarization curves for mild steel in 1 M HCl + 2 ml DMF (blank) and 1 M HCl + 2 ml containing 200 ppm of the polyisoxazolidine **105a** of DP = 2 at 60 ^{o}C.

.

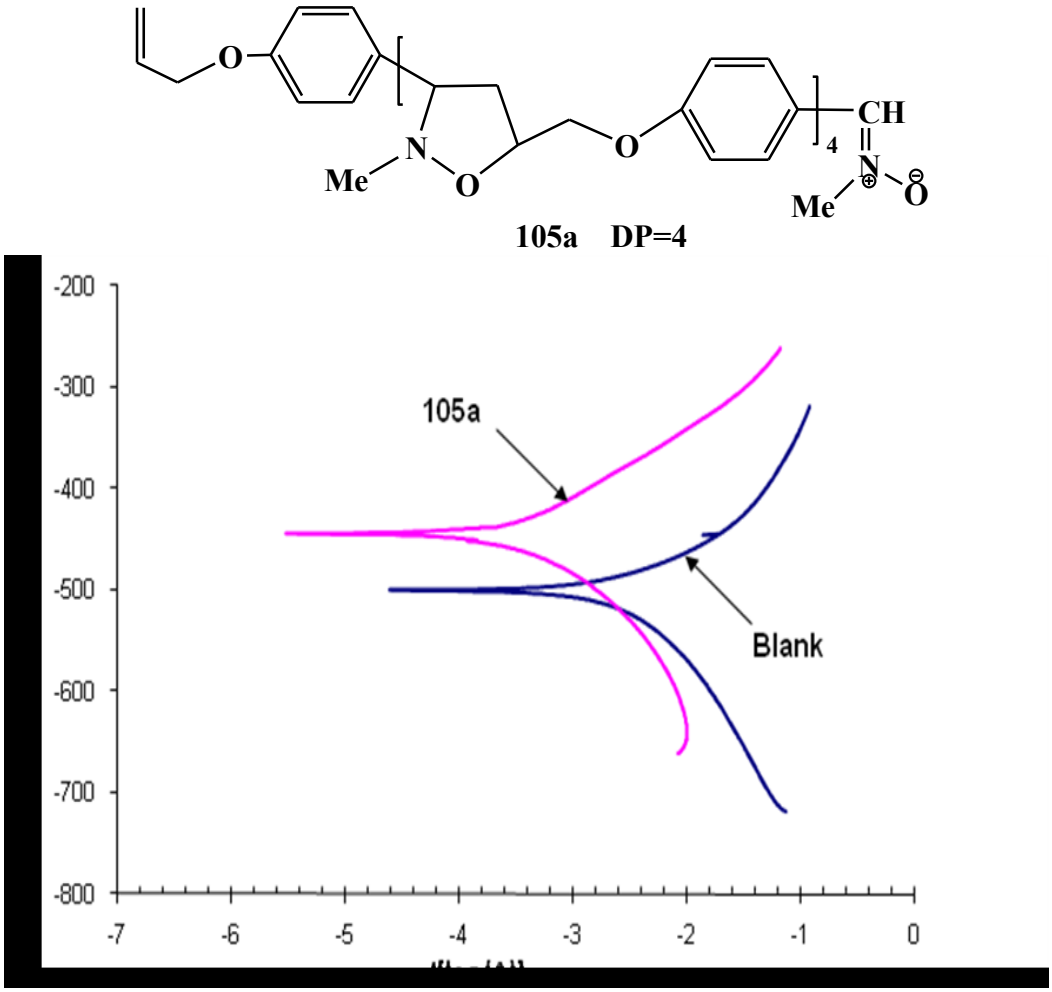

Figure 24. Potentiodynamic polarization curves for mild steel in 1 M HCl + 2 ml DMF (blank) and 1 M HCl + 2 ml containing 200 ppm of the polyisoxazolidine **105a** of DP = 4 at 60 ^{o}C**.**

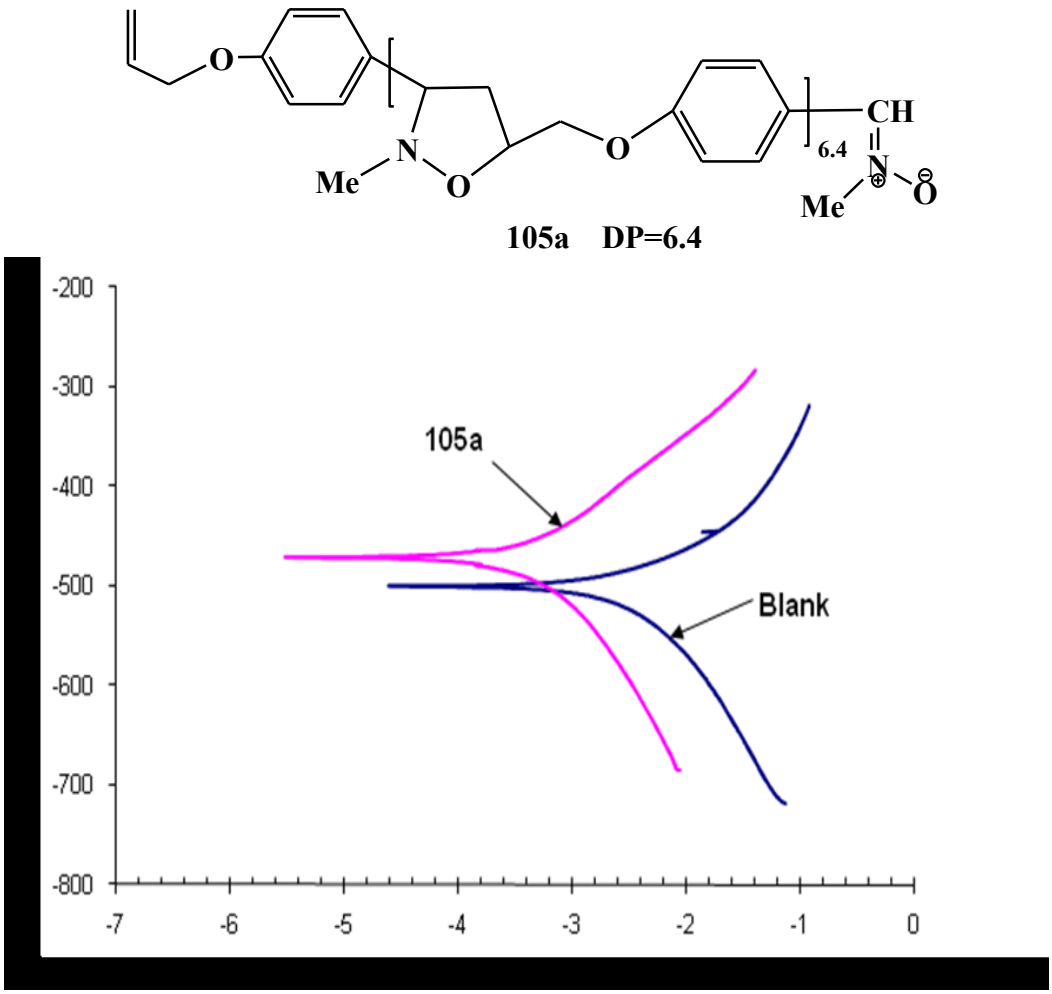

Figure 25. Potentiodynamic polarization curves for mild steel in 1 M HCl + 2 ml DMF (blank) and 1 M HCl + 2 ml containing 200 ppm of the polyisoxazolidine **105a** of DP = 6.4 at 60 ^{o}C**.**

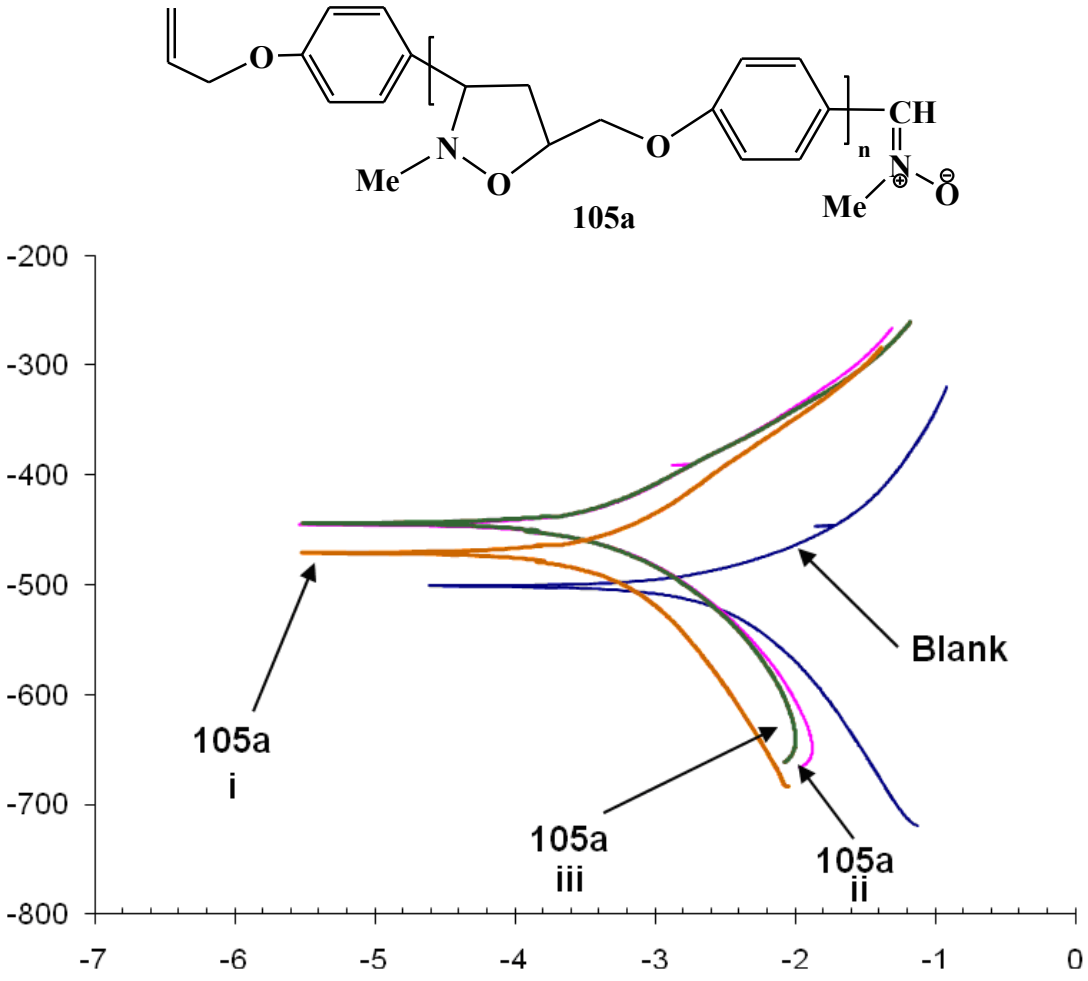

Figure 26. Potentiodynamic polarization curves for mild steel in 1 M HCl + 2 ml DMF (blank) and 1 M HCl + 2 ml containing 200 ppm of the polyisoxazolidine **105a** (i), **105a** (ii) and **105a** (iii) of DP = 2, 4, and 6 respectively at 60 ^{o}C.

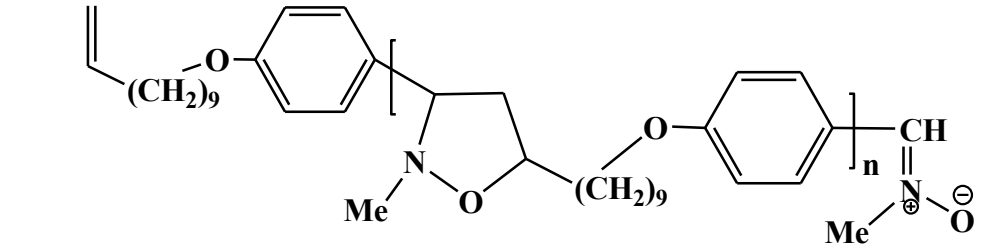

105b

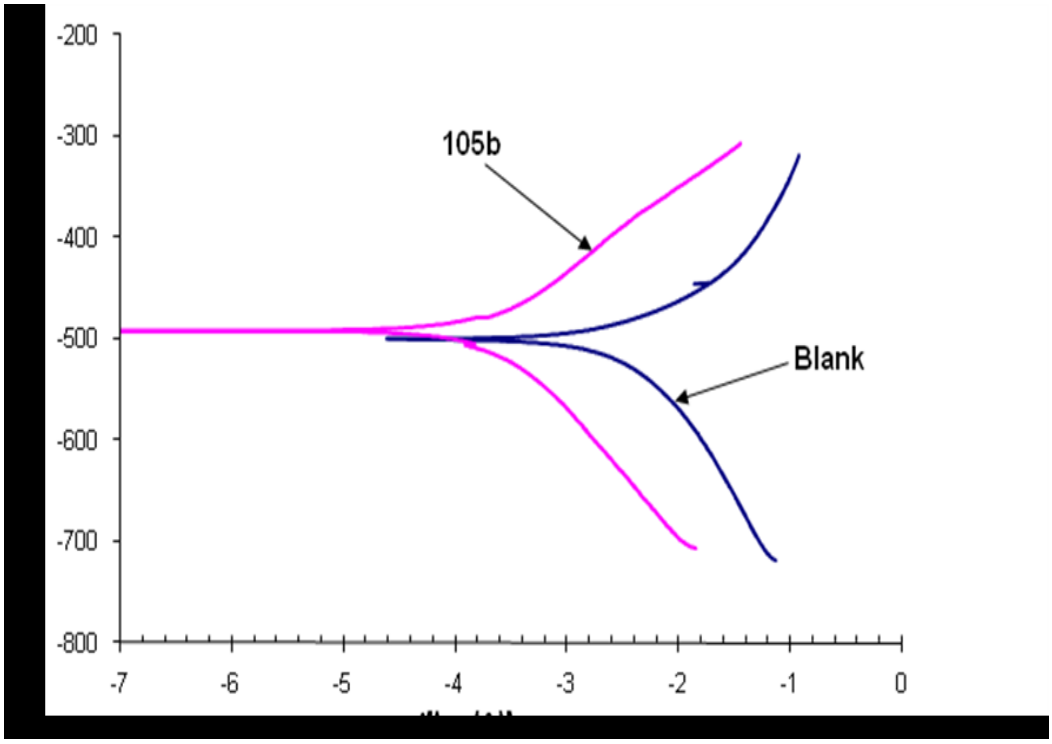

Figure 27. Potentiodynamic polarization curves for mild steel in 1M HCl + 2 ml DMF (blank) and 1 M HCl + 2 ml containing 200 ppm of the polyisoxazolidine **105b** at 60 ^{o}C.

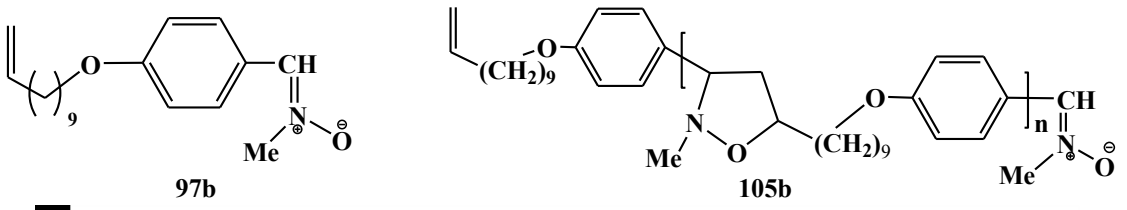

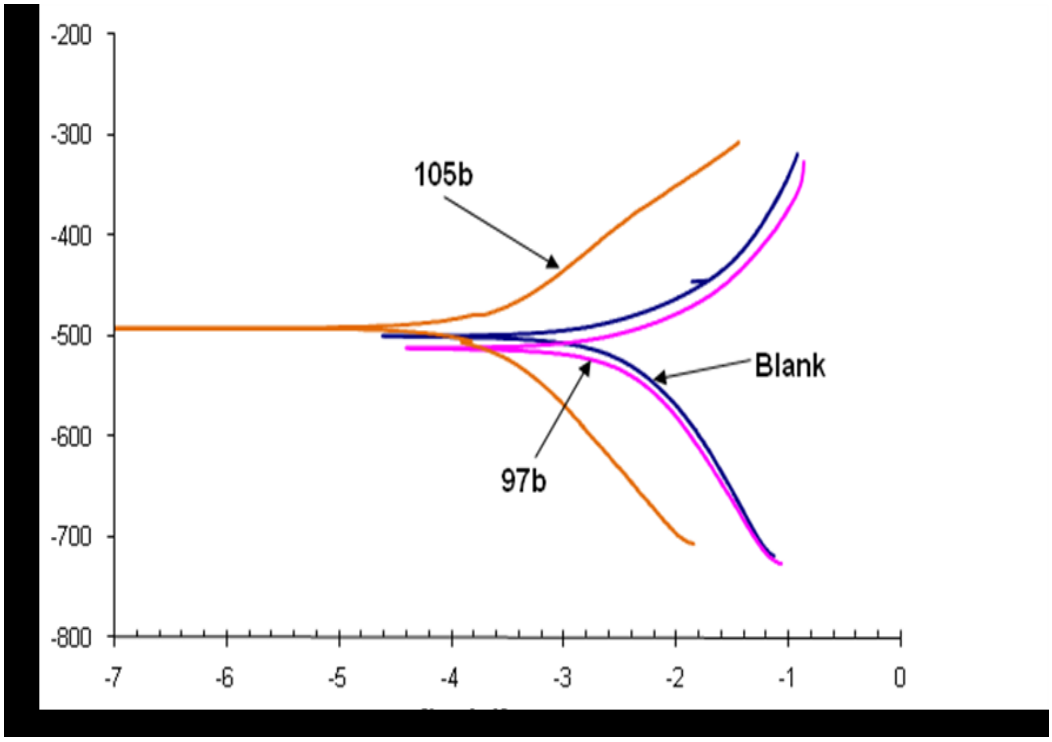

Figure 28. Potentiodynamic polarization curves for mild steel in 1M HCl + 2 ml DMF (blank) and 1 M HCl + 2 ml containing 200 ppm of the monomer **97b** and polyisoxazolidine **105b** at 60 ^{o}C.

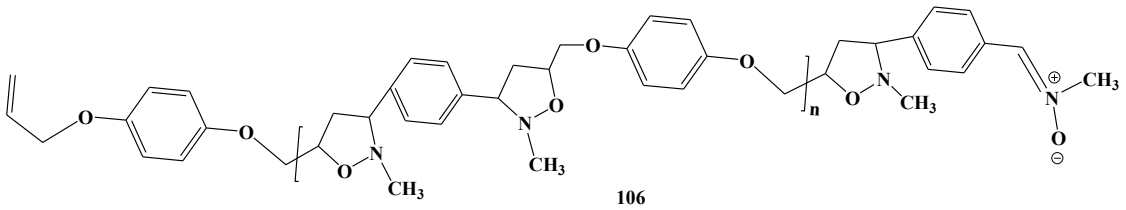

106

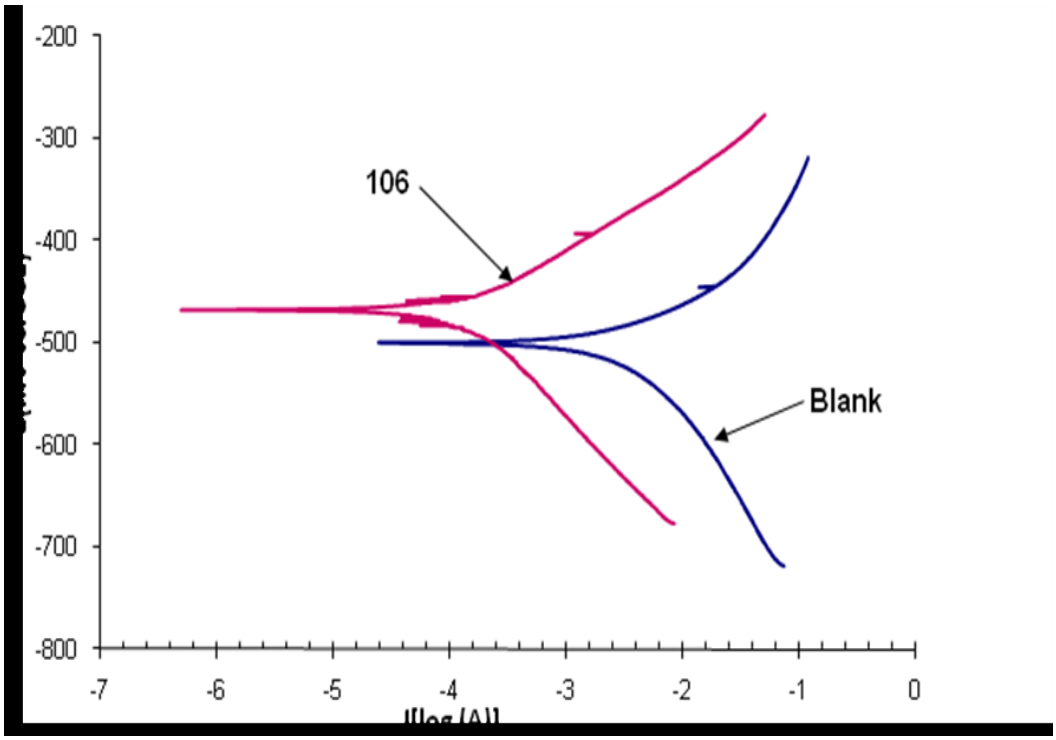

Figure 29. Potentiodynamic polarization curves for mild steel in 1M HCl + 2 ml DMF (blank) and 1 M HCl + 2 ml containing 200 ppm of the polyisoxazolidine **106** at 60 ^{o}C.

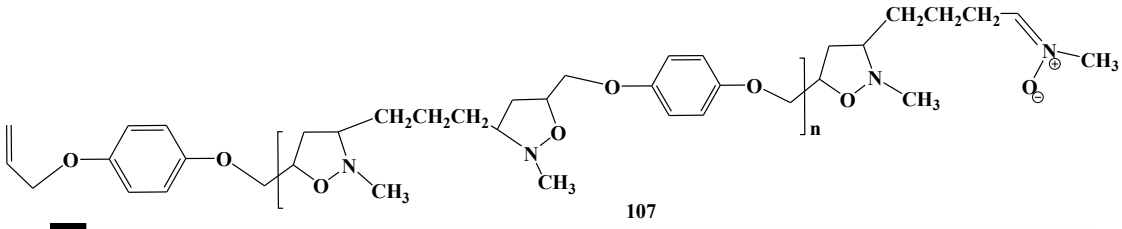

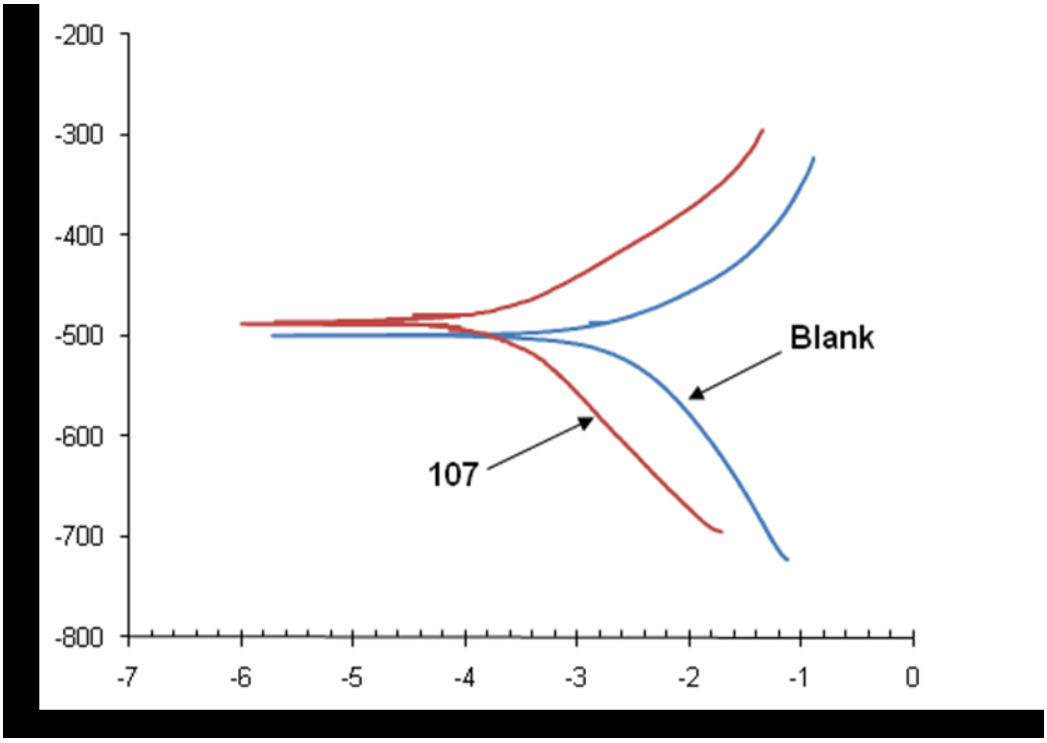

Figure 30. Potentiodynamic polarization curves for mild steel in 1 M HCl (blank) and 1 M HCl containing 200 ppm of the polyisoxazolidine **107** at 60 ^{o}C.

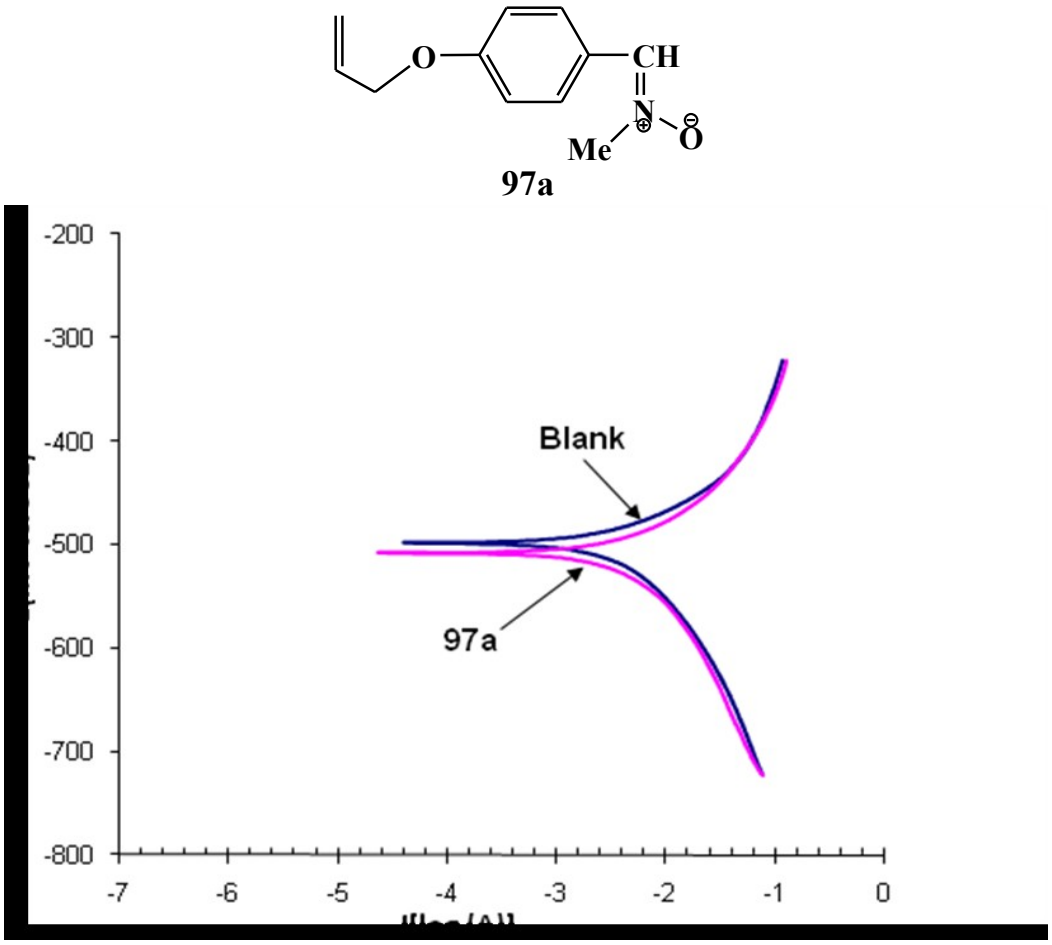

Figure 31. Potentiodynamic polarization curves for mild steel in 0.5 M H_2SO_4 (blank) and 0.5 M H_2SO_4 containing 200 ppm of the monomer **97a** at 60 ^oC.

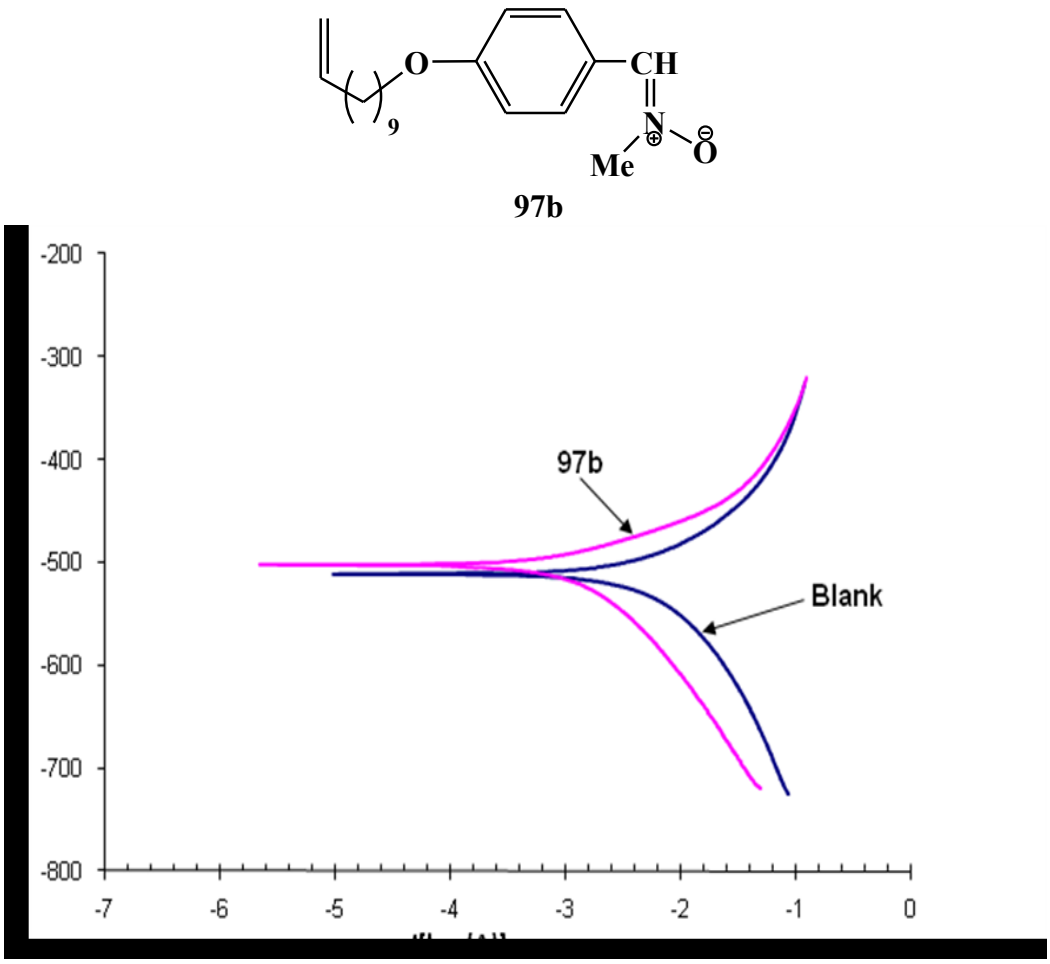

Figure 32. Potentiodynamic polarization curves for mild steel in 0.5 M H_2SO_4 + 2 ml DMF (blank) and 0.5 M H_2SO_4 + 2 ml DMF containing 200 ppm of the monomer **97b** at 60 ^{o}C.

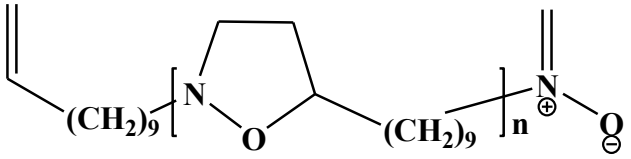

104a

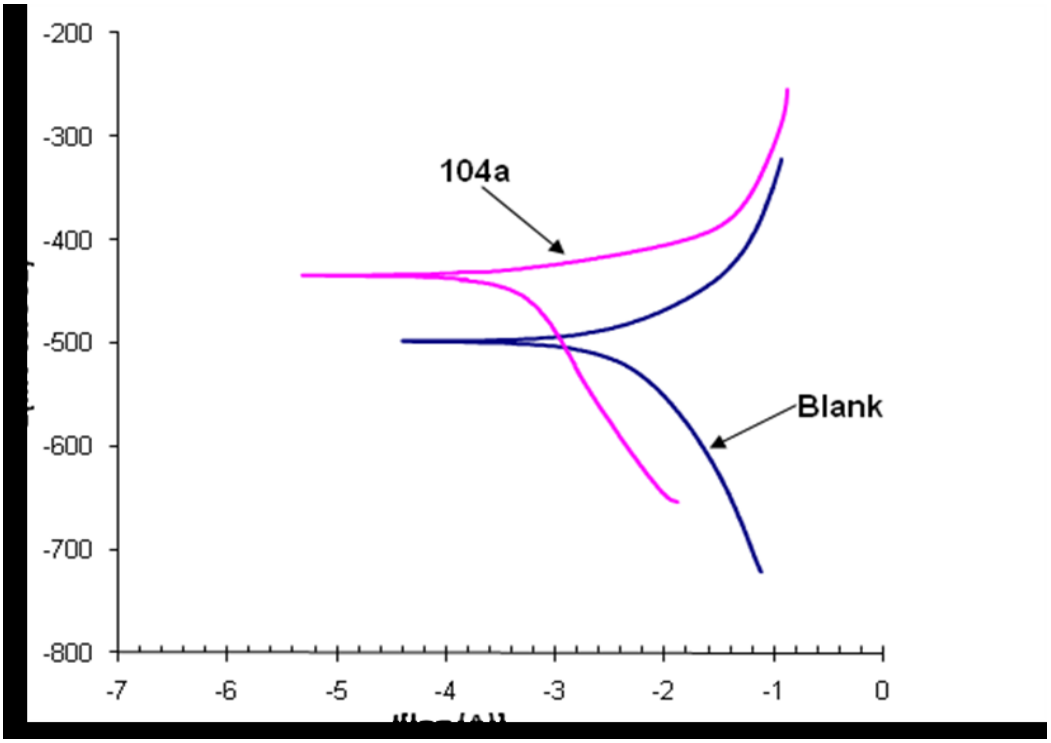

Figure 33. Potentiodynamic polarization curves for mild steel in 0.5 M H_2SO_4 (blank) and 0.5 M H_2SO_4 containing 200 ppm of the polyisoxazolidine **104a** at 60 ^oC.

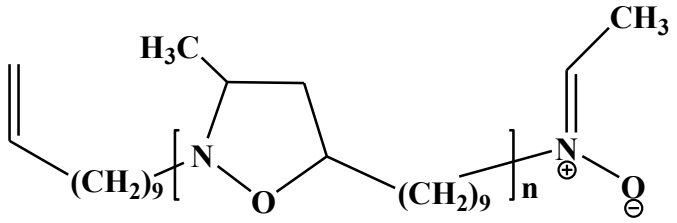

104b

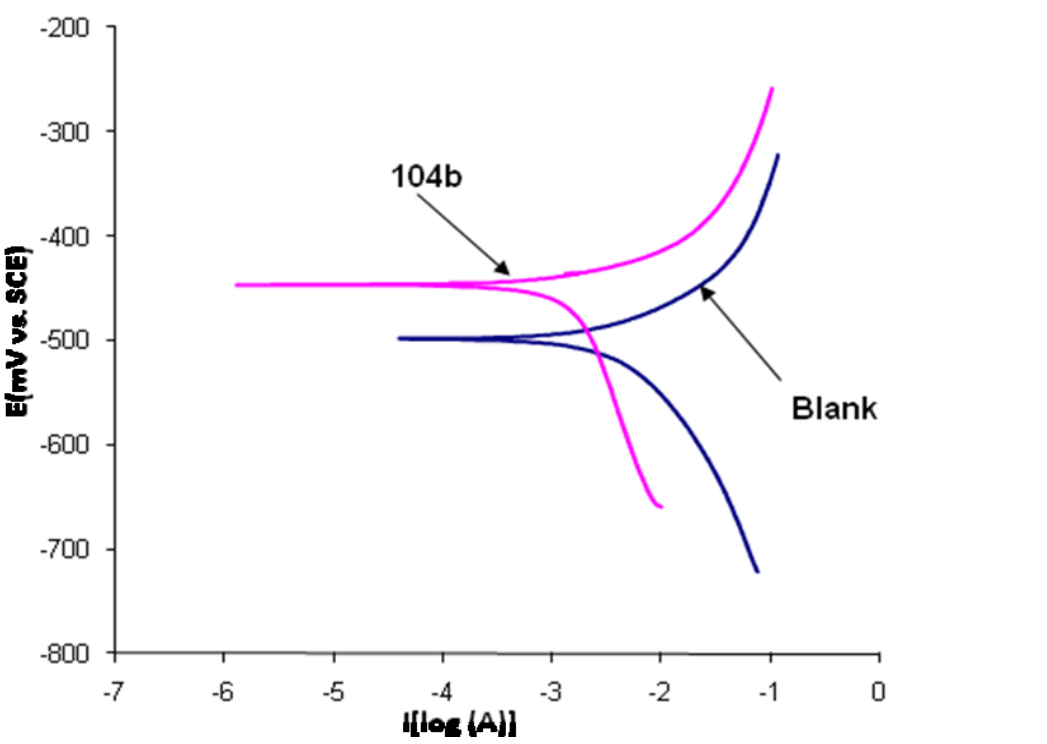

Figure 34. Potentiodynamic polarization curves for mild steel in 0.5 M H_2SO_4 (blank) and 0.5 M H_2SO_4 containing 200 ppm of the polyisoxazolidine **104b** at 60°C.

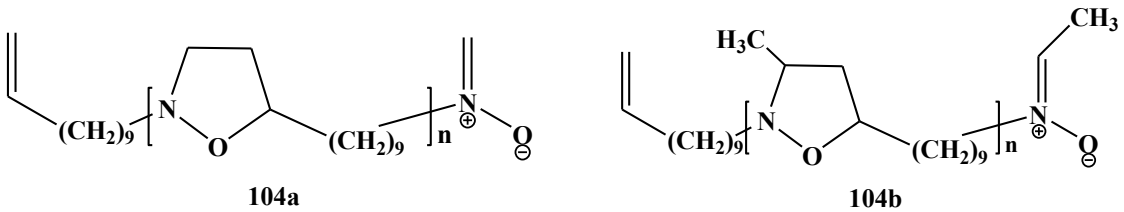

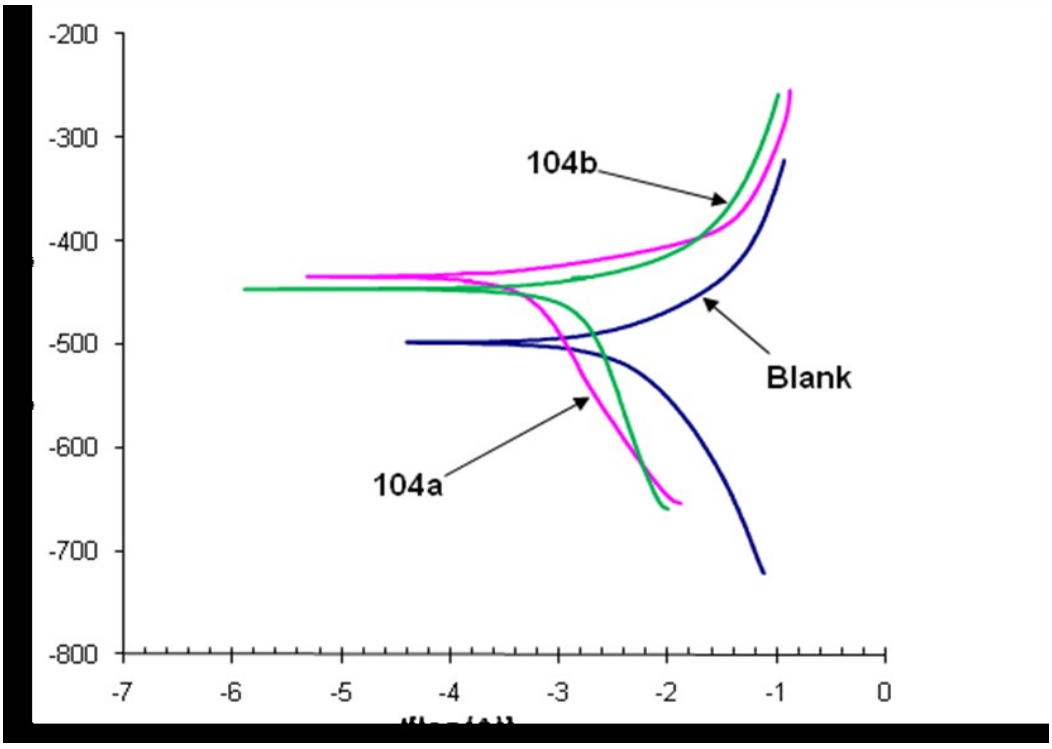

Figure 35. Potentiodynamic polarization curves for mild steel in 0.5 M H_2SO_4 (blank) and 0.5 M H_2SO_4 containing 200 ppm of the polyisoxazolidines **104a** and **104b** at 60^{o}C.

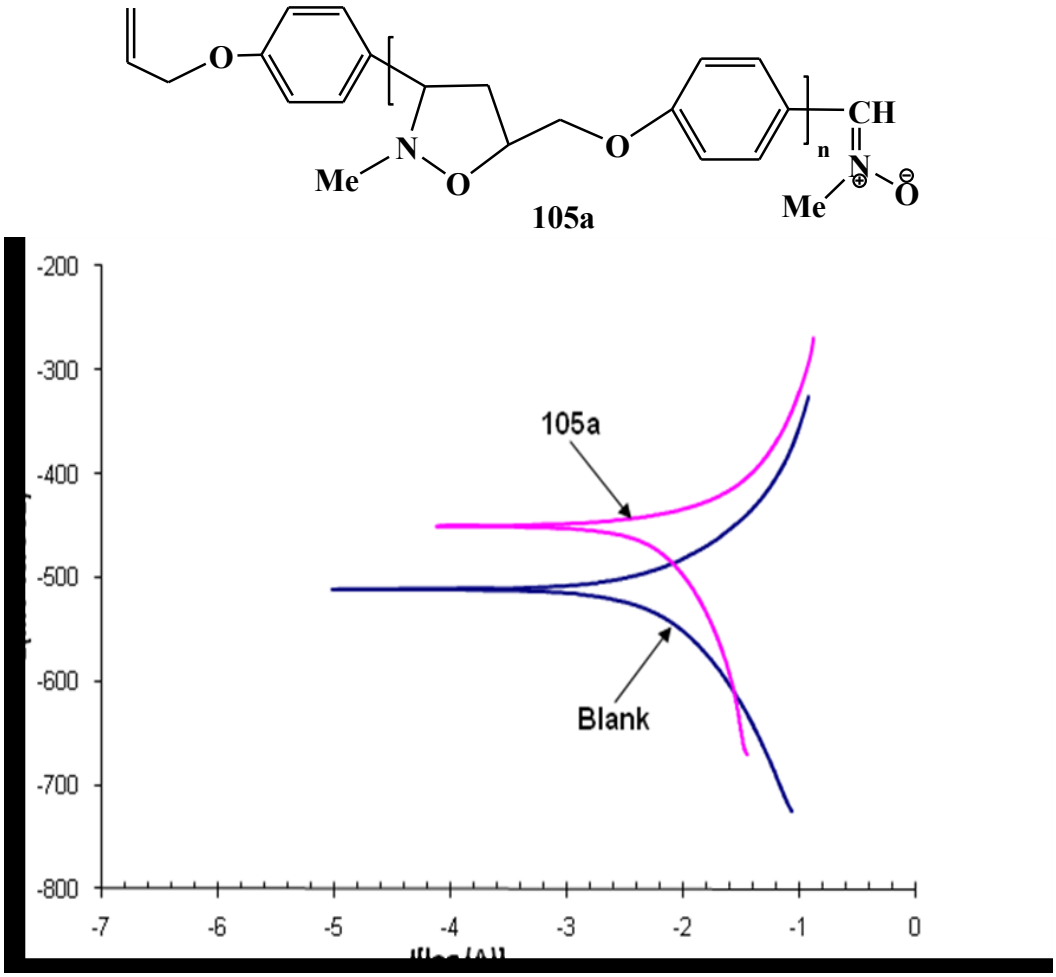

Figure 36. Potentiodynamic polarization curves for mild steel in 0.5 M H_2SO_4 + 2 ml DMF (blank) and 0.5 M H_2SO_4 + 2 ml DMF containing 200 ppm of the polyisoxazolidine **105a** at 60 ^{o}C.

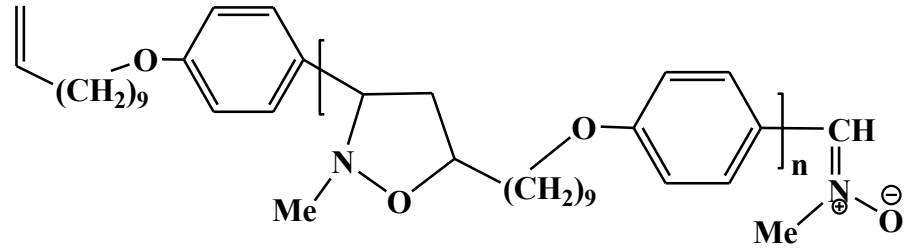

105b

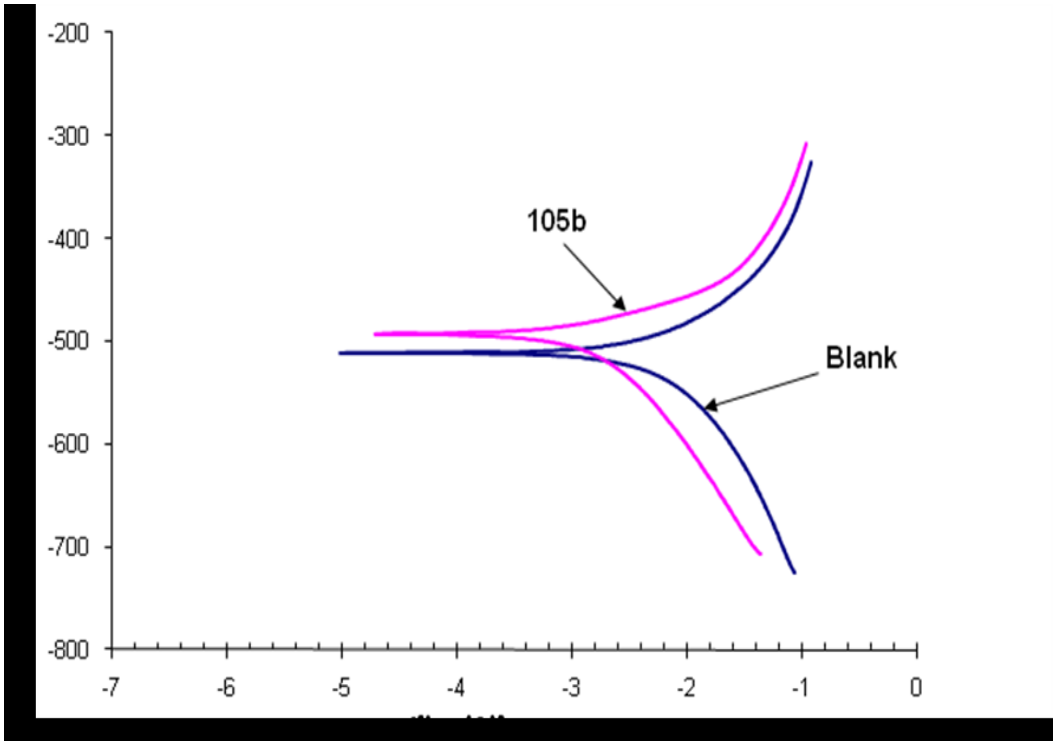

Figure 37. Potentiodynamic polarization curves for mild steel in 0.5 M H_2SO_4 + 2ml DMF (blank) and 0.5 M H_2SO_4 + 2 ml DMF containing 200 ppm of the polyisoxazolidine **105b** at 60 ^oC.

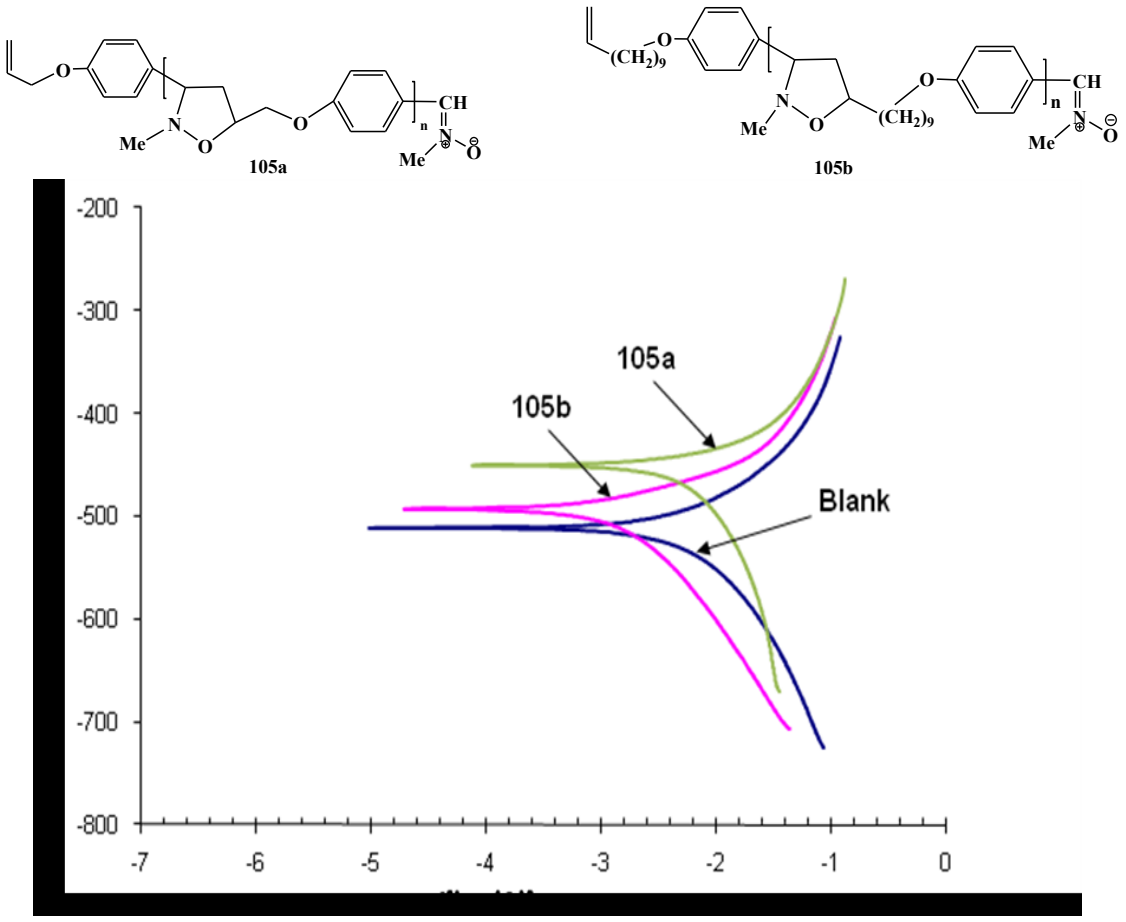

Figure 38. Potentiodynamic polarization curves for mild steel in 0.5 M H_2SO_4 + 2 ml DMF (blank) and 0.5 M H_2SO_4 + 2 ml DMF containing 200 ppm of the polyisoxazolidines **105a** and **105b** at 60 ^{o}C.

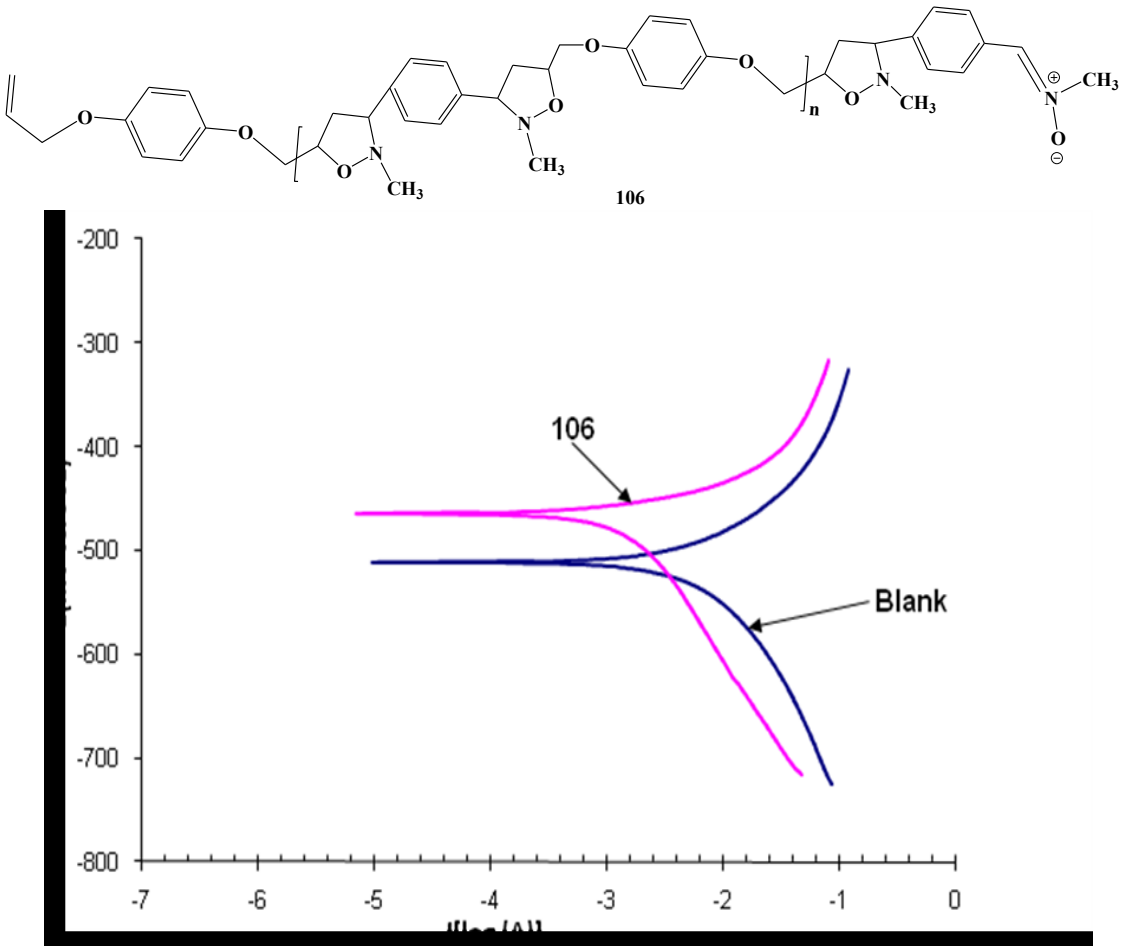

Figure 39. Potentiodynamic polarization curves for mild steel in 0.5 M H_2SO_4 + 2 ml DMF (blank) and 0.5 M H_2SO_4 + 2 ml DMF containing 200 ppm of the polyisoxazolidine **106** at 60 ^oC.

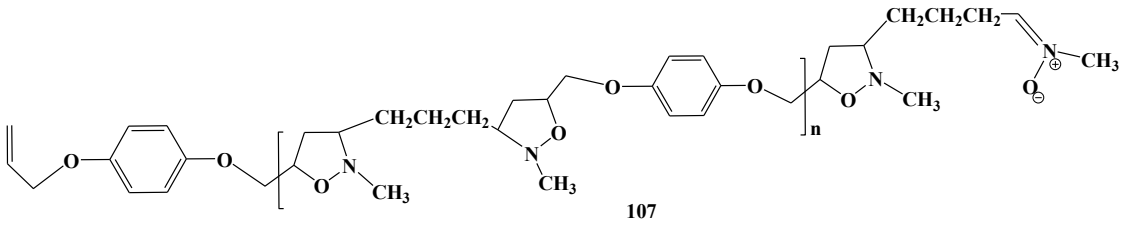

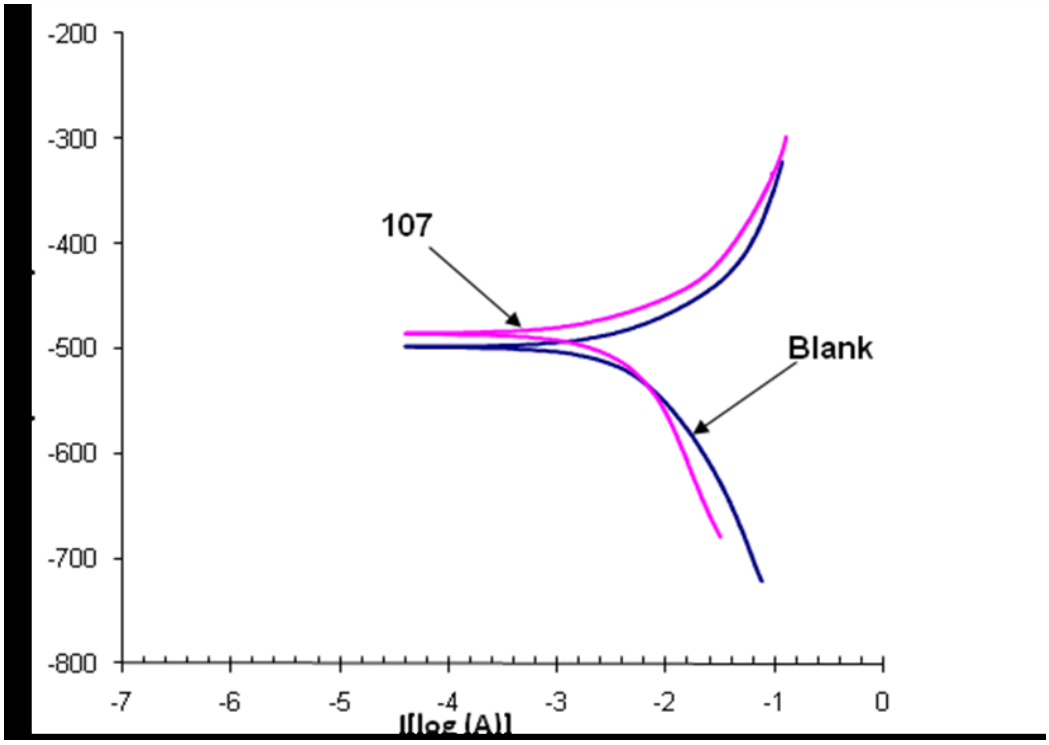

Figure 40. Potentiodynamic polarization curves for mild steel in 0.5 M H_2SO_4 (blank) and 0.5 M H_2SO_4 containing 200 ppm of the polyisoxazolidine **107** at 60 ^oC.

4.8. Discussion

The newly synthesized inhibitor oligomers have been tested for their %IEs by various methods. The results of the inhibition study in 1 M HCl and 0.5 M H_2SO_4 at 60°C using gravimetric method are given in Table 5. Gravimetric method is indeed the most simple and reliable method for the determination of inhibition efficiency, nonetheless the results (Tables 6-9) for the inhibition efficiency by the electrochemical method using Tafel plots corroborate the results from gravimetric method.

All the oligomers used in this study are highly surface-active and showed excellent inhibition of corrosion in 1 M HCl (Table 5); the inhibitor **104b** achieved inhibition efficiencies of ~ 99% in the presence of 400 ppm. Most of the inhibitors achieved maximum efficiencies at a concentration of 50 ppm, thereafter the %IE is leveled off upon further increasing the inhibitor concentrations. The decrease in %IE for **105b**, in comparison with **105a**, could be attributed to the solubility problem associated with the longer chain length. It is worth mentioning that the dimer, tetramer and hexamers of **105a** gave similar protection in the acidic media. Note that the molecules **97a** and **97b**, the corresponding monomers of the oligomeric **105a** nad **105b**, gave considerably lower %IEs (Table 5).

While the cationic ammonium compounds are known to be very effective inhibitors in HCl against corrosion of mild steel, these are not good inhibitors in plain sulfuric acid media as a result of the sulfate ions being strongly adsorbed on the metal surface, thereby leaving less space available for the inhibitor molecules to adsorb[82].

Several derivatives of indoles[83], azoles[84], triazoles[85] and a quaternary ammonium salt[86] have been shown to be moderately effective, while a group of isoxazolidines demonstrated better efficiency in arresting corrosion of steel in sulfuric acid media[14,87-89]. Note that the inhibitors **105a** demonstrated very good protection both in HCl as well as H_2SO_4 media, while its corresponding monomer **97a** faired very poorly.

The results obtained from the Tafel plots and linear polarizations (Table 6-9) corroborated the findings of the gravimetric method. The oligomers gave very good to excellent protection while the monomers **97a** (Table 6) and **97b** (Table 7) faired poorly. The presence of inhibitors has resulted in lowering the corrosion current density significantly, thereby confirming their inhibitive nature. It is evident from the Tafel plots of the compounds that the inhibitor adsorption shifted the corrosion potential (E_{corr}), in most cases (Table 6) in the negative direction with reference to the blank in 1 M HCl, signifying that suppression of the cathodic reaction is the main effect of these corrosion inhibitors.

The Tafel plots in 0.5 M H_2SO_4 (Tables 8 and 9) revealed that the inhibitor adsorption shifted the corrosion potential (E_{corr}) in the noble (less negative) direction with reference to the blank, signifying that suppression of the anodic reaction is the main effect of these corrosion inhibitors.

4.9. Conclusions

A study of oligiomerization involving a new series of alkene-nitrones, dinitrones, and dialkenes has been carried out. This has given us the isoxazolidine-based inhibitor molecules of lower degree of polymerization. One of the objectives of the study was to find out inhibitor molecules that would provide effective protection of corrosion of mild steel in HCl as well as H_2SO_4 media. This is a preliminary study; however, it paves the way to investigate further to prepare molecules having higher degree of polymerization. The study indeed reflected the scope and limitation inherent in the cycloaddition of the alkene-nitrones in the current study. The precedent literature always used activated alkenes, so the cycloaddition rates were faster than the ones observed in our cycloaddition reaction involving nonactivated alkenes. The activating group in an alkene is the presence of electron withdrawing groups like ester, anhydride or amide groups. However, one of the disadvantages of these carbonyl terminals is their hydrolytic instability. Even though our alkenes are less reactive, but they do not contain hydrolytically unstable alkene substituents. The study has also revealed that the methylene nitrone are much more reactive than the more substituted nitrones. Hence, any future study must utilize the methylene nitrones (monosubstituted) and monosubstitued alkene of the alkene-nitrone type A-N, and should avoid the dialkene-dinitrone cycloaddition as it is very difficult to maintain stoichiometry. The reactivity of the cycloadditions may be improved using Lewis acid catalysts.

CHAPTER 5

EXPERIMENTAL

5.1. General

All mps are uncorrected. Melting points were recorded in a calibrated Electrothermal-IA9100-Digital Melting Point Apparatus. IR spectra were recorded on a Perkin Elmer 16F PC FTIR spectrometer. ^{1}H and ^{13}C NMR spectra were measured in $CDCl_3$ using TMS as internal standard on a JEOL LA 500 MHz NMR spectrometer operating at 500.00 MHz. Silica gel chromatographic separations were performed with silica gel 100 from Fluka Chemie AG (Buchs, Switzerland). All the starting materials were purchased from Aldrich Chemical Company and were used as received without any further purification. All the solvents were of reagent grade. Dichloromethane was passed through alumina before use. All reactions were carried out under N_2.

5.2. N-(10-undecenyl) hydroxylamine (91)

In a round bottom flask were taken hydroxylamine hydrochloride (34.0 g, 489.3 mmol), sodium hydroxide (17.5 g, 437.5 mmol) and ethanol (200 cm^3). The mixture was stirred using a magnetic stir bar at room temperature for about 10 minutes. The mixture became homogeneous to give hydroxylamine alone. 11-Bromo-1-undecene **(90)** was added portion wise to the mixture and heated at 90 ^oC for 7 h. Approximately 180 cm^3 of Ethanol was then removed by distillation at 100 ^oC. Water was added to the mixture, basified by K_2CO_3 and the solution was extracted with ether (4 x 100 cm^3). The organic layer was dried using Na_2SO_4. The ether was removed by gentle steam of N_2 at 25 ^oC. The residual liquid was purified by chromatography over silica gel using 1:4 ether/hexane mixture as eluant to give hydroxylamine **91** as colorless liquid. Crystallizing the product

from ether/hexane gave a white hydroxylamine crystal. Hydroxylamine **91** crystals were dried under vacuum at ambient temperature (3.3 g, 29.8 %); Mp. 68-68.5 ^{o}C, $\nu_{max.}$ (neat) 3261, 3152, 3078, 2921, 2850, 1642, 1559, 1508, 1461, 1377, 1149, 1058, and 721 cm^{-1}; δ_H ($CDCl_3$): 1.28-1.52 (16H, m), 2.03 (2H, m, *J* 7 Hz), 2.91(2H, t, *J* 7.35 Hz), 4.91 (2H, q, *J* 9.15), 5.80 (1H, m, *J* 6.7). δ_C($CDCl_3$): 26.77, 27.10, 28.92, 29.11, 29.34, 29.43, 29.49, 33.80, 53. 76, 114.13, 139.21.

5.3. N-(10-undecenyl) methylideneamine N-oxide (93a)

To a solution of the hydroxylamine **91** (1.51 g, 8.15 mmol) in toluene (10 cm^3) was added paraformaldhyde (**92a)** (317.85 mg, 10.60 mmol) and the mixture was stirred using a magnetic stir bar at 75 ^{o}C for 1 h or until the complete conversion of the hydroxylamine to the corresponding nitrone N-(10-undecenyl) methylideneamine N-oxide **(93a)**. The mixture was filtered to get rid of the excess white solid paraformaldhyde. The alkene-nitrone was used in the next step without further purification. δ_H ($CDCl_3$): 1.23-1.33(12H, m), 1.91 (2H, p), 2.02 (2H, t, J 7.5 Hz), 3.78 (2H, t, J 7.35), 4.91 (2H, q, J 10.3 Hz), 5.77 (1H, m), 6.31 (1H, d, 7.7 Hz), 6.49 (1H, d, 7.7 Hz).

5.4. N-(10-undecenyl) 1-ethylideneamine N-oxide (93b)

Distilled acetaldehyde (**92b)** (313 mg, 8.41 mmol) was added to a solution of the hydroxylamine **91** (1.2 g, 6.47 mmol) in ethanol (10 cm^3). The reaction mixture was stirred using a magnetic stir bar at room temperature for about 2 h or until the nitrone **93b** was formed. At the end of the reaction, ethanol was removed by a gentle steam of N_2 at 40 ^{o}C. Crystallizing the nitrone from hexane give a white crystal but the melting point is very low. $\nu_{max.}$ (neat) 3416, 3076, 2921, 2852, 1732, 1640, 1606, 1461, 1350, 1183, 1103, 994 and 456 cm^{-1}; δ_H ($CDCl_3$): 1.27-1.36 (12H, m), 1.90 (2H, t), 2.00-2.04 (5H, m), 3.73 (2H, t, *J* 7.05 Hz), 4.91 (2H, q, *J* 10.1 Hz), 5.79 (1H, m), 6.75 (1H, q, *J* 5.8 Hz).

$\delta_C(CDCl_3)$: 12.43, 26.26, 27.23, 28.67, 28.83, 28.89, 29.15, 29.16, 33.56, 65.11, 113.94, 134.11, 138.90.

5.5. *p*-Allyloxybenzaldehyde (96a)

To a stirring solution of sodium ethoxide (0.13 mol; prepared by adding 3.0 g sodium) in ethanol (65 cm^3) was added *p*-hydroxybenzaldehyde **(94)** (15.9 g, 0.13 mmol) at 20°C. After the mixture became homogeneous (*ca.* 5 min), allyl bromide (**95)** (15.7 g, 0.13 mol) was added and the mixture was heated in a closed vessel at 65°C for 12 h. Within an hour, the formation of NaBr was visible on the wall of the flask. After removal of most of the ethanol by a gentle stream of N_2, the residual mixture was taken up in ether (50 cm^3) and washed with water (2x100 cm^3), 5% NaOH solution (2x50 cm^3), followed again by water (2x50 cm^3). The organic layer was dried (Na_2SO_4) and concentrated to give *p*-allyloxybenzaldehyde (**96a)** (18.7 g, 88.7%) as a brown liquid. ^{1}H NMR spectrum revealed the product as very pure and as such used without further purification. (Found: C, 74.0; H, 6.1. $C_{10}H_{10}O_2$ requires C, 74.06; H, 6.21%); $\nu_{max.}$ (neat) 3076, 2828, 2737, 1687, 1600, 1577, 1508, 1458, 1424, 1392, 1364, 1312, 1258, 1161, 1111, 996, 932, 857, 832, 761, and 656 cm^{-1}; δ_H ($CDCl_3$): 4.63 (2H, d, *J* 5.2 Hz), 5.35 (2H, m), 6.05 (1H, m), 7.02 (2H, d, *J* 8.7 Hz), 7.83 (2H, d, *J* 8.8Hz), 9.89 (1H, s); $\delta_C(CDCl_3)$: 69.00, 115.00 (2C), 118.37, 130.02, 131.97 (2C), 132.28, 163.60, 190.82.

5.6. *p*-10-Undecen-1-yloxybenzaldehyde (96b)

The above procedure was repeated with 11-bromo-1-undecene (**90**) (15.2 g, 0.065 mol); half the quantity of the other materials was used. The temperature of the reaction was maintained at 65 °C for 12 h and at 90 °C for a further period of 12 h in a closed vessel. Similar workup procedure afforded the *p*-10-undecen-1-yloxybenzaldehyde **96b** (15.7 g, 88%) as a brown liquid. ^{1}H NMR spectrum revealed the product as very pure and as such used without further purification. (Found: C, 78.6; H, 9.4. $C_{18}H_{26}O_2$ requires C, 78.79; H,

9.55%). $\nu_{max.}$ (neat) 3074, 2926, 2853, 2733, 1693, 1640, 1601, 1577, 1509, 1467, 1429, 1393, 1311, 1258, 1216, 1160, 1109, 1015, 910, 832, 723 and 617 cm-1; δ_H ($CDCl_3$): 1.20-1.60 (12 H, m), 1.82 (2H, quint, *J* 6.8 Hz), 2.04 (2H, q, *J* 7.0 Hz), 4.04 (2H, t, *J* 6.6 Hz), 4.96 (2H, m), 5.81 (1H, m), 6.98 (2H, d, *J* 8.6 Hz), 7.82 (2H, d, *J* 8.8 Hz), 9.88 (1H, s). δ_C($CDCl_3$): 25.95, 28.91, 29.05, 29.10, 29.32, 29.41, 29.48, 33.80, 68.41, 114.16, 114.75 (2C), 129.74, 131.99 (2C), 139.17, 164.27, 190.80.

5.7. N-methyl-(*p*-Allyloxyphenyl)methylideneamine N-oxide (97a)

4-Allyloxy-benzaldehyde (**96a)** (5.057 g, 31.17 mmol), absolute ethanol (30 cm^3), N-methyl hydroxylaminehydrochloride (4.026 g, 48.21 mmol) and sodium acetate.$3H_2O$ (7.094 g, 52.13 mmol) were placed in 100 ml around bottom flask, and the mixture was stirred for about 1 h at room temperature. After removal of the solvent by blowing a gentle stream of N_2 at 40 ^oC, the solid residue was transferred to separatory funnel with dichloromethane (25 cm^3) and diluted with water (15 cm^3). At the end of the reaction, the solution was basified by K_2CO_3 and extracted with dichloromethane (4 x 25 cm^3). The organic layer was dried over $MgSO_4$ and then filtered. A gentle stream of N_2 at 40 ^oC was used to remove dichloromethane and the solution was crystallized from dichloromethane/ether/little pentane at room temperature. The crystals were dried under vacuum at room temperature to give nice white crystals (4.4599 g, 74.75%); Mp. 81.5-83.4 ^oC, $\nu_{max.}$ (KBr) 3425, 2984, 1598, 1504, 1417, 1306, 1249, 1161, 991, 938, 879 and 839 cm^{-1}; δ_H ($CDCl_3$): 3.83 (3H, s), 4.56 (2H, d, *J* 4.85 Hz), 5.29 (1H, d, *J* 10.35 Hz), 5.4011 (1H, d, *J* 17.4), 6.04 (1H, m), 6.93 (2H, d, *J* 8.55), 7.29 (1H, s), 8.19 (2H, d, *J* 8.55). δ_C($CDCl_3$): 53.82, 68.65, 114.44 (2C), 117.91, 123.46, 130.26 (2C), 132.59, 134.78, 159.93.

5.8. N-methyl-*(p*-10-Undecen-1-yloxyphenyl)methylideneamine N-oxide (97b)

A solution of 4-(10-undecenyloxy)benzaldehyde **(96b)** (2.765 g, 10.076 mmol), absolute ethanol (20 cm^3), N-methylhydroxylamine hydrochloride (1.34 g, 16.044 mmol) and sodium acetate.$3H_2O$ (1.77 g, 13 mmol) was stirred in a closed vessel at room temperature for about 15 minutes or until the TLC (silica, ether) indicated the presence of the nitrone. Another portion of 4-(10-undecenyloxy) benzaldehyde **(96b)** (1.15 g, 4.19 mmol), N-methyl hydroxylamine hydrochloride (0.417 g, 4.99 mmol) and sodium acetate.$3H_2O$ (0.680 g, 5.00 mmol) was added to the vessel and stirred for about 30 minutes. The solution was extracted with dichloromethane (4 x 30 cm^3) and the organic layer was dried over $MgSO_4$. The dichloromethane was removed by gentle steam of N_2 at 40 ^oC, crystallized from hexane/ether and dried under vacuum at ambient temperature to give white crystals (2.99 g, 76.37 %); Mp. 72-72.8 ^oC, $\nu_{max.}$ 3448, 2924, 2849, 2366, 1599, 1502, 1467, 1420, 1303, 1250, 1167 and 942 cm^{-1}; δ_H ($CDCl_3$): 1.29-1.60 (12H, m), 1.80 (2H, p, *J* 6.4 Hz), 2.05 (2H, t, *J* 6.75 Hz), 3.84 (3H, s), 3.99 (2H, t, *J* 6.7 Hz), 4.98 (2H, m), 5.82 (1H, m), 6.93 (2H, d, *J* 8.85 Hz), 7.26 (1H, s), 8.18 (2H, d, *J* 9.2 Hz). δ_C($CDCl_3$): 25.92, 28.84, 29.04, 29.08, 29.29, 29.34, 29.43, 33.74, 53.85, 68.01, 114.07 (2C), 114.26, 123.17, 130.33 (2C), 134.89, 139.15, 160.64.

5.9. *p*-Diallyloxybenzene (99)

In around bottom flask were taken *p*-dihydroxybenzene **(98)** (14.822 g, 134.61 mmol) and ethanol (140 cm^3). The mixture was stirred using a magnetic stir bar at room temperature and the *p*-dihydroxybenzene was dissolved immediately to give homogeneous mixture. After adding the first portion of sodium hydroxide (5.3176 g, 132.94 mmol) and allyl bromide **(95)** (16.35 g, 135.12 mmol), the color of the mixture was turned to dark brown. The mixture was heated in a closed vessel at 80^oC for 2 h and then the second portion of sodium hydroxide (5.322 g, 133.05 mmol) and allyl bromide **(95**) (16.2991 g, 134.73 mmol) was added. After removal of most of the ethanol by a gentle stream of N_2, the residual mixture was taken up in hexane (100 cm^3), washed with

5% NaOH solution (40 cm^3) and extracted with water and 5% NaOH solution. At the end of the reaction, most of the hexane was removed by blowing N_2 and the product was dried under vacuum distillation at 115 ^oC to give nice orange liquid product (10 g, 40%); $\nu_{max.}$ (KBr) 3425, 3019, 2909, 2861, 1858, 1649, 1506, 1284, 1226, 1024, 931, 824, and 788; δ_H ($CDCl_3$): 4.51 (4H, d, *J* 5.2 Hz), 5.30 (2H, d, *J* 10.65 Hz), 5.42 (2H, d, *J* 17.07), 6.088 (2H, m), 6.86 (4H, s).

5.10. *N,N'*-dimethyl-*p*-phenylenedinitrone (101)

Terephthaladehyde **(100)** (7.06 g, 52.6 mmol), N-methyl hydroxylamine hydrochloride (11.931 g, 142.85 mmol), sodium acetate.$3H_2O$ (23.65 g, 173.8 mmol) and ethanol (150 cm^3) were placed in a round bottom flask, and the mixture was stirred for about 18 h at 50 ^oC. After removal of the solvent by blowing a gentle stream of N_2 at 70 ^oC, the solution was basified by K_2CO_3 and extracted with boiling dichloromethane. At the end of the reaction, the solution was crystallized from dichloromethane/ether/little pentane at room temperature. The crystals were dried under vacuum at room temperature to give nice crystals (8.88 g, 87.85%); Mp. >250 ^oC, $\nu_{max.}$ (KBr) 3752, 3386, 3077, 2368, 1653, 1580, 1415, 1310, 1168, 937, 865, and 589; δ_H ($CDCl_3$): 3.90 (6H, s), 7.41 (2H, s), 8.25 (4H, s). δ_C($CDCl_3$): 54.58 (2 × CH_3), 128.29 (4 × Ar-C), 131.81 (2 × Ar-C), 134.66 (2 × N=C).

5.11. *N,N'*-Dimethyl-1,5- pentylidenedinitrone (103)

A solution of glutaraldehyde (pentanedial) **(102)** (15.356 g, 76.69 mmol), ethanol (150 cm^3), N-methyl hydroxylamine hydrochloride (13.42 g, 160.7 mmol) and sodium acetate.$3H_2O$ (22.0712 g, 162.2 mmol) was stirred in a closed vessel at room temperature for about 4 h. Most of the ehanol was removed by blowing N_2 The solution was extracted with dichloromethane (4 x 30 cm^3) and the organic layer was dried over ($MgSO_4$). The mixture was washed with boiling $CHCl_3$ which was removed by blowing a gentle stream of N_2. At the end of the reaction, the solution was crystallized from Methanol/ether at

room temperature. $\nu_{max.}$ (KBr) 3750, 3245, 3041, 2927, 2869, 1603, 1432, 1403, 1044, 1174, 1121, 920; δ_H ($CDCl_3$): 1.66 (2H, t, *J* 7.6 Hz), 2.33 (4H, m), 3.53 (6H, s), 7.16 (2H, t, *J* 4.85Hz). δ_C($CDCl_3$): 21.17 (2×CH_2), 26.37 (2×CH_2), 52.36 (2×CH3), 139.3 (2×C=N).

5.12. Poly(5-nonanyl isoxazolidine) (104a)

5.12.1.Kinetics at 65°C in $CDCl_3$

Kinetics of polymerization of the alkene-nitrone **93a** was carried out at 65°C for about 204 h. Thus, a mixture of the hydroxylamine **91** (55.6 mg, 0.280 mmol) and paraformaldehyde (**92a**) (18.6 mg, 0.6 mmol) in $CDCl_3$ (0.58 g) in an NMR tube was reacted and ^{1}H NMR spectra were recorded at various times. The reaction volume was determined to be 0.60 mL during the polymerization which translates into an initial concentration [M_o] of the monomeric nitrone **93a** as 0.280/0.60 or 0.467 M. The analysis of the proton spectra were used to determine the concentration of the polymer and end groups, and a plot of degree of polymerization versus time afforded the rate constant for the polymerization.

5.12.2. Polymerization at 80°C in Toluene

A solution of the hydroxylamine **91** (1.51 g, 8.15 mmol) and paraformaldehyde (**92a**) (321 mg, 10.7 mmol) in toluene (10 cm^3) was reacted at 80°C, and ^{1}H NMR spectra were recorded at various times. The reaction was stirred using magnetic stir bar and, after 24 h, the color of the reaction mixture became brownish. The toluene was removed and the residual mixture was dried under vacuum at room temperature to give brown gel material. $\nu_{max.}$ 3341, 3075, 2922, 2852, 1729, 1639, 1503, 1463, 1372, 1286, 908, and 787.

5.13. Poly(3-methyl-5-nonanylisoxazolidine) (104b)

In round bottom flask were taken monomer **93b** (92.3 mg, 0.437 mmol) and about 5 cm^3 of toluene and heated for 80 h at 100 ^oC. At the end of the polymerization, the toluene was removed by using CCl_4 and gentle stream of N_2 at about 60 ^oC and dried under vacuum at room temperature to give black gel material. $\nu_{max.}$ 3327, 3074, 2926, 2853, 1735, 1640, 1375, 1284, 1134, 1074, 993, 908, and 786.

5.14. Poly(2-methyl-5-methyleneoxy-*p*-phenylisoxazolidine) (105a)

Toluene (20 g) was heated at 120 ^oC to get rid of the moisture. Homopolymerization of the alkene-nitrone **97a** (3.01 g, 15.75 mmol) was carried out in toluene (10.327 g, 11.94 cm^3) (total volume 12.5 cm^3, i.e. 15.75/12.5 = 1.26 M) at 120 ^oC for about 125 h using magnetic stir bar for stirring the mixture, and this gave viscous brownish material. At several interval a portion of the reaction mixture was taken and exchanged with $CDCl_3$ and NMR recoreded to find out the concentration of several end groups and polymer repeating units. The polymer **105a** was dissolved in toluene at 100 ^oC and precipitated in methanol and hexane. Drying the polymer in a vacuum gave white solid polymer. $\nu_{max.}$(KBr) 3424, 2953, 2867, 2773, 2065, 1687, 1609, 1509, 1455, 1241, 1173, 1030, and 832.

5.15. Poly(2-methyl-5-nonanyloxy-*p*-phenylisoxazolidine) (105b)

Monomer **97b** (1.01 g, 3.33 mmol) in moisture-free toluene (5.97 g, 6.9 cm^3) (total volume 7.22 cm^3, i.e. 3.33/7.22 = 0.461 M) was homopolymerized for 162 h at 120 ^oC. After removing the solvent, the polymer was dissolved in dichloromethane at room temperature. The dichloromethane was removed by gentle stream of N_2 at 40 ^oC, and the polymer was precipitated in pentane and ether and dried under vacuum. $\nu_{max.}$ 3360, 3064, 2924, 2853, 2770, 1578, 1513, 1302, 1245, 1172, 1024, and 831.

5.16. Polymer 106

To avoid solubility problem, the polymerization was carried out in DMF. Thus a solution of the dialkene **99** (2.00 g, 10.5 mmol) and dinitrone **101** (2.02 g, 10.5 mmol) in DMF (total volume of the solution 13 cm^3) was heated at 120 ^oC for 140 h. The solution was thus 0.808 M in both the dialkene and dinitrone and the concentration of the alkene and nitrone functionalities will then be 2 × 0.808 i.e 1.62 M each. The ^1H NMR spectra were recorded at several intervals. The reaction mixture was precipitated in water and dried under vacuum to give polymer **106** as a white solid. $\nu_{max.}$ (KBr) 3415, 3048, 2952, 2868, 2770, 1608, 1506, 1455, 1342, 1223, 1111, 1038, 893, 824,708, and 546.

5.17. Polymer 107

p-Diallyloxybenzene **(99)** (2.285 g, 12.0 mmol), *N,N*'-Dimethyl-1,5- pentylidenedinitrone **(103)** (2.04 g, 12.9 mmol) and toluene (5 g) were placed in a round bottom flask and the mixture was stirred at 110 ^oC for about 92 h. The dinitrone was partially soluble in the reaction mixture. The ^1H NMR spectrum revealed the absence of protons attributed to the nitrone functionality (CH=NO(CH_3), while the dialkene end group protons are present in considerable amount. In order to react with the terminal alkene end groups more of the dintrone **103** (5. 0 mmol) was added and the mixture was polymerized for a further 24 h. After removing the solvent, the polymer was dissolved in dichloromethane at room temperature and precipitated in ether to give very elastic polymer.

The above reaction was repeated in ethanol solvent in which a homogeneous starting solution was obtained. However, the ^1H NMR spectrum again revealed the presence of protons attributed to the nitrone functionality (CH=NO(CH_3) in minor quantity, while the dialkene end group protons are present in considerable amount. $\nu_{max.}$ (KBr) 3395, 3207, 2921, 2858, 2778, 2026, 1502, 1446, 1339, 1217, 1032, 823. A pure sample of the dinitrone **(103)** was thermolyzed in toluene at 110 ^oC for 24 h. The ^1H NMR spectrum revealed the complete decomposition of the nitrone into intractable matter.

5.18. End-capping of Polymer 105a

To different chain length (8 h, 46 h, 72 h and 150 h) of polymer **105a** in $CDCl_3$ was added excess methyl acrylate and stirred in a closed NMR tube at 55 ^oC for 48 h. The reaction mixture was cooled to ambient temperature and the $CDCl_3$ and excess methyl acrylate were removed by gentle stream of N_2 at 40 ^oC.

5.19. Corrosion Measurement

5.19.1 Gravimetric Method (Weigh Loss Measurements)

The gravimetric experiments were performed in glass vessels containing 1M HCl with various amounts of the corrosion inhibitors. The gravimetric experiments were also carried out in 1N H_2SO_4 containing different concentrations of the corrosion inhibitors. The mild steel was suspended through a nylon thread in the HCl and in the H_2SO_4 solutions with various concentrations of the corrosion inhibitors. The glass container was placed without stirring in a water bath heated to 60 ^oC and kept for 6 h.

Solutions of 1M HCl and 1N H_2SO_4 were prepared from reagent A.C.S. concentrated HCl (Fisher Scientific Company) using distilled water. The coupons employed in the gravimetric method were prepared from mild steel having the composition: 0.089% (C), 0.34% (Mn), 0.037 (Cr), 0.022 (Ni), 0.007 (Mo), 0.005 (Cu), 0.005 (V), 0.010 (P) and 99.47% (Fe).

Before immersion test, the coupons were washed with deionized, cleaned with acetone and finally dried. After the elapsed time, the cleaning procedure consisted of wiping the coupons with a paper tissue, polishing lightly with emery paper, washing with distilled water, degreased with acetone and again washed with deionized water. The weight loss was determined at 60 ^oC for 6 h by hanging the steel coupon measuring 2.5 x

2.0 x 0.1 cm^3 into 1M HCl solution (140 cm^3) containing various amounts (0, 10, 25, 50, 100, 200, 400 ppm) of the synthesized corrosion inhibitors. The same procedure was carried out for solutions of 1N H_2SO_4. Corrosion inhibition efficiency was calculated based on the following equation:

$$\%IE = \frac{\text{Weight loss (blank)} - \text{Weight loss (inhibitor)}}{\text{Weight loss (blank)}} \times 100$$

Weight loss (blank) and weight loss (inhibitor) represent weight loss in absence and presence of inhibitor, respectively.

5.19.2 Electrochemical measurements

Two types of electrochemical techniques have been used in this study, Tafel Plots and Linear Polarization.

5.19.2.1 Tafel Plots

The Mild steel employed in electrochemical method was prepared from mild steel having the composition**:** 0.184% (C), 0.070% (Si), 0.29% (Mn), 0.097 (Cr), 0.071 (Ni), 0.021 (Mo), 0.065 (Cu), 0.014 (V), 0.012 (P), 0.029% (S), and 99.15% (Fe). The test specimens for the electrochemical measurements were machined in a flag shape from a mild steel sheet of 1 mm thickness. The stem of the flag, which measured approximately 3 cm, was insulated by an insulating paint. The remaining area was about 1 cm^2 and provided 2 cm^2 of exposed area. The exposed area was cleaned by increasing grades of emery papers (100, 400, 600 and 1500 grit size). Finally it was washed with acetone to remove any grease/oil.

The experiments were carried out in 200 cm^3 of 1M HCl containing various concentration of the inhibitors at 60 ^oC with the exposure time of 30 min (or until a steady-state open circuit potential was obtained). The same procedure was performed for solutions of 1N H_2SO_4. The electrochemical cell was assembled in a 250 ml round-bottomed flask consisting of carbon steel working electrode; the graphite electrode of approximately 5 mm diameter as a counter electrode and a saturated calomel electrode (SCE) was used as a reference electrode. All three electrodes were connected to a potentiostat (Model 283, EG&G PARC) through an electrometer. The potentiostat was hooked to a personal computer via a GPIB card. In this fashion the potentiostat could be controlled through the computer. Values of parameters in the electrochemical experiments were as follows: inhibitor concentration, 0 ppm and 200 ppm; potential range, ±250 mV with respect to open circuit potential. A scan rate of 0.16 mV/s was applied. Log of the generated current between the working electrode (mild steel specimen) and the counter electrode was plotted versus the over potential.

Each pair of Tafel plots {inhibitor in 1M HCl solution and of 1M HCl (blank)} were analyzed to obtain corrosion current density and corrosion potential. The same technique was used for each pair of Tafel plots for 1N H_2SO_4 solutions. The corrosion rate was determined in mils per year (mpy) using:

$$CR = 0.129 \frac{a * i}{n * D}$$

where,

CR = corrosion rate in mpy

a = atomic weight of the metal

n = number of electrons in the reduction of the metal ions.

D = density of the metal in g/cm^3.

i = corrosion current density $\mu A/cm^2$.

Finally, the corrosion inhibition efficiency of each solution was determined by:

$$\text{Corrosion Inhibition Effeciency} = \frac{CR_{blank} - CR_{inhibitor}}{CR_{blank}}$$

5.19.2.2 Linear Polarization (LP)

Linear polarization (polarization resistance) values were obtained from current potential plots. The polarization resistance was measured by scanning through a potential range that was very close to the corrosion potential. The potential range was ±15 mV around E_{corr} and the β_a and β_c slopes were fixed at 100 mV/decade.

REFERENCES

1. K. V. Gothelf and K. A. Jørgensen*, Chem. Rev.*, 98, 863*,* (1998).
2. P. N. Confalone and Edward M. Huie, "The [3+2] nitrone-olefin cycloadditions reaction", *Organic Reaction*, 36, 1-172 (1988).
3. G. R. Delpierre and M. Lamchen, *Quarterly Reviews*, 19, 329-348, (1965).
4. Kurt B.G. Torssell. *"Nitrile Oxides, Nitrones, and Nitronates in Organic Synthesis"*. VCH, (1988).
5. Glenn W. Goodall and Wayne Hayes*, Chem. Soc. Rev.*, 35, 280–312, (2006).
6. Padwa, General Heterocyclic Chemistry: 1,3-Dipolar Cycloaddition Chemistry, John Wiley and Sons, Chichester, Vol. 2, (1984).
7. Lyudmyla Vretik and Helmut Ritter, *Macromolecules,* 36, 6340-6345, (2003).
8. Helen M. I. Osborn, Natasha Gemmell and Laurence M. Harwood, *J. Chem. Soc., Perkin Trans. 1*, 2419–2438*,* (2002).
9. R. Sustmann, *Pure Appl. Chem.,* 40, 565-593, (1974).
10. V. G. Manecke and J. Klawitter, *Makromol. Chem.*, 108, 292, (1967)
11. V. G. Manecke and J. Klawitter, *Makromol. Chem.,* 142, 253, (1971).
12. Glenn W. Goodall, Kevin Cosstick, Simon C. Richards, Wayne Hayes, *European Polymer Journal,* 44,1881–1890, (2008).
13. Iida, Hideo; Kibayashi, Chihiro. "Synthesis of natural products via 1,3-dipolar cycloadditions of nitrones", *Yuki Gosei Kagaku Kyokaishi* 41(7), 652-66, (1983).
14. S. A. Ali, M. T. Saeed, S. Rahman, *Corros. Sci.,* 45, 253-266, (2003).
15. S. A. Ali, A. M. El-Shareef, R. F. Al-Ghamdi and M. T. Saeed, *Corros. Sci.*, 47, 2659-2678, (2005).
16. A. Yıldırım and M. Cetin, *Corrosion Science*, 50, 155–165, (2008).
17. Glenn W. Goodall, Kevin Cosstick, Simon C. Richards and Wayne Hayes, *European Polymer Journal*, 44, 1881–1890, (2008).
18. Michael Heinenberg, Bernhard Menges, Silvia Mittler and Helmut Ritter, *Macromolecules,* 35, 3448-3455, (2002).
19. V. S. Sastri, *Corrosion Inhibitors*, Principles and Application, John wiley and sons, (1998).

20. V. S. Sastri, G. R. Hoey, and R. W. Revie, *CIM Bulletin,* 87, 87, (1994).
21. The folowing textbook describes corrosion process in some details: by S. A. Bradford,*Corrosion Control,* Van Nostrand Reinhold, New York.
22. Gerhardus H. Koch, Michiel P. H.Brongers, Neil G. Thompson, Y. Paul Virmani and Joe H. Payer *"CORROSION COSTS AND PREVENTIVE STRATEGIES IN THE UNITED STATES"* Report by CC Technologies Laboratories, Inc. to Federal Highway Administration (FHWA), Office of Infrastructure Research and Development, Report FHWA-RD-01-156, September 2001.
23. H.B. Rudreesh, S. M. Mayanna, *J. Electrochem. Soc.*, 124, 340-342, (1977).
24. R.K. Dinnappa and S.M.Mayanna, *J. Appl. Electrochem. Soc.*, 11, 111-116, (1981).
25. R.K. Dinappa and S.M.Mayanna, *Corrosion,* 38, 525-530, (1982).
26. O.L. Riggs, NACE, Houston, Texas, 7, (1973).
27. N. Hackerman and R. M. Hurd, Proc. Int. *Congress of Metallic Corrosion*, London, Butterworths, P.166, (1962).
28. R. G. Pearson, *J. Chem. Education*, 45, 581, (1968).
29. V. S. Sastri, and P.R. Roberge, *Proc. 11th Int. Congress*, Florence, Italy,2-6 April v-3, 55, (1990).
30. K. Aramaki, T. Mochizuki and H. Nishihara, Proc. *10th Int. congress on metallic corrosion,* New Delhi, India, vol. 3. Oxford & IBH Pub. Co., P.2759, (1987).
31. P. Dupin, A.de Savignace, A. Lattes, *Information Chimie*, 228/224, p. 169, (1982).
32. R. Walker, Corrosion, *Corrosion,* 31, 97-100, (1975).
33. R. C. Ayers, N. Hackerman, *J. Electrochem. Soc.*, 110 , 507-513, (1963).
34. F. B. Growcock, *Corrosion,* 45 , 1003-1006, (1989).
35. S. L. Granese, "Study of inhibiting action of nitrogen-containing compounds," *Corrosion,* 44 , 322-327, (1988).
36. V. P. Grigorev and V. V. Ekilic, *Chemical Structure and Protective Action of Corrosion Inhibitors,* Restov University Edn, Ukraina, (1978).
37. A. Popova, E. Sokolova and S. Raicheva, *Khimia i industria*, 6, 275, (1987).
38. A. Popova, E. Sokolova and S. Raicheva, *Khimia i industria*, 2, 72, (1988).
39. S. N. Raicheva, B. V. Aleksiev and E. I. Sokolova, *Corrosion Sci.*, 34, 343, (1993).
40. H. F. Finley and N. Hackerman, *J. Electrochem. Soc.*, 107, 259, (1960).

41. F. M. Donahue, and K. Nobe, *J. Electrochem Soc*., 112, 886, (1965).
42. V. S. Sastri and J. R. Perumareddi, *Corrosion,* 50, 432, (1994).
43. N. Eldakar and K. Nobe, *Corrosion,* 33, 128, (1977).
44. A. Frignani, C. Monticelli, G. Brunoro, and G. Trabanelli, proc. 6th European symposium on *Corrosion inhibitors,* Ann. univ. Ferrara, n. s. Sez. V. Suppl. no. 8, P.1519, (1985) .
45. N. B. Lykina, A. I. Marshkov and Y. N. Mikhailovskii, *Zashch. Metall.,* 26, 333, (1990).
46. Y. Y. Bogatchuk, S. A. Nesterenko, G. G. Vrzhosek and V. V. Trachevskii, *Izv. Vyssh. Uchebn. Zaved., Khim. Tekhnol.,* 31, 68, (1988).
47. N. I. Podobaev, N. V. Kardash and A. N. Levichev, Metall. Koksokhim., 98, 71, (1989).
48. N. M. Agaev, T. A. Aslanov, R. I. Mustafaev, I. R. Eminova and G. D. Geidarova, *Zasch. Metall.,* 25, 992, (1989).
49. A. A. Al-Suhybani, *Corros. Prev. Control,* 37, 11, (1990).
50. A. N. Levichev and N. V. Kardash, *Zashch. Metall.,* 27, 971, (1991).
51. R. D. Braun, E. E. Lopez and D. P. Vollmer, *Corros. Sci.,* 34, 1251, (1993).
52. L. Haupt and J. Meissner, *Korrosion (Dresden),* 20, 31, (1989).
53. G. Trabanelli, F. Zucchi, G. Giullini and V. Carassiti, *Werkst und korros,* 20, 1012, (1969).
54. E. Mclafferty, *Corrosion Control by Coatings ,* princeton, NJ, Science press, P.279, (1979).
55. F. B. Growcock, W. W. Frenier and V. R. Lopp, *Proc. 6th European Symposiumon Corrosion Inhibitors,* Ann. Univ. Ferrara, n.s., Sez, V. Suppl. no. 7, p.1185, (1980).
56. a) F. Zucchi, G. L. Zucchini and G. Trabanelli, *Proc. 3rd Eurpean Symposium on Corrosion Inhibitors,* Ann. Univ. Ferrara, n.s. Sez. V, Suppl. 5, P.415, (1970). b) D. Jayaperumal, S. Muralidharan, P. Subramanium, G. Venkatachari and S. Senthilrel, *Anti-Corrosion Method and Material ,* 44, 265, (1997).
57. G. Lendvay-Gyrik, G. Meszaros, B. Lengyel, G. Lendvay, *Corros. Sci.,* 45, 1685-1702, (2003).

58. M. S. Morsi, Y. F. Barakat, R. El-Sheikh, A. M. Hassan, and A. Baraka, Werkstof *und Korrosion,* 44, 304, (1993).
59. N. Hackermn, and A. C. Mackrides, *Ind. Eng. Chem.,* 46, 523, (1954).
60. V. Carrasiti, F. Zucchi, G. Trabanelli: *Proc. 3rd European Symposium on Corrosion Inhibitors,* Ferrara 1970; University of Ferrara, 525, (1971).
61. N. Hackerman: Proc. 1st International Congress *"Metal Corrosion",* London, 313, (1961).
62. M. A. Quraishi, M. A. W. Khan and M. Ajmal, *Bull. Electrochem.,* 11(6), 274-277, (1995).
63. H. Luo, Y. C. Guan and K. N. Han, *Corrosion,* 54, 721-731, (1998).
64. S. Hettiarachchi, Y. W. Chan, R.B.Wilson, Jr., and V.S. Agarwala, *Corrosion,* 45, 30-34, (1989).
65. M. Kralji, Z. Mandi and Lj. Dui, *Corros. Sci.*, 45, 181-198, (2003).
66. M. Hosseini, S. F. L. Martens, A. R. arshadi, *Corros. Sci.,* 45, 1473-1489, (2003).
67. G. Smith, Br. *Corros. J.,* 9, 165, (1984).
68. Dickie, Ray A.; Floyd, F. Louis, *ACS Symposium Series*, 322, 1-16, (1986).
69. Oh, Se Yong; Park, Chan Eon; Song, Sang Min, *U.S. Pat. Appl. Publ*., 7 pp. US 2002035222 A1 20020321 CAN 136:263639 AN 2002:221233 (Pat No. 6455654), (2002).
70. Annand, Robert R.; Woodson, Aldred E., *U.S. Pat*., 10 pp. (US Patent No.3982894) 19760928 CAN 89:10128 AN 1978:410128, (1976).
71. Carpenter, Clint W.; De Haan, Jeanne M., *U.S. Pat*., 10 pp. US 5389139 A 19950214 CAN 123:317015 AN 1995:420683, (1995).
72. Ghosh, Tirthankar; Hann, William M.; Weinstein, Barry., *Eur. Pat. Appl.,* 19 pp. (US Patent No. 6,646,082), (2003).
73. Bakeev, Kirill N.; Chuang, Jui-Chang; Winkler, Thomas; Drzewinski, Michael A.; Graham, David E. "Copolymer-based corrosion inhibitor in steel pipelines during transport of water and hydrocarbons", U.S, 4 pp., Cont.-in-part of U.S., (2002).
74. Mengoli, G.; Musiani, M. M.; Pagura, C.; Paolucci, F., *Corrosion Science* 32(7), 743-53, (1991).

75. R. Hariharaputhran, A. Subramanian, A. A. Antony, P. Manisankar, T. Vasudevan, S. V. Iyer, *Anti-Corrosion Methods and Materials*, 46, 35-39, (1999).
76. R. Behrends, K. Leuchs, *Angew. Chem.*, 257, 239, (1890).
77. O. H. Wheeler, P. H. Gore, *J. Am. Chem. Soc.*, 78, 3365,(1956).
78. Iwakura, Yoshio; Akiyama, Masayasu; Shiraishi, Shinsaku., *Bulletin of the Chemical Society of Japan*, 38(3), 513-14, (1965).
79. Michael Heinenberg and Helmut Ritter, *Macromol. Chem. Phys.,* 200, 1792–1805, (1999).
80. Kenta Tanaka, Tetsutaro Igarashi, and Tadamitsu Sakurai*, Macromolecules*, 37, 5482, (2004).
81. G. R. Delpierre, M. Lamchen, *Quaterly Reviews,* 19, 329-348, (1965).
82. T. Murakawa and Hackerman, N., *Corros. Sci., 4, 387-397, (1964).*
83. G. Moretti, G. Quartarone, A. Tassan, A. Zingales, *Electrochim. Acta.,* 41, 1971-1980, (1996).
84. R. H. Chaturvedi and R. S. Chaudhury, Corros. *Prevent. Contr.,* 37, 53-55, (1990).
85. S. Muralidharan, M. A. Quraishi and S. V. K. Iyer, *Corros. Sci.,* 37, 1739-1750, (1995).
86. H. A. ElDahan, T. Y. S. Mohamed and S. A. Abo El-Enin, *Anti-Corros. Meth. Mater*., 46, 358-363, (1999).
87. S. A. Ali, A. M. El-Shareef, R. F. Al-Ghamdi and M. T. Saeed, *Corros. Sci.,* 47, 2659-2678, (2005).
88. S. A. Ali, H. A. Al-Muallem, M. T. Saeed, S. U. Rahman, *Corros. Sci*., 50, 664-675, (2008)
89. S. A. Ali, H. A. Al-Muallem S. U. Rahman, and M. T. Saeed, *Corros Sci.,* 50, 3070-3078, (2008)

VITA

Name:	Abdullah Ali Lajami**.**
Place of Birth:	Jarodiah, Saudi Arabia.
Nationality:	Saudi.
Date of Birth:	09-05-1976
Present Address:	King Fahd University of Petroleum and Minerals.
Permanent Address:	Qatif, Saudi Arabia.
Phone:	(03)8527692
E-mail:	g200501090@kfupm.edu.sa
	g250109@gmail.com